Abstract

Title of Dissertation: SHIFTING INPUTS AND TRANSFORMATIONS OF NITROGEN IN FORESTED AND MIXED LAND USE BASINS: IMPLICATIONS FOR HYDROLOGIC NITROGEN LOSS

Robert D. Sabo, Doctor of Philosophy, 2018

Dissertation Directed By: Dr. Keith N. Eshleman

Professor

University of Maryland Center for Environmental Science, Appalachian Laboratory

Increased N inputs along with changes in population, land use, and climate have globally altered the N cycle. This alteration has been associated with increased food, energy, and fiber availability, but has also contributed to the degradation of human health conditions and diminishment of expected ecosystem services in many regions throughout the world. In this context, my research explored the impact of shifting anthropogenic N inputs and other environmental drivers on terrestrial N surpluses and linked changes in terrestrial surpluses to observed changes in N loss to aquatic systems. Working in both forested and mixed land use catchments in the eastern USA, I hypothesized that processes that reduced terrestrial N surpluses in catchments by 1) reducing N inputs, 2) increasing plant uptake, and/or 3) increasing gaseous efflux would result in decreased hydrologic N export. Identification of potential processes was accomplished by first generating long-term atmospheric, remote sensing, terrestrial, and hydrologic datasets for individual catchments. The first two components of my dissertation highlighted potential interactions between atmospheric N deposition, acidic deposition, climate, and disturbance in influencing terrestrial N availability, as indicated by N isotopes in tree rings, in forested catchments. Leveraging trend analysis and statistical models, I identified continued long-term declines in terrestrial N availability in forests, but this decline was likely being modified by disturbance and long-term reductions in acidic deposition. The final component of my dissertation involved developing a lumped conceptual model to explain water quality trends in three mixed land use catchments within the Chesapeake Bay watershed. This study assessed the relative influence of point source N loading, agricultural practices, and atmospheric N deposition on long-term trends in riverine N loss. Insights from the simple N loading model strongly suggested that declines in atmospheric N deposition and point source loading were key drivers of historical water quality improvement. Whether relying on quasi-mass balances or dendroisotopic records, findings from this research emphasize the usefulness of constructing proxy datasets of terrestrial N surpluses in identifying likely processes driving changes in hydrologic N loss in forested and mixed land use catchments.

SHIFTING INPUTS AND TRANSFORMATIONS OF NITROGEN IN FORESTED AND MIXED LAND USE BASINS: IMPLICATIONS FOR HYDROLOGIC NITROGEN LOSS

By

Robert Daniel Sabo

Dissertation submitted to the Faculty of the Graduate School of the
University of Maryland, College Park, in partial fulfillment
of the requirements for the degree of
Doctor of Philosophy
2018

Advisory Committee:

Professor Keith N. Eshleman, Chair
Professor David M. Nelson
Professor Eric A. Davidson
Professor Andrew J. Elmore
Professor Thomas R. Fisher
Professor Kaye L. Brubaker

Dedication

"*Your wife shall be like a fruitful vine within your house, your children like olive plants around your table*."

-Ps. 128:3

This work is dedicated to my wife, Sarah Sliviak Sabo. From the mountains of western Maryland to the urban bustle of Washington D.C., she has been my rock and a spring of joy throughout my graduate school career. Thank you for your unwavering faith and encouragement, our beautiful children, and our irreplaceable popcorn nights.

Acknowledgements

Many thanks to Dr. Keith N. Eshleman for his willingness to advise and mentor me for the past seven years throughout both my Masters and Doctoral studies. I would like to also acknowledge Dr. David M. Nelson for his tireless efforts in improving my scientific writing skills and for introducing me to the wonders of stable isotopes. I am grateful to Drs. Eric A. Davidson and Andrew J. Elmore for offering two of the most influential classes of my graduate career and their invaluable guidance and encouragement offered on field trips and conferences. Thank you also to Dr. Tom R. Fisher for our edifying conversation on nitrogen dynamics in forested and mixed land use catchments and your dedication in improving my doctoral research program. Many thanks to all my fellow research collaborators, undergraduate researchers, and research assistants in making this ambitious research program possible. They are specifically acknowledged in individual chapters. Special thanks also to the administrative staff at Appalachian Lab who not only coordinated my research funds, but who always strove to ensure that my family was best supported under tightening budgets. This research was made possible through the support of an Environmental Protection Agency Science to Achieve Results Graduate Fellowship, National Geographic Young Explorer's Grant, research assistantship from Appalachian lab, and a teaching assistantship through the Marine-Estuarine-Environmental Sciences (MEES) Graduate Program. This research was also supported in part by an appointment to the Research Participation Program for the U.S. Environmental Protection Agency, Office of Research and Development, administered by the Oak Ridge Institute for Science and Education through an inter-agency agreement between the U.S. Department of Energy and EPA.

Table of Contents

List of Tables

List of Figures

Chapter 1: Processes driving the loss of N to surface waters: Opportunities and Challenges

The release of excess nitrogen through fossil fuel combustion and activities associated with food production has altered the global nitrogen (N) cycle. Historically, the productivity of ecosystems was often limited by the supply of N, but humanity has applied energy-intensive measures to convert N_2 into ammonia through the Haber-Bosch process. After factoring in the unintentional release of N from fossil fuel combustion, anthropogenic activities input ~190 Tg N yr^{-1} into the Earth's atmosphere and biosphere (Galloway et al. 2008), whereas current estimates of N fixed through natural terrestrial processes stands at only ~127 Tg N yr^{-1} (Cleveland et al. 2013). The >100% increase in reactive N production has been associated with increased food, energy, and fiber availability (Galloway et al. 2003), but the majority of anthropogenically created N does not end up in food, fiber, or other products because it is transported to downwind or downstream systems (Houlton et al. 2013). Transport of excess N has contributed to eutrophication of surface waters (Carpenter et al. 1998, Conley et al. 2009), N enrichment of forests and grasslands (MacDonald et al. 2002, Simkin et al. 2016), hypoxia (Conley et al. 2009), smog (Haagen-Smit 1952), accumulation of atmospheric particulate matter (Zheng et al. 2005), and acidification of terrestrial and aquatic ecosystems (Bobbink et al. 2010) over the past century. The degradation of human health conditions and diminishment of expected ecosystem services has prompted many nations to develop integrated management strategies to promote nitrogen use efficiency and decreased the release of nitrogen (Galloway et al. 2008, Sutton et al. 2011). Air and water quality improvements have been observed in industrial countries that have cut NO_x emissions from stationary and vehicular sources (Eshleman et al. 2013, Garmo et al. 2014,

Eshleman and Sabo 2016), reduced TN flux from wastewater treatment plants through nutrient removal technologies (Mallin et al. 2005), and increased agricultural nitrogen use efficiency through increased crop yields and application of nutrient management strategies (Mueller et al. 2012, Velthof et al. 2014). It is imperative to identify the relative influence of specific management and technological applications on air and water quality improvements in order to gauge and potentially enhance the assimilative capacity of N in ecosystems and reduce N loss to downwind or downstream areas (Sobota et al. 2013).

The hydrologic loss of N in large mixed land use basins throughout Europe, China, and North America is primarily driven by climate and anthropogenic nitrogen inputs (Boyer et al. 2002, Chen et al. 2016b). Riverine N exports generally rise as N inputs increase through fertilizer application, food imports, atmospheric NO_y deposition, and cultivation of leguminous crops, but can also be attenuated with high rates of crop removal. The net difference in anthropogenically mediated input and removal processes is termed the net anthropogenic nitrogen input (NANI, (Howarth et al. 2012)). Increased riverine N export, however, can be attenuated by climatic forces that either promote greater denitrification or reduce riverine discharge (Boyer et al. 2002, Howarth et al. 2012). Based on comparative catchment analyses, warmer catchments that have lower discharge are generally more retentive of N inputs then cooler catchments with higher discharge (Howarth et al. 2012). This suggests catchments inherently have a "baseline" assimilative capacity to either efflux or retain N inputs partly based on their hydroclimatology. Even though N inputs and discharge can generally explain global patterns of riverine N export, there is substantial variability in riverine N export among

catchments with similar annual discharges and N inputs. This variability is informative because it indicates riverine N export can be attenuated by not only reducing nitrogen inputs into the catchment, but by modifying atmospheric and terrestrial processes that may prevent hydrologic loss of N to downstream ecosystems (Hale et al. 2015, García et al. 2016). Since greatly reducing N inputs may be unfeasible in many mixed land use catchments throughout the globe (Doering et al. 2011, Sutton et al. 2011), identifying the primary drivers of N retention and N export is paramount to informing water quality restoration initiatives throughout the USA and elsewhere.

Discerning the primary drivers of hydrologic N loss in smaller mixed land use basins is difficult due to uncertainty over the multiple sources that input N into the system and the variable influence that different land uses have on N retention (Howarth et al. 2012). Thus, much of the conceptual knowledge on the transport and transformation of N in ecosystems has stemmed from the study of "simpler" forested catchments (Likens 2013). Focusing on forested catchments eliminates the issue of multiple land uses and reduces the number of N sources generally to three categories: biologically fixed nitrogen, atmospheric N deposition, and soil N reservoirs (Hedin et al. 1995). Similar to the insights stemming from the NANI studies, climate and N inputs play a large role in governing the annual hydrologic loss of N (Brookshire et al. 2011, Adams et al. 2014, Hwang et al. 2014). Generally, warmer temperate forested catchments on the east coast of the USA display greater retention of atmospheric N deposition and less N leaching to surface waters than cooler sites (Aber and Driscoll 1997, Eshleman et al. 2013). Processes that govern these regional retention patterns likely stem from the influence of temperature and precipitation on plant uptake and gaseous efflux. Warmer areas that

experience longer growing seasons are likely to be more productive and have a greater N demand relative to cooler sites (Hwang et al. 2014). The capacity of a forest to accumulate or efflux nitrogen determines its ability to retain atmospherically deposited nitrogen (Aber et al. 1989), in turn preventing nitrate leaching to surface water. The recently proposed conceptual model of kinetic N saturation by Lovett and Goodale (2011) describes the dynamic between source and sink rates of N in forests through a simple mass balance:

$$Y = D - A - G \qquad 1)$$

where the N yield (*Y*) is determined by the amount of atmospherically deposited nitrogen (*D*) less the amount immobilized through net annual assimilation of N into forest vegetation and soil organic matter (*A*) and/or effluxed through various gaseous pathways (*G*). This conceptual model has been empirically supported in long-term observational studies, which have revealed that forested catchments generally retain or efflux a constant proportion (*a*) of atmospheric inorganic nitrogen (IN) deposition through time (Grigal 2012, Eshleman et al. 2013). Based on this conceptual model, N yields, primarily in the form of nitrate, are responsive to changes in *D* if processes governing *A* and *G* are not greatly altered (Figure 1, left panel). Vegetative uptake can be offset by disturbances (Eshleman et al. 1998), drought (Kaushal et al. 2008), ozone damage (Ollinger et al. 2002), successional processes (McLauchlan et al. 2007), and other factors, however. Storage of N in soil organic matter can also become saturated leading to enhanced mineralization/nitrification or altered via regime shifts (Aber et al. 1998, Webster et al. 2016). Intense periods of rainfall or large snowmelts may cause activation of preferential

hydrologic pathways by which nitrate is flushed to streams prior to its processing (Piatek et al. 2005, Sabo et al. 2016a). Inter-annual variation in runoff also affects year to year variability in retention with higher annual runoff leading to diminished retention (Adams et al. 2014, Eshleman and Sabo 2016). Identifying the drivers that alter the net accumulation rates of atmospheric N deposition in forested catchments can help identify parallel processes that are likely important in governing the retention and loss of N in mixed land use catchments.

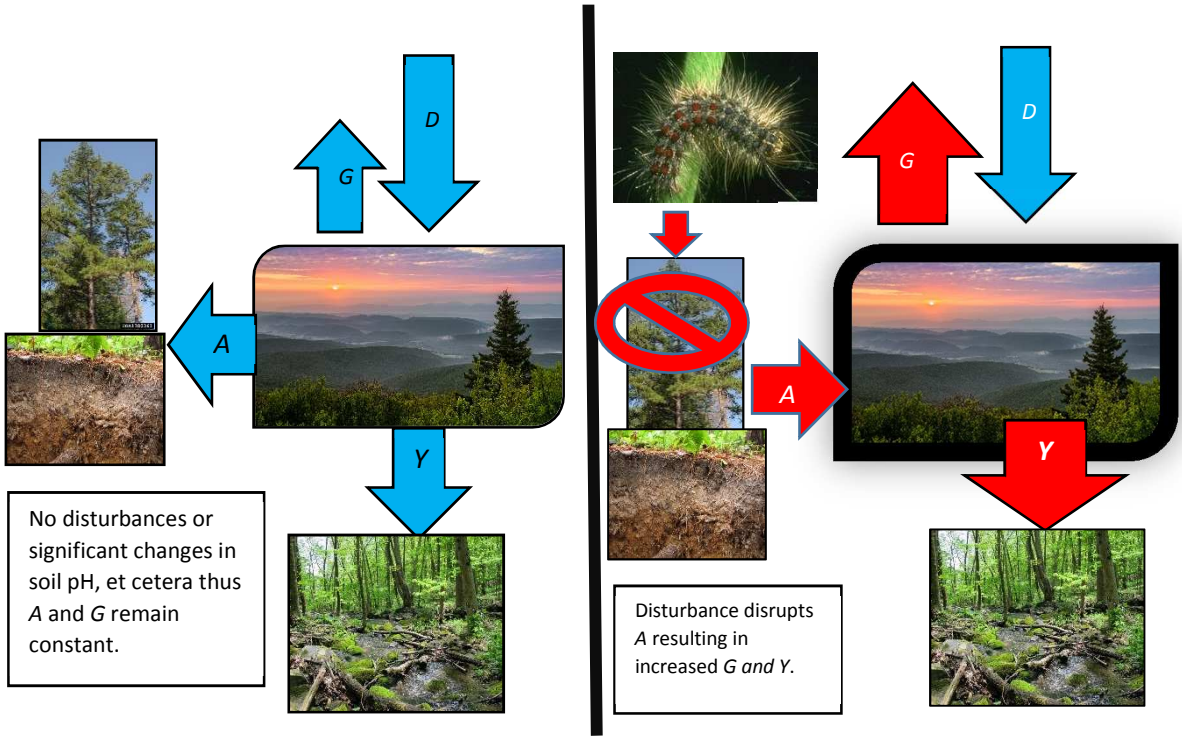

Figure 1. Conceptual diagram illustrating the kinetic N saturation model in a forested catchment. If the atmospheric inputs and the net aggradation of N in soils/vegetation and gaseous efflux of N is steady through time, then hydrologic N loss to streams will be constant (left panel). These processes are often not constant in forests, however. One possible scenario is illustrated in the right panel where canopy disturbance by gypsy moth larvae results in a net negative accumulation of N in forest soils and vegetation resulting in elevated gaseous and hydrologic losses of N.

The recent emergence of long-term datasets that estimate the flux of N in atmospheric, terrestrial, and hydrologic compartments of catchments potentially offer empirical insight into the predominant drivers of water quality changes in forested and

mixed land use catchments. Datasets that estimate changes in terrestrial N availability or mass balance are particularly useful for assessing the direct influence of N inputs, crop N uptake, and disturbance on potential N loss to surface waters. These datasets, unlike inference of N availability from water quality data, do not display 1) co-linearity with discharge or 2) lag issues associated with groundwater residence time (Hirsch et al. 2010, Chen et al. 2016a). Thus, the relationships between identifiable processes (e.g., satellite-based observations of forest disturbance or recorded changes in crop N removal) and changes in terrestrial N availability as inferred from impartial mass balances or dendroisotopic records can become firmly established. Establishing these relationships can subsequently informing efforts looking to assess the relative influence of specific management actions and technological applications (e.g., wastewater treatment upgrades) on observed water quality trends (Doering et al. 2011, Keisman et al. 2015). This approach is based on recent efforts to link changes in atmospheric N deposition with water quality improvement through a modified kinetic N saturation model (MKNSM), an adaptation of the kinetic N saturation model, in the Potomac River Basin (Eshleman and Sabo 2016). The findings of the study challenged conventional wisdom that agricultural best management practices and wastewater treatment plants were the primary drivers of water quality improvements in the Chesapeake Bay drainage (Shenk and Linker 2013). There is uncertainty, however, over parallel changes in other N sources and processes in the Potomac that has inspired further investigation. In my dissertation, I explored how changes in the inputs and the terrestrial transformation/flux of N impact hydrologic N loss in both forested and mixed land use catchments (Figure 1; Figure 2).

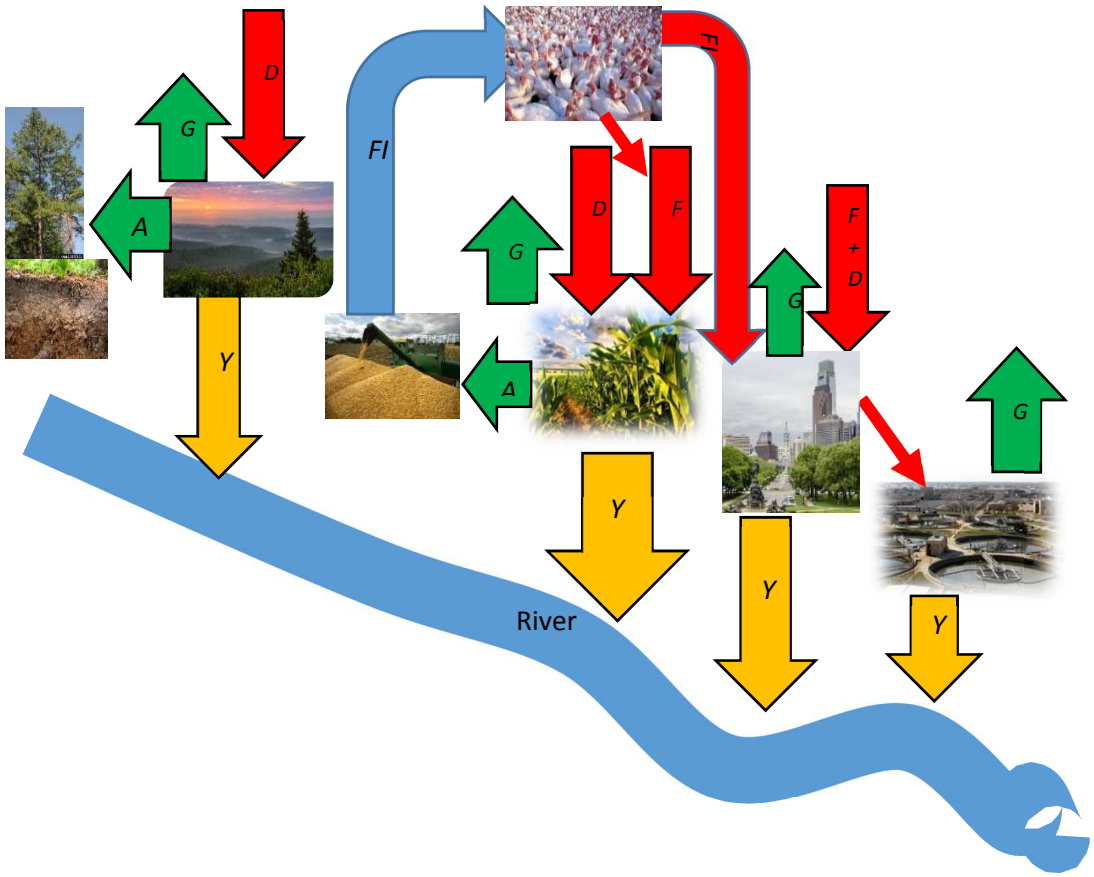

Figure 2. Simplified conceptual diagram highlighting major N fluxes for different land cover types in a mixed land use catchment. Generally, the kinetic N saturation model can be applied to all land use types, but additional fluxes need to be considered. These include net food transfers within a catchment (FI), cultivated biological N fixation (not illustrated), and manure/fertilizer N application to agricultural areas and urban landscapes (F). It should be noted gaseous emissions, if not in the form of N_2 or N_2O, likely partly contribute to atmospheric N deposition within a catchment (not illustrated). Red arrows highlight N inputs, green indicates gaseous efflux and soil/plant N removal, and orange highlights N loss to surface water. Steps to reduce inputs (red) or enhance A/G pathways (green) will result in decreased hydrologic N loss to surface waters (orange).

I assessed temporal changes in terrestrial N availability in agricultural lands and forests, and attributed long-term temporal shifts in terrestrial N availability to changes in N inputs, disturbance, and crop N uptake. I hypothesize that processes that reduce N inputs, increase plant uptake, or increase gaseous efflux in catchments would result in reduced hydrologic N loss in both forested and mixed land use catchments. I predicted that reductions in atmospheric N deposition would decrease terrestrial N availability and nitrogen loss in forested catchments. This response, however, would be disrupted if

parallel processes that impact net vegetative uptake and soil aggradation (*A*) like disturbance, deposition of mineral acids, and drought were co-occurring within the forested catchment (Figure 1). I also predicted decreasing N inputs (e.g., fertilizer/manure or atmospheric N deposition) onto mixed land use catchments would result in decreased terrestrial N availability and TN loss to surface water. In addition, planting of more productive crop cultivars and technological upgrades to wastewater treatment plants would increase plant N uptake and gaseous efflux, respectively, in turn leading to less N vulnerable to being lost to surface waters (Figure 2). This dissertation accounted for the predominant N inputs and transformations into both forested and mixed land use catchments, in hopes of explaining past changes in terrestrial N availability and surface water TN loss.

The dissertation consists of three studies that explored how shifts in the inputs and processing of N impact terrestrial N availability and hydrologic N loss in both forested and mixed land use catchments. The first two components of my dissertation highlighted potential interactions between atmospheric N deposition, acidic deposition, climate, and disturbance in influencing terrestrial N availability, as indicated by N isotopes in tree rings, in forested catchments. Leveraging trend analysis and statistical models, I identified likely drivers of shifting terrestrial N availability in forested catchments. The third primary component of this dissertation conceptually builds on research from chapters two and three but transitions to a quasi-mass balance approach to explain water quality trends in three mixed land use catchments in the Chesapeake Bay. This study developed a lumped, land use specific nitrogen loading model to assess the relative influence of point source N loadings, agricultural practices, and atmospheric N deposition

on long-term trends of total nitrogen loading. This chapter was the most applied and socially pertinent of the chapters because it will inform watershed managers and policy makers developing strategies to improve water quality in the Chesapeake Bay. I expected this research to highlight that shifts in N inputs are not necessarily the sole driver of terrestrial N surpluses and water quality trends in forested and mixed land use catchments.

Chapter 2: Watershed-scale changes in terrestrial nitrogen cycling during a period of decreased atmospheric nitrate and sulfur deposition

(At the time of dissertation submission, this chapter has been published in a special edition of *Atmospheric Environment* titled "Watershed-scale changes in terrestrial nitrogen cycling during a period of decreased atmospheric nitrate and sulfur deposition". I contributed substantially to the design and implementation of the study and was the lead author of this paper. Please also note some of the terminology differs from the rest of the dissertation (e.g., NO_3-N instead of nitrate or watershed instead of catchment).)

Abstract

Recent reports suggest that decreases in atmospheric nitrogen (N) deposition throughout Europe and North America may have resulted in declining nitrate export in surface waters in recent decades, yet it is unknown if and how terrestrial N cycling was affected. During a period of decreased atmospheric N deposition, we assessed changes in forest N cycling by evaluating trends in tree-ring $\delta^{15}N$ values (between 1980 and 2010; n = 20 trees per watershed), stream nitrate yields (between 2000 and 2011), and retention of atmospherically-deposited N (between 2000 and 2011) in the North and South Tributaries (North and South, respectively) of Buck Creek in the Adirondack Mountains, USA. We hypothesized that tree-ring $\delta^{15}N$ values would decline following decreases in atmospheric N deposition (after approximately 1995), and that trends in stream nitrate export and retention of atmospherically deposited N would mirror changes in tree-ring $\delta^{15}N$ values. Three of the six sampled tree species and the majority of individual trees showed declining linear trends in $\delta^{15}N$ for the period 1980–2010; only two individual trees showed increasing trends in $\delta^{15}N$ values. From 1980 to 2010, trees in the watersheds of both tributaries displayed long-term declines in tree-ring $\delta^{15}N$ values at the watershed scale ($R = -0.35$ and $p = 0.001$ in the North and $R = -0.37$ and $p < 0.001$ in the South). The decreasing $\delta^{15}N$ trend in the North was associated with declining stream nitrate concentrations (-0.009 mg N L^{-1} yr^{-1}, $p = 0.02$), but no change in the retention of

atmospherically deposited N was observed. In contrast, nitrate yields in the South did not exhibit a trend, and the watershed became less retentive of atmospherically deposited N ($-7.3\%\ yr^{-1}$, $p < 0.001$). Our $\delta^{15}N$ results indicate a change in terrestrial N availability in both watersheds prior to decreases in atmospheric N deposition, suggesting that decreased atmospheric N deposition was not the sole driver of tree-ring $\delta^{15}N$ values at these sites. Other factors, such as decreased sulfur deposition, disturbance, long-term successional trends, and/or increasing atmospheric CO_2 concentrations, may also influence trends in tree-ring $\delta^{15}N$ values. Furthermore, declines in terrestrial N availability inferred from tree-ring $\delta^{15}N$ values do not always correspond with decreased stream nitrate export or increased retention of atmospherically deposited N.

Introduction

Nitrogen and sulfur oxide emissions (NO_x and SO_x, respectively) from fossil fuel combustion have contributed to atmospheric acid deposition (defined herein as the wet and dry deposition of nitric and sulfuric acids) and the acidification and eutrophication of many terrestrial and aquatic ecosystems throughout Europe and North America for more than a century (Driscoll et al. 2001). To prevent further ecosystem deterioration and protect human health, regulations requiring NO_x and SO_x emission reductions were implemented in many industrialized nations, resulting in declines in acid deposition in recent decades (Vet et al. 2014). Observational studies indicate that resultant long-term declines in NO_3-N deposition have sometimes occurred concomitantly with decreased NO_3-N export in surface waters, suggesting potential declines in ecosystem N availability (Kothawala et al. 2011, Rogora et al. 2012, Waller et al. 2012, Eshleman et al. 2013). Catchment-scale clean roof experiments have also demonstrated that ecosystem N availability and stream NO_3-N yields can decline in response to decreased N and S inputs (Corre et al. 2003, Corre and Lamersdorf 2004). Experimental approaches, however, cannot be easily replicated in multiple watersheds across broad spatial scales. In addition, factors such as forest succession (McLauchlan et al. 2007), changing denitrification rates (Morse et al. 2015), insect-caused defoliation (Eshleman et al. 1998), disturbance (Bernal et al. 2012), in-stream processes (Peterson et al. 2001), and timber harvest (Vitousek and Melillo 1979) can also influence stream NO_3-N yields, which may make it difficult to detect a direct influence of declining NO_3-N deposition on stream NO_3-N yields or to infer changes in terrestrial N availability (Argerich et al. 2013, Kopáček et al. 2016). A proxy that captures information about past changes in N availability within catchments is

needed to help assess the influence of decreased NO_3-N deposition on N cycling in terrestrial ecosystems (Tomlinson et al. 2016).

Recent theoretical and empirical advances indicate that the nitrogen isotope ($\delta^{15}N$; $^{15}N/^{14}N$ ratio of a sample relative to a standard) values of tree rings provide an integrated metric of historical changes in soil N availability, defined as the supply of N relative to its demand by plants (McLauchlan et al. 2007, Gerhart and McLauchlan 2014, Howard and McLauchlan 2015). Tree-ring $\delta^{15}N$ values record changes in multiple pathways that fractionate N isotopes, including gaseous N losses during denitrification and nitrification, nitrate leaching, and transfer of N to plants via mycorrhizal fungi (Craine et al. 2009). Overall, greater N availability tends to result in relatively low $\delta^{15}N$ values in the N that is lost (e.g. through denitrification or nitrification followed by leaching of NO_3-N), which results in more positive $\delta^{15}N$ values within residual soil inorganic nitrogen (IN) pools, and thus more positive $\delta^{15}N$ values in plant tissues. Furthermore, high N availability tends to cause plants to be less dependent on mycorrhizal fungi, which are known to provide them with N that has low $\delta^{15}N$ values (Michelsen et al. 1998, Hobbie et al. 2000). High $\delta^{15}N$ values typically occur in soil and leaves of forests with high rates of nitrification (Pardo et al. 2007), denitrification (Nadelhoffer et al. 1996, Templer et al. 2007), nitrate leaching (Pardo et al. 2006), and low input of N from mycorrhizal fungi (Pardo et al. 2006).

Some of the recent declines in stream NO_3-N yields attributed to decreased atmospheric N deposition in the northeastern US may be partly explained by declining terrestrial N availability (as recorded by tree-ring $\delta^{15}N$ values) due to decreased inorganic nitrogen (IN) inputs. However, the relative importance of declining N deposition on

terrestrial N availability as recorded in plant $\delta^{15}N$ values is uncertain (Gerhart and McLauchlan 2014). Declines in stream NO_3-N yields and tree-ring $\delta^{15}N$ values in a forested watershed in the northeastern United States over a 30 year period were attributed to successional processes that drove a decline in N availability (McLauchlan et al. 2007), suggesting that stream NO_3-N export and tree-ring $\delta^{15}N$ records may be complementary approaches that provide independent validation of each other in terms of changes in ecosystem N availability. However, species-specific tree ring $\delta^{15}N$ trends have also been observed (Cairney and Meharg 1999, McLauchlan and Craine 2012), indicating that species may exhibit temporal variation in their partitioning of available forms of N due to changing factors such as nitrification rates, ammonium deposition, and/or changes on reliance of mycorrhizal fungi (Gerhart and McLauchlan 2014). Comparison of tree-ring $\delta^{15}N$ and stream N datasets can help to disentangle the influence of local changes in terrestrial N cycling from larger, regional factors, such as decreased IN inputs via declines in atmospheric N deposition, to explain catchment-scale trends in terrestrial N availability and stream NO_3-N yields (McLauchlan et al. 2007, Eshleman et al. 2013).

We conducted a comparative analysis at two well-studied forested watersheds (North and South Tributaries of Buck Creek) in the Adirondack Mountains, New York, USA (Lawrence 2002, Ross et al. 2012). Hydrologic and stream water-quality monitoring have been carried out at these Buck Creek tributaries since the fall of 1999, along with periodic vegetative and soil surveys (Lawrence 2002, NYSERDA 2012, Ross et al. 2012). Stream NO_3-N yields in the North Tributary (North) are typical of other forests in New England and the Adirondacks ($\sim$1.2 kg N ha^{-1} yr^{-1}), whereas stream NO_3-N yields in the South Tributary (South) are elevated ($\sim$5.10 kg N ha^{-1} yr^{-1}) relative to other

northeastern forests (Ross et al. 2012). Trends in acid deposition (1986–2011), $\delta^{15}N$ in tree cores (1980–2010), and stream NO_3-N export (2000–2011) were evaluated and compared. A multiple regression model was also constructed to assess the relationship between IN and sulfate deposition and stand-level tree-ring $\delta^{15}N$ values. We hypothesized that tree-ring $\delta^{15}N$ values would only begin to decline following decreased atmospheric N deposition (~post-1995), and that trends in stream NO_3-N export and retention of atmospherically deposited N would mirror changes in tree-ring $\delta^{15}N$ values. Specifically, we expected watershed-scale tree-ring $\delta^{15}N$ values to remain stable for the 1980–1995 period, but decline due to declining N availability following declines in atmospheric IN deposition. We also hypothesized that stream NO_3-N export would show a decline and thus coincide with a declining trend in tree-ring $\delta^{15}N$ values between 2000 and 2010.

Methods

Site description

The North and South Tributaries of Buck Creek (referred to as North and South below; Figure 3) have been continuously gaged since October 1999. They have been the subject of multiple hydrobiogeochemical investigations assessing the impacts of acid deposition on Adirondack forests (Burns et al. 2009, Lawrence et al. 2011, Ross et al. 2012). These mountainous catchments were last logged in the early 1900s, and currently contain mature forests typically found throughout the northeastern United States (NYSERDA 2012). The climate of the Buck Creek watershed (*Figure 3*) is characterized by cold winters and cool summers with mean monthly temperatures in January and July averaging −10 °C and 18 °C, respectively (Lawrence et al. 2004, PRISM 2015). Over the period of record (1986–2013), mean annual precipitation was ~1300 mm according to

data extracted from NADP/PRISM gradient maps (NADP 2015, PRISM 2015). The typical growing season for the forest surrounding Buck Creek extends from late May to mid-September, and is followed by the development of a significant snowpack, which usually melts in mid-April.

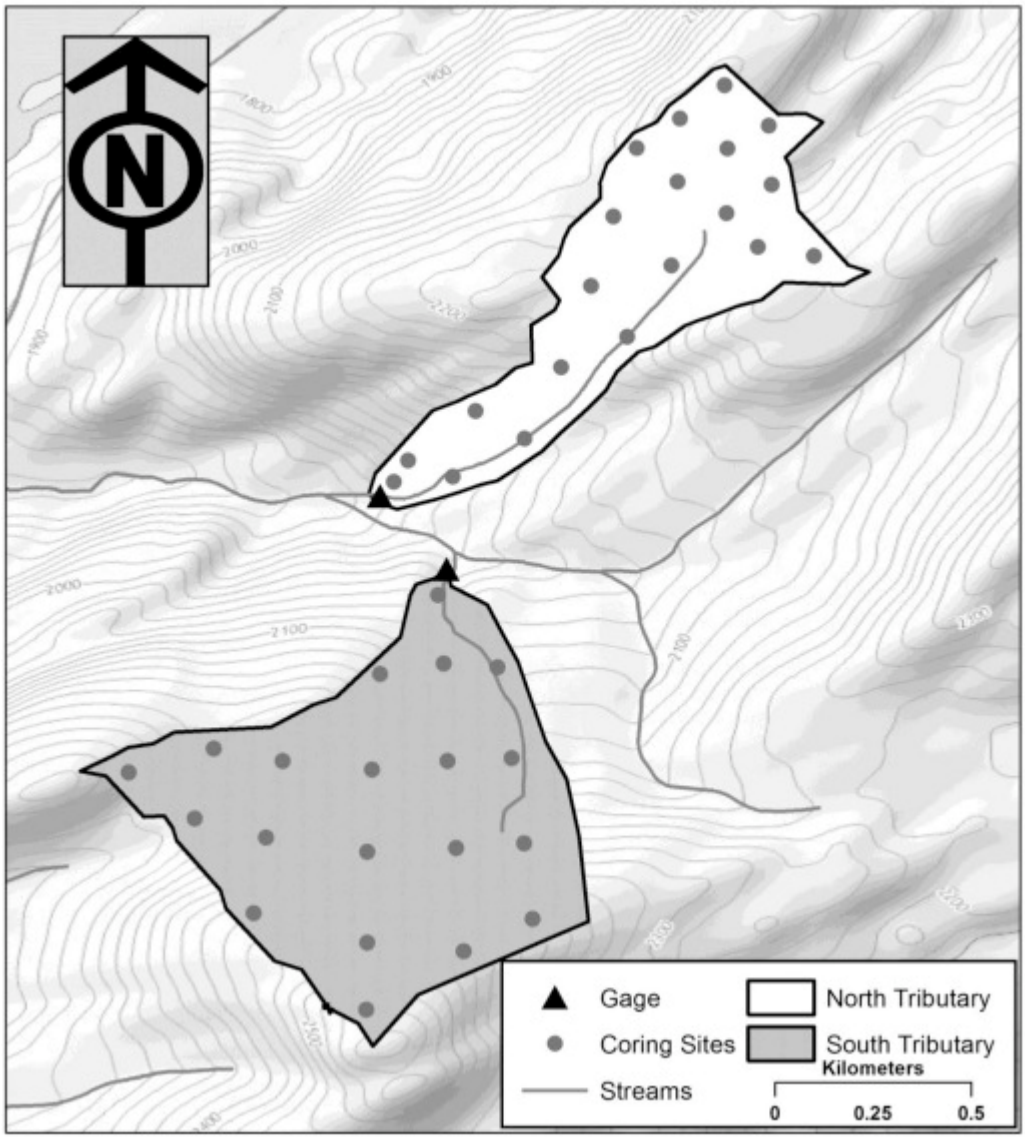

Figure 3. Map of tree coring sites and stream gages in the North and South Tributaries of the Buck Creek watershed.

The mixed forest of the North watershed (27 ha) is dominated by red spruce (*Picea rubens*), American beech (*Fagus grandifolia*), and red maple (*Acer rubrum*)

with *Sphagnum*-dominated wetlands in the headwaters (Lawrence 2002, NYSERDA 2012). There was a reported decrease in basal area in this catchment between 2005 and 2010 due to (1) an unexplained red spruce decline across all size classes (DBH > 5 cm) and (2) beech bark disease, which is eliminating older beech trees in the watershed (NYSERDA 2012). Beech bark disease is a fungal infection that makes beech trees vulnerable to drought and insect infestations (Houston 1994). The North watershed contains well-drained Spodosol soils lying above metasedimentary rock and various forms of gneiss (Lawrence 2002). Fractured bedrock is exposed at the surface in many locations within the catchment, which may result in a loss of water to deep groundwater before exiting the watershed. The stream tends to dry up for a few weeks in late summer with flow restarting in September. Stream NO_3-N yields in the North ($\sim$1.2 kg N ha^{-1} yr^{-1}) are close to the median values of forested watersheds in the northeastern U.S. (Ross et al. 2012). Potential mineralization and nitrification rates are also similar to those of other forests in the region, and nitrification potentially consumes up to $\sim$22% of the mineralized ammonium (Ross et al. 2012).

American beech is the dominant tree species in the South watershed (52 ha). However, beech bark disease has infected virtually all beech trees in this catchment, with higher mortality rates among larger individuals (Ross et al. 2012). Despite the prevalence of beech bark disease, the total basal area of American beech increased from 2000 to 2010 (NYSERDA 2012), because saplings increased in size to be included in the tree monitoring. The South contains well-drained Spodosol soils and generally has more till deposits than the North (Lawrence 2002). Stream NO_3-N yields in the South ($\sim$5.10 kg N ha^{-1} yr^{-1}) are among the highest in the region, but potential mineralization

and nitrification rates in the South are consistent with those in other regional forests (Ross et al. 2012). Potential nitrification rates are higher in the South than North watershed, and nitrification consumes a relatively greater proportion (~33%) of the mineralized ammonium in the South watershed (Ross et al. 2012).

Dendroisotopic records

Twenty mature trees were sampled in each watershed. The trees were randomly spread along transects that were perpendicular to the fall line and spaced approximately 200 m apart (Figure 3). In the field, the largest tree nearest to the pre-selected sampling point was usually chosen to optimize time-series data per sampled tree, but trees that were apparently diseased or in decline (based on visual inspection of the bark) were not sampled; the next nearest healthy, co-dominant or dominant canopy tree was sampled instead. As a result of this sampling strategy, no beech trees were cored. Two cores were taken from opposite sides of each bole at breast height using a 5.15 mm incremental borer and stored in paper straws. The cores were returned to the lab, dried in an oven at 60 °C, sanded, and stored until ring widths were measured using CooRecorder software (Larsson 2009). A detailed visual examination of each increment bore was used to assign ages to each ring. Individual annual increments were cut from one bore per tree using a razor blade and stored in 96-well plates prior to $\delta^{15}N$ and %N analysis.

Approximately 10 mg of wood from every other annual increment for the 1980–2010 period was subsampled and used for $\delta^{15}N$ and %N analysis. In cases where the annual rings were too narrow to yield ~10 mg, multiple rings were aggregated (e.g., 2002–2004) and the midpoint of the aggregated range (e.g., 2003) was used in subsequent statistical analyses. Prepared samples (n = 580) were analyzed for $\delta^{15}N$ using a Carlo

Erba NC2500 elemental analyzer (CE Instruments, Milano, Italy) interfaced with a Thermo Delta V+ isotope ratio mass spectrometer (Bremen, Germany). A Carbosorb trap was used to remove CO_2 and a magnesium perchlorate trap was used to remove water vapor after combustion in the elemental analyzer. The $\delta^{15}N$ data were normalized to the AIR scale using a two-point normalization curve with internal standards calibrated against USGS40 and USGS41(Qi et al. 2003, Brand et al. 2014). The analytical precision among runs (1σ) of an internal wood standard was 0.3‰.

Measurements of $\delta^{15}N$ were normalized by subtracting the mean $\delta^{15}N$ value of the 1980–2010 period from the $\delta^{15}N$ value of each sample from each bore such that each bore had a mean $\delta^{15}N$ value of 0‰ (McLauchlan et al. 2007). Pearson correlation values were calculated to assess trends in normalized $\delta^{15}N$ (n-$\delta^{15}N$) for the period of 1980–2010 for individual trees, species, watersheds, and both watersheds combined to facilitate comparison among sites, species, and scales. The significance of the correlation was evaluated using a block bootstrap and two-tailed significance test procedure in R (Tian et al. 2011). The procedure involved resampling time series of individual trees, species, watersheds, and both watersheds combined 10,000 times in blocks of three consecutive time periods (i.e., 1980–1981, 1982–1983, and 1984–1985) to generate a bootstrap distribution of Pearson correlation values. A two-tailed significance test was then used to assess if the correlation was still significant after accounting for temporal autocorrelation. In addition, trends for the 1980–1995 and 1995–2010 periods were assessed in both watersheds and the combined dataset. Complementing the correlation analysis, a simple arithmetic two-year mean of all 20 individual trees (1980–1981, 1982–1983, etc.) sampled in each watershed was used to scale up from individual tree observations to

further visualize trends in watershed-scale n-$\delta^{15}N$ and $\delta^{15}N$ values. Likewise, all 40 trees were used to calculate a two-year mean, combining the entire dataset.

Stream NO3-N export and acid deposition

The annual wet atmospheric deposition rates and precipitation-weighted mean concentrations of NO_3-N, NH_4-N, IN, and sulfur (S) for the Buck Creek watershed were extracted using geographic information software from wet deposition annual gradient maps published by the National Atmospheric Deposition Program (NADP 2015) for years 1986–2011. These continuous gradient maps are based on observations from the NADP National Trends Network and a high resolution precipitation model developed by the PRISM Climate Group (Latysh and Wetherbee 2012). Trends through time in the wet atmospheric NO_3-N, NH_4-N, and IN deposition rates (1986–1995 and 1995–2011) and wet atmospheric S deposition rate (1986–2011) were assessed using simple linear regression analysis. Time periods for regression analysis were determined *a priori*, based on the observation of decreased SO_x emissions since the early 1970s following implementation of emissions reduction programs through the Clean Air Act of 1970 and implementation of NO_x emission reduction programs following implementation of Phase 1 of the Acid Rain Program in 1995 (Driscoll et al. 2003).

In addition, a multiple regression model was developed to estimate average n-$\delta^{15}N$ through time for the combined watershed dataset (1980–2010) using annual NH_4-N, NO_3-N, and S deposition rates reported at Huntington Wildlife Monitoring Station (NY20), which is about ~50 km from our study area. This dataset was used because it contains annual wet deposition values going back to 1980, whereas the NADP PRISM maps only extend to 1986. Similar deposition values and trends were found between

NADP PRISM maps and measured deposition rates from NY20 for S deposition ($R^2 = 0.88$, $y = 1.28x$) and IN deposition ($R^2 = 0.77$, $y = 1.27x$) for the 1986–2011 period (data not shown). The annual deposition data were aggregated by calculating the 2-year mean deposition rate (1980–1981, 1982–1983), thus allowing direct comparison with n-$\delta^{15}N$ data. Analysis for multi-collinearity and model building was carried out in R using the **ltm**, **leaps**, and **car** packages (Fox 2002, Rizopoulos 2006, Lumley and Miller 2009, R 2014). Model selection was based on variance inflation factor (VIF), the Bayes' Information Criterion (BIC), and adjusted R^2.

Flow and stream NO_3-N concentration data for the North and South Tributaries were provided by the U.S. Geological Survey (USGS) and Adirondack Lake Survey Corporation (Lawrence 2002, Lawrence et al. 2008) for the 2000–2012 period. Periodic (every two weeks, year round) and episodic (high flows between April and November) stream sampling has been carried out since 2000. Based on a time series of daily estimated concentration and daily mean discharge, a statistical load estimator (LOADEST) developed by the USGS (Runkel et al. 2004) was calibrated with inputs of time, daily flow and NO_3 concentration to estimate daily NO_3-N yields (kg ha^{-1} d^{-1}) for the same period. The same seven explanatory variables based on daily streamflow and time were used for each watershed. Observed daily concentrations were typically composed of an individual grab sample, but for days with multiple samples, a mean concentration was used to calibrate LOADEST to model daily NO_3-N concentrations on days when no sampling occurred. Some summer samples collected in the North (n = 21) were not included in the calibration because no flow was measured in the stream. In total, 394 and 455 daily concentrations for the North and South, respectively, were used to

parameterize the LOADEST model. Estimates of the daily yields were summed to produce monthly and annual yields (kg N ha^{-1} mo^{-1} and kg N ha^{-1} yr^{-1}) and flow-weighted mean concentrations (mg N L^{-1}). For the dates when NO_3-N measurements were made, the LOADEST model explained 89% and 86% of the variation of natural-log daily NO_3-N yields in the South and North, respectively. Slopes of the graphs of observed versus predicted daily loads were 1.04 for the South and 1.08 for the North, which indicates only a small positive bias in the LOADEST estimates. Trends in annual NO_3-N yield, retention of wet IN deposition (Yield/Wet Deposition), and flow-weighted mean concentrations were assessed using simple linear regression analysis.

Results

We observed declining n-δ^{15}N trends between 1980 and 2010 for 21 of the 40 sampled trees (Figure 4; Figure 5; Table 1; Table 2). Three of six sampled species displayed declining n-δ^{15}N values over time in the two watersheds (Figure 6 and Table 3). Both maple species (red maple, n = 8; sugar maple, *A. saccharum*, n = 12) and red spruce (n = 12) declined over the period of record. Yellow birch (*Betula alleghaniensis,* n = 6), balsam fir (*Abies balsamea*, n = 1) and eastern hemlock (*Tsuga canadensis*, n = 1) showed no trends over time. No species showed positive trends in n-δ^{15}N, and only two individual sugar maple trees in the South showed significant positive trends. Despite variation in n-δ^{15}N trends observed at the individual tree level, watershed-level n-δ^{15}N was similar in the North and South watersheds for the 1980–2010 period, respectively (Figure 6; Table 4). At the watershed level, n-δ^{15}N trends were both declining for the 1980–1995 period in the North and South (Table 4; Figure 4; Figure 5). Values of n-δ^{15}N continued a decline in the 1995–2010 period in both watersheds, but the trends were more apparent in the South ($p = 0.001$) than the North ($p = 0.0895$). Despite

similar trends, average non-normalized $\delta^{15}N$ values of the South were consistently higher than the North (Figure 5).

Table 1. Results of $\delta^{15}N$ bootstrap analyses for individual trees in the North, including Pearson correlation coefficient (r) and p values

By individual tree

Watershed	Species	Tree number	r	p-value
North	red spruce	N1	0.60	0.065
North	red maple	N2	0.04	0.46
North	red maple	N3	-0.33	0.13
North	red spruce	N4	**-0.82**	**0.0063**
North	red maple	N5	**-0.60**	**0.043**
North	sugar maple	N6	**-0.53**	**0.046**
North	red spruce	N7	-0.24	0.23
North	E. hemlock	N8	0.37	0.11
North	red spruce	N9	-0.45	0.087
North	yellow birch	N10	0.25	0.2
North	red maple	N11	-0.06	0.38
North	red maple	N12	**-0.68**	**0.031**
North	red spruce	N13	-0.42	0.083
North	red maple	N14	-0.03	0.45
North	red spruce	N15	**-0.69**	**0.034**
North	balsam fir	N16	-0.65	0.1
North	red spruce	N17	**-0.56**	**0.024**
North	red maple	N18	**-0.74**	**0.0046**
North	red spruce	N19	**-0.93**	**0.0011**
North	red spruce	N20	0.04	0.57

Table 2. Results of $\delta^{15}N$ bootstrap analyses for individual trees in the North, including Pearson correlation coefficient (r) and p values

By individual tree

Watershed	Species	Tree number	r	p-value
South	sugar maple	S1	**-0.68**	**0.006**
South	red spruce	S2	-0.57	0.06
South	sugar maple	S3	-0.02	0.49
South	sugar maple	S4	-0.55	0.055
South	yellow birch	S5	0.03	0.49
South	sugar maple	S6	**-0.55**	**0.02**
South	yellow birch	S7	-0.03	0.46
South	sugar maple	S8	**-0.64**	**0.028**
South	sugar maple	S9	**-0.85**	**0.0058**
South	sugar maple	S10	**-0.92**	**0.0043**
South	yellow birch	S11	**-0.63**	**0.029**
South	sugar maple	S12	-0.07	0.38
South	sugar maple	S13	**0.58**	**0.036**
South	red spruce	S14	0.15	0.35
South	sugar maple	S15	**-0.91**	**< 0.001**
South	sugar maple	S16	**-0.62**	**0.013**
South	red spruce	S17	**-0.94**	**< 0.001**
South	sugar maple	S18	**0.47**	**0.047**
South	red maple	S19	**-0.68**	**0.0049**
South	yellow birch	S20	0.39	0.1485

Table 3. Results of $\delta^{15}N$ bootstrap analyses by tree species, including Pearson correlation coefficient (r) and p values

By species

Species	r	p-value
balsam fir (*n=1*)	-0.65	0.1022
red maple (*n=8*)	**-0.43**	**0.0019**
sugar maple (*n=12*)	**-0.45**	**< 0.001**
yellow birch (*n=6*)	-0.06	0.3524
red spruce (*n=12*)	**-0.43**	**0.0016**
Eastern hemlock (*n=1*)	0.37	0.1212

S deposition declined between 1986 and 2011, whereas no trend in precipitation amount was detected during this period (Figure 7). Deposition of IN declined during 1995–2011 despite substantial variability in precipitation amount, but no IN deposition trend was observed during 1985–1995. Decreases in IN deposition were driven by

declining NO_3-N deposition (data not shown). Deposition of NH_4-N was constant throughout the period of record, and its proportion of total IN deposition increased from ~30 to ~50% as NO_3-N deposition declined (data not shown).

Table 4. Results of $\delta^{15}N$ bootstrap analyses for all trees in the study and by watershed, including Pearson correlation coefficient (r) and p values.

Total dataset

Time Period	r	p-value
1980-2010	**-0.36**	**< 0.001**
1980-1995	**-0.26**	**0.002**
1995-2010	**-0.21**	**0.0095**

By watershed

Watershed (Time Period)	r	p-value
North (1980-2010)	**-0.35**	**0.0013**
North (1980-1995)	**-0.26**	**< 0.001**
North (1995-2010	-0.14	0.0895
South (1980-2010)	**-0.37**	**< 0.001**
South (1980-1995)	**-0.26**	**0.0084**
South (1995-2010)	**-0.30**	**0.001**

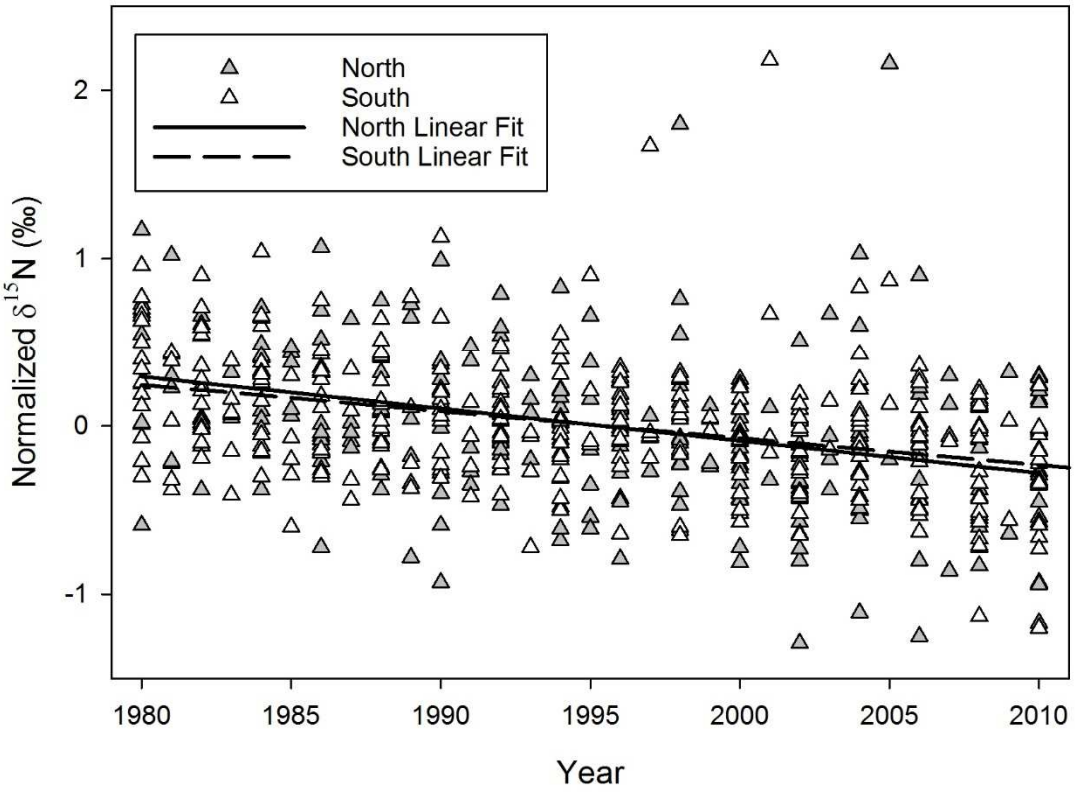

Figure 4. Time series of watershed-level tree-ring $\delta^{15}N$ values from the North ($r = -0.35$, $p < 0.0013$, $n = 20$) and South ($r=-0.37$, $p<0.0001$, $n = 20$) watersheds at Buck Creek.

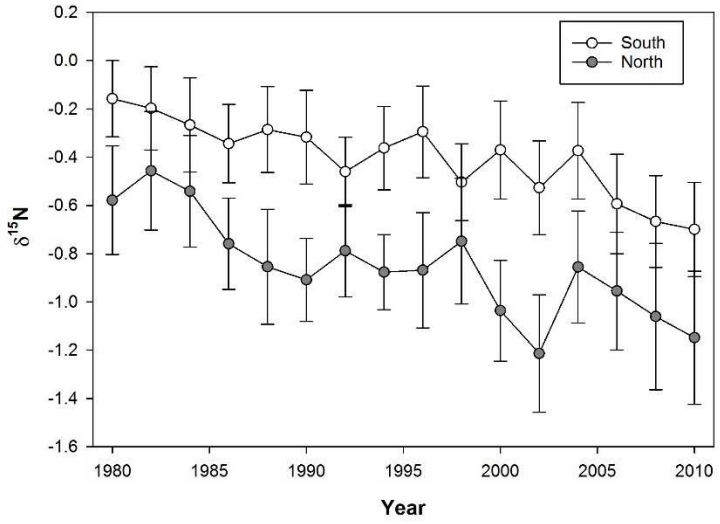

Figure 5. Time series of two-year mean $\delta^{15}N$ values (± 1 S.E.) in the North (grey circles) and South (white circles).

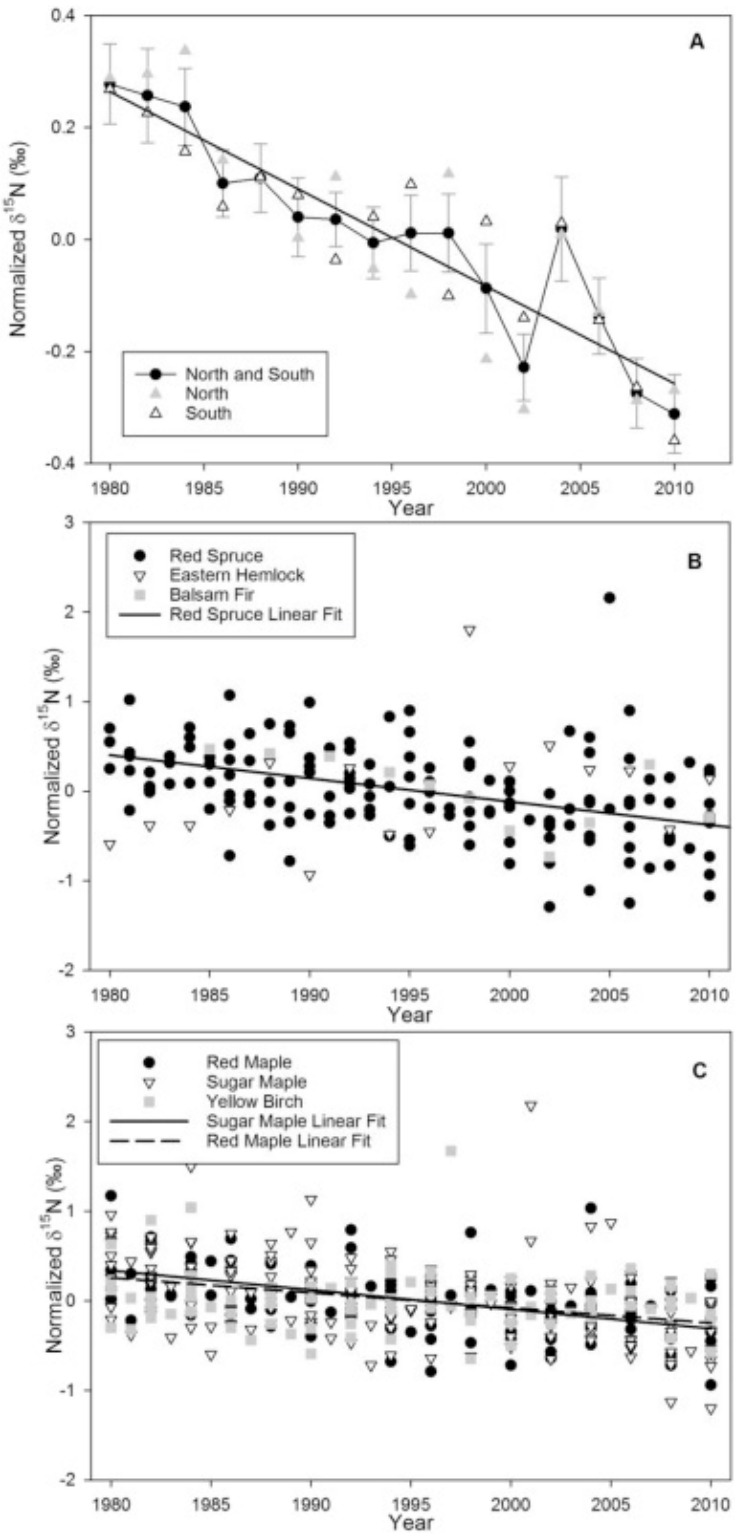

Figure 6. A) Two-year mean n-δ^{15}N values (±1 S.E.) in the North (grey triangles), South (white triangles), and both watersheds combined (black circles; along with the linear line of best fit). Species-specific time series of n-δ^{15}N in coniferous (B) and deciduous trees (C) along with linear lines of best fit for significant negative correlations.

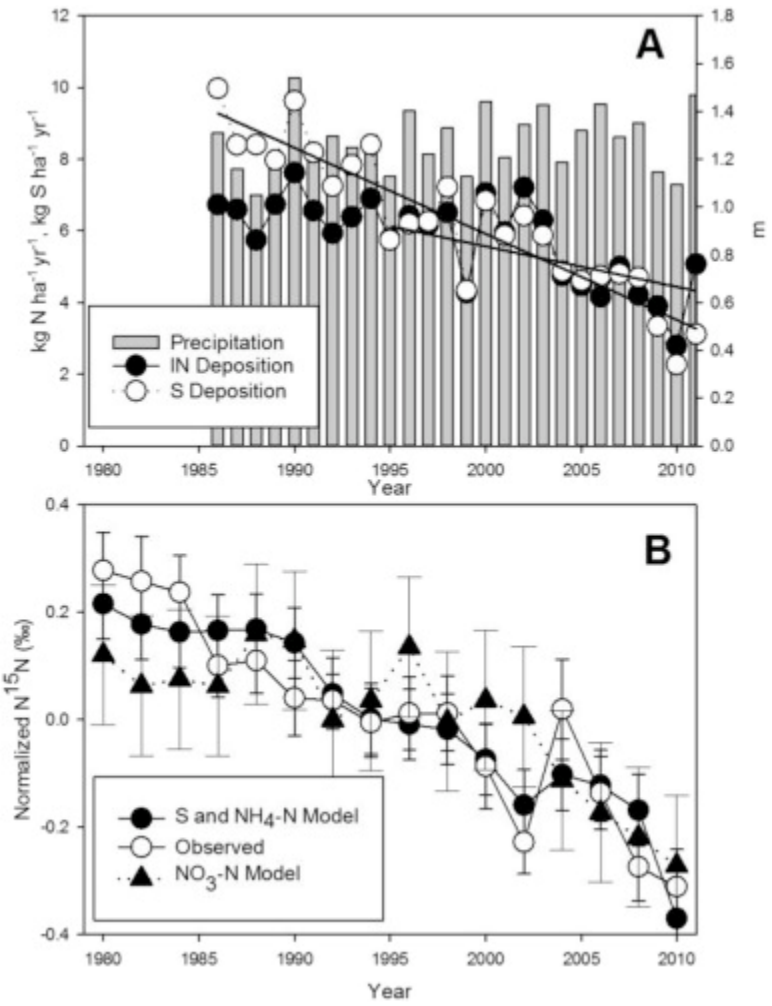

Figure 7. A) Precipitation and wet deposition of inorganic nitrogen (IN) and sulfur (S). Wet S deposition decreased during 1986–2011 ($R^2 = 0.83$, $p < 0.0001$, $n = 25$) and IN deposition decreased during 1995–2011 ($R^2 = 0.49$, $p < 0.01$, $n = 16$). No trend in precipitation was observed in either period. B) Time series of predicted and observed combined watershed n-$\delta^{15}N$ values; NH_4-N and S deposition multiple regression model and simple NO_3-N model ($R^2 = 0.83$, $p < 0.01$, $n = 30$ and $R^2 = 0.51$, $p < 0.01$, $n = 30$, respectively).

Both SO_4-S and NO_3-N deposition rates from the NY20 NADP station displayed a positive relationship with the combined n-$\delta^{15}N$ dataset (SO_4-S: $R^2 = 0.78$, $p < 0.01$; NO_3-N: $R^2 = 0.54$, $p < 0.01$), whereas NH_4-N had little influence ($R^2 = 0.07$, $p = 0.76$). Both SO_4-S and NO_3-N deposition were highly correlated and failed the VIF test (calculated value > 5), so these variables could not be included together in the same multiple-regression model. NH_4-N deposition showed no issues of multi-collinearity with either SO_4-S and NO_3-N deposition variable. After model building, a combined NH_4-N

and SO_4-S deposition model generated the lowest BIC score and highest adjusted R^2 of the seven models, with no issues of multi-collinearity among parameters (BIC = −22.38, R^2 = 0.83; Figure 7; Table 5). This model demonstrated that lower annual n-$\delta^{15}N$ values were associated with higher NH_4-N deposition rates (β_1 = −0.22, p = 0.03) and lower SO_4-S deposition rates (β_2 = 0.11, p < 0.01). A NO_3-N and NH_4-N deposition model was also applied (R^2 = 0.48, BIC = −4.4), but NH_4-N deposition was not a significant parameter in this model (p = 0.82, data not shown); furthermore, this model explained less variance in the combined Buck Creek watershed n-$\delta^{15}N$ record than did a simplified NO_3-N deposition model (R^2 = 0.51, p < 0.01; Figure 7). Overall, annual n-$\delta^{15}N$ values in the North and South were declining prior to declines in atmospheric N deposition.

Table 5. Summary of evaluation criteria (R^2 and BIC) and results from the variance inflation factors VIF test for all combinations of model parameters (S, NO_3-N, NH_4-N) in the model

Model	S, NH_4*	S, NO_3, NH_4	S	S, NO_3	NO_3*	NO_3, NH_4	NH_4
Adjusted R^2	0.83	0.82	0.77	0.76	0.51	0.48	-0.064
BIC	-22	-20	-19	-17	-7.1	-4.4	5.4
VIF Test	Passed	Failed	NA	Failed	NA	Passed	NA

During the 2000s, the North typically yielded 30% of IN deposition on an annual basis, whereas the South retained little IN deposition, and even yielded more NO_3-N than wet-deposited IN in the latter half of the record (Figure 8). Stream-water mean annual flow-weighted NO_3-N concentrations declined in the North (p = 0.02; Figure 8), whereas a weaker trend in concentration was observed in the South (p = 0.09; Figure 8). Stream NO_3-N yields and runoff showed no trends in the North or South (Figure 8). Mean monthly flow-weighted concentrations were lowest during the growing season and highest in the late winter and early spring (Figure 9). Generally, the mean monthly flow-

weighted concentrations for the dormant season in the North declined until ~2005–2006, after which they stabilized during the latter half of the record (Figure 9). Monthly concentrations in the South displayed an initial decline (2000–2004) but peak dormant season concentrations have dramatically increased from ~1.0 mg NO_3-N L^{-1} in the mid-2000s to 1.4 mg NO_3-N L^{-1} after 2010 (Figure 9).

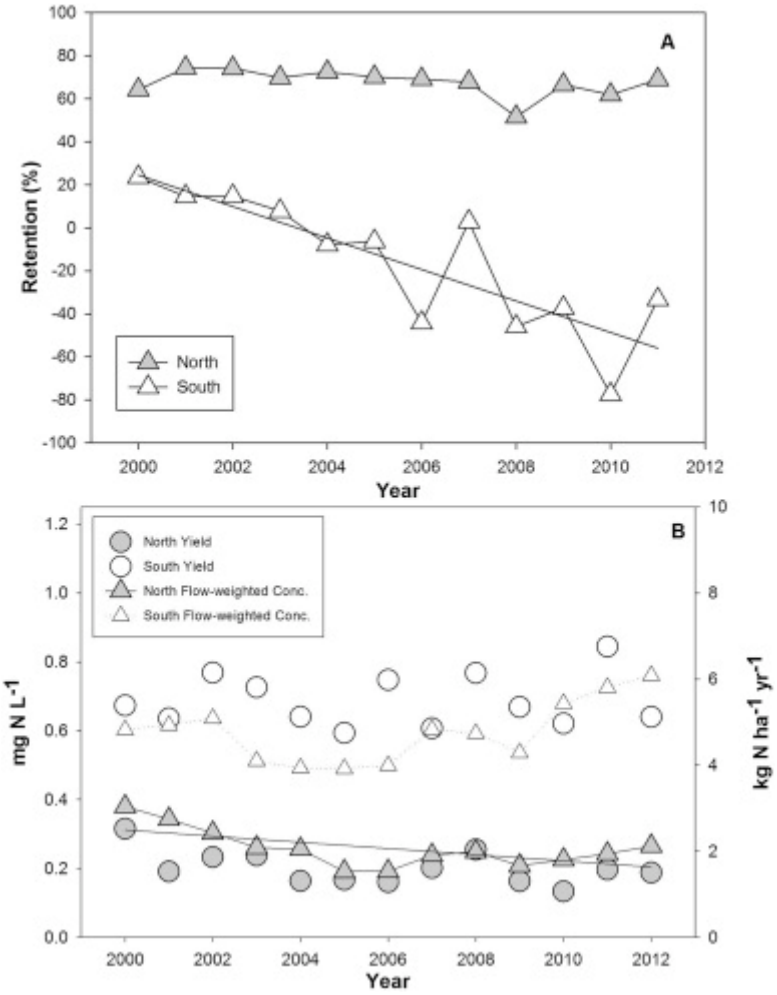

Figure 8. A) Retention of wet IN deposition from 2000 to 2011. Retention has declined in the South (R^2 = 0.68, $p < 0.0001$), but has remained constant in the North. B) Annual stream runoff, NO_3-N yield, and mean flow-weighted concentration of NO_3-N for the North and South watersheds. Mean annual flow-weighted concentration of NO_3-N in the North has declined since 2000 (R^2 = 0.33, p = 0.02), but there was no trend in the South.

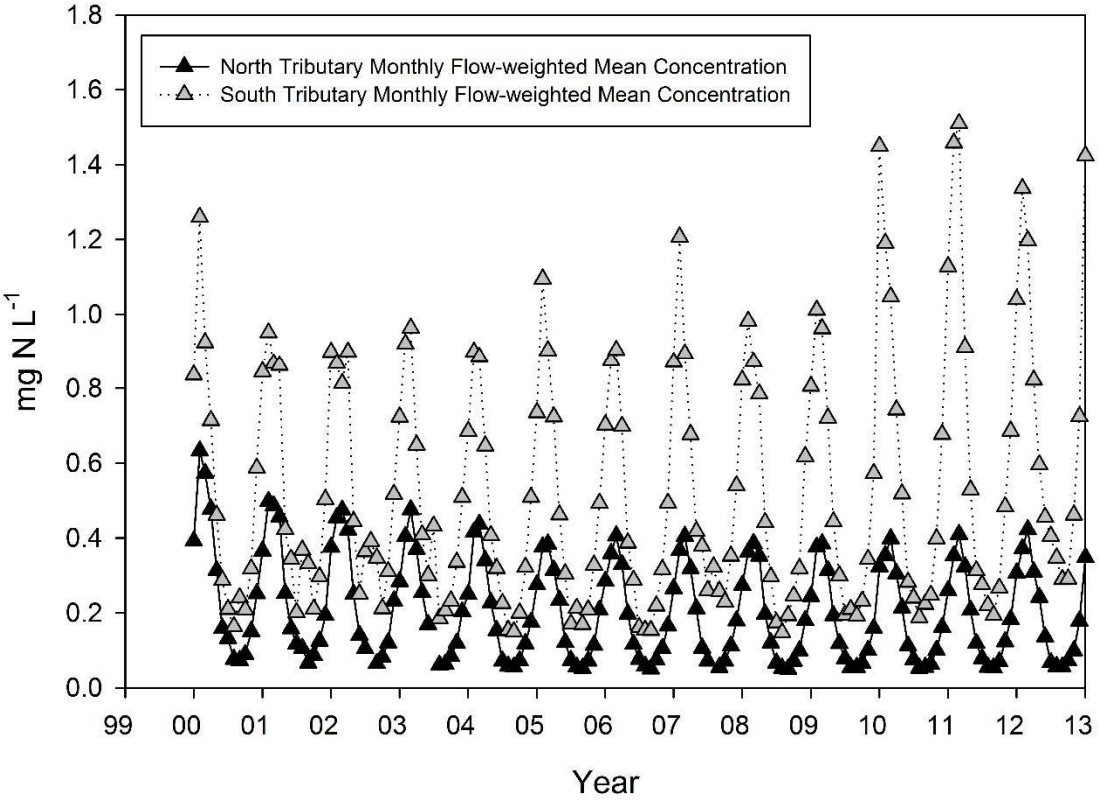

Figure 9. LOADEST estimated mean monthly flow-weighted NO_3-N concentrations from the North and South Tributary of Buck Creek.

Discussion

Changes in terrestrial N cycling prior to declines in atmospheric IN deposition

Despite differences in tree species composition, soil composition, N retention, terrestrial N availability relative to plant demand, and hydrology between the North and South (Burns et al. 2009, NYSERDA 2012), both watersheds demonstrated near equivalent declines in tree ring n-δ^{15}N throughout the 30-year study period. The n-δ^{15}N values began to decline prior to decreases in atmospheric N deposition, which is inconsistent with our hypothesis that terrestrial N availability would only decline following declines in atmospheric N deposition. Thus, factors other than declining atmospheric N deposition must have a greater relative influence on changes in terrestrial N availability (as inferred from tree-ring δ^{15}N values) at Buck Creek.

Decreased mineral acid (i.e., H^+) deposition, rather than N deposition, is one potential factor than may influence ecosystem N cycling in our study watersheds. For example, the clean-roof experiments of Corre et al. (2003) and Corre and Lamersdorf (2004) decreased the amount of both deposited N and acidity onto the catchments, so recovery from acidification may have at least partly driven the observed decline in N availability in the experimental catchment. Recovery of forests, soils, lakes, and streams from chronic acid deposition has been documented throughout the Adirondacks over the past three decades (Stoddard et al. 1999, Driscoll et al. 2003, Lawrence et al. 2013, Driscoll et al. 2016). At our study sites, decreases in soil aluminum (Al) mobilization as a result of decreased acidic deposition were indicated by pronounced decreases in exchangeable Al concentrations between 1997 and 2009–2010 in the North and between 1998 and 2014 in the South (Lawrence et al. 2015a). Thus, the forests in the North and South may be experiencing reduced Al toxicity and enhanced nutrient cation availability (Ca, Mg, K) as the systems continue to recover from terrestrial acidification (Driscoll et al. 2001, Oulehle et al. 2011, Battles et al. 2013, Sullivan et al. 2013). Alleviation of these ecosystem stressors would potentially 1) enhance carbon accumulation in aboveground biomass and soil organic matter, thus increasing N immobilization and inducing N limitation (Monteith et al. 2007) and/or 2) increase decomposition rates in soils, in turn causing a shift in available N (McLauchlan and Craine 2012, Sawicka et al. 2016).

Factors other than decreases in acid deposition may also contribute to explaining the declines in tree-ring $\delta^{15}N$ values in the North and South. Multiple studies have reported that the isotopic signature of atmospheric N deposition can be recorded in tree rings (Saurer et al. 2004, Savard et al. 2009, Doucet et al. 2012, Jung et al. 2013). Results

from the multiple regression analysis indicated that atmospheric NH_4-N deposition was a significant and influential parameter when paired with SO_4-S deposition. δ^{15}N-NH_4 values are typically quite negative, ranging from about −1 to −20‰ (Garten Jr 1992, Jia and Chen 2010, Xiao et al. 2012), so it is possible that NH_4-N deposition may be depositing more negative δ^{15}N-NH_4 into soil IN pools, thus influencing our observed tree-ring δ^{15}N trends. Yet, deposition typically comprises only a small proportion of tree N uptake, so the potential influence of δ^{15}N-NH_4 on tree-ring δ^{15}N values requires further study (Gerhart and McLauchlan 2014). Increased atmospheric CO_2 concentrations during the period of our study may also influence δ^{15}N trends by contributing to progressive N limitation through enhanced plant uptake and increased C:N ratios in plants and soils (McLauchlan et al. 2010, Norby et al. 2010). However, neither watershed has progressively increased its N retention, suggesting that progressive N limitation may not be occurring in these watersheds. A recent study reported a decrease in nitrogen pools and mineralization rates at Hubbard Brook (Durán et al. 2016), and the authors posited that declining terrestrial N pools may be driven by warming temperatures and reduced snow accumulation. Reduced snowpack and warming temperatures have also been observed in the Adirondacks, but other studies have indicated that climate change may actually increase or have a minimal impact on terrestrial N availability and stream NO_3-N loss (Sebestyen et al. 2009, Brookshire et al. 2011) thus making the influence of climate change uncertain.

Forest successional processes are another plausible explanation for the declining n-δ^{15}N trends in the North and South. As forest succession proceeds, the N immobilization potential of a forest has been postulated to increase due to greater plant

uptake, organic matter accumulation, and coarse woody debris production thereby contributing to declining N availability (McLauchlan et al. 2007). Disturbances ranging from low intensity surface fires to canopy gap formations, however, have been shown to disrupt any trends in N availability that may be brought about by successional processes (Bukata and Kyser 2007, Beghin et al. 2011, Howard and McLauchlan 2015). In the North, beech bark disease and spruce decline have caused a decline in tree basal area during the study period, whereas beech bark disease has killed a large proportion of mature beech trees in the South (NYSERDA 2012). Disturbance has clearly happened in the North and South (as indicated by NYSERDA vegetative surveys from 2000 to 2010), yet n-δ^{15}N values declined between 1980 and 2010 at the watershed level. The ongoing disturbance in both watersheds thus reduces the likelihood that n-δ^{15}N trends observed in the North and South are being primarily driven by successional processes.

Individual tree and species-specific δ15N trends

Downscaling observations to the level of individual trees revealed substantial variability in δ^{15}N trends. Only half of the trees exhibited long-term declines in δ^{15}N values in our study, and two trees actually demonstrated increased tree-ring δ^{15}N through time. Furthermore, some records displayed sudden and discordant positive peaks in δ^{15}N, which suggests relatively rapid and transient increases in N availability as the result of local-scale processes. Such processes may override the drivers of the declining δ^{15}N trends at the watershed scale. For example, the release of sub-canopy trees following canopy decline and/or mortality of dominant trees, due to disease or weather events, could increase access to nutrients due to 1) greater root production and coverage in the soil matrix and 2) possibly enhanced nutrient mineralization (White and Pickett 1985). If local disturbances mask long-term trends in tree-ring δ^{15}N, then our results reinforce the

importance of designing field sampling efforts to include high sampling density, multiple species, and extensive spatial coverage to assess changes in terrestrial N cycling across a watershed.

Our results also highlight the importance of understanding how species-specific characteristics influence changes in forest N cycling. The growth of some species in our watersheds, including yellow birch and American beech, is thought to be insensitive to N deposition (Thomas et al. 2010, Halman et al. 2014). The results for the six yellow birch trees sampled in our study support this understanding, because they showed relatively constant $\delta^{15}N$ values over time despite significant decreases in N deposition. This lack of trend suggests that the amount of N available to yellow birch has not significantly changed through time. In contrast, other tree species, including the sugar maples in our study, may strongly respond to the reduced loss of base cations from soils and foliage as acid deposition declines (Lovett and Mitchell 2004, Huggett et al. 2007). For example, in the northeastern United States, trees in sugar maple-dominated plots treated with lime to remediate acidified soils showed increased plant growth, greater recruitment, and reduced mortality (Groffman et al. 2006, Halman et al. 2014), which ultimately led to decreased ammonium available for nitrification (Simmons et al. 1996, Groffman et al. 2006). Soils at Buck Creek show signs of recovery from acidification (Lawrence et al. 2015a), and similar declines in N availability may be occurring, at least for sugar maples, in the North and South.

Differing trends in watershed N retention

Declines in stream flow-weighted NO_3-N concentrations in the North were consistent with long-term declines in terrestrial N availability as inferred from declining

watershed-scale tree-ring $\delta^{15}N$ values. This result was expected since a decline in terrestrial N availability would be associated with "tighter" N cycling thus minimizing the loss of N to streams (Aber et al. 1998). Relative to the South, the North was apparently more retentive of wet atmospheric N deposition for the period of record, which is consistent with the North potentially having lower terrestrial N availability as indicated by dendroisotopic records (*Figure 5*). The North is consistent with other mid-Atlantic forests that seem to retain a fixed proportion of wet deposited IN (~70%) over time (Eshleman et al. 2013), despite the fact that wet atmospheric IN deposition ranged from 3 to 7 kg N ha yr^{-1}. Although the hydrobiogeochemical mechanisms that can explain the relatively constant retention over time are uncertain (Grigal 2012, Eshleman et al. 2013), it is clear from the mass balance that less total N is being deposited and retained in the North over time on an absolute basis. Somewhat inconsistent with stream NO_3-N trends in the North, however, was the negative but still not statistically significant $\delta^{15}N$ trend for the 1995–2010 period. Ongoing spruce decline and beech bark disease has caused a decrease in stand-level basal area in the North, and this disturbance may be masking the influence of N deposition on the short-term $\delta^{15}N$ trend by providing new sources of terrestrial N or depressing plant uptake of N in the North.

Unlike the consistent N retention over time in the North, the South displayed decreasing retentiveness during a period of declining N deposition and N availability, as inferred from declining watershed-scale tree-ring $\delta^{15}N$ values. These results indicate that dendroisotopic and stream NO_3-N records may not always provide similar information about terrestrial N availability (McLauchlan and Craine 2012, Gerhart and McLauchlan 2014, Tomlinson et al. 2016). The decline in N retention indicates that a source of N from

within the catchment is being mineralized but not being retained by plants and soils in the South. At Buck Creek, a possible source includes the decomposition of more recalcitrant material in soils recovering from acidification (Lawrence et al. 2011, Lawrence et al. 2015a, Sawicka et al. 2016). The decline of beech trees could also explain decreased N retention as a result of diminishing rates of plant uptake and death of older trees. However, the total basal area of beech in the South actually increased by 16% between 2000 and 2010 (NYSERDA 2012), which argues against this explanation. Many other forested watersheds have also shown reductions in retentiveness of N during periods of decreased N and acid deposition (Argerich et al. 2013, Kopáček et al. 2016), yet the relative importance of the various factors contributing to declining retention remain unclear. Besides changes in terrestrial biogeochemical cycling, higher dormant season flows and increased flood peak frequency may be enhancing NO_3-N transport (Bernal et al. 2012). The inconsistency between declining tree-ring $\delta^{15}N$ values and retention trends in the South could also originate from sampling bias during field collections of tree cores for $\delta^{15}N$ analysis. The sampling protocol required the sampling of healthy, large trees, so no mature American beech trees were sampled in this study. The extensive coverage of diseased beech in the South raises the prospect that the other randomly sampled species may not completely represent changes in tree-ring $\delta^{15}N$ values across the watershed. In previous studies, beech showed no particular sensitivity in growth or survival to atmospheric N deposition or calcium amendments (Thomas et al. 2010, Halman et al. 2014); so, similar to yellow birch, the changes in acid deposition over time may not have greatly influenced tree-ring $\delta^{15}N$ trends in beech. Thus, the apparent contradiction in the

South between the stream water NO_3-N and watershed-level dendroisotopic data should be interpreted with caution.

Conclusions

We observed that changes in N availability, as inferred from declining watershed-scale tree-ring $\delta^{15}N$ values, were occurring prior to decreases in atmospheric N deposition (pre-1995) in the North and South Tributaries of Buck Creek. Declines in N deposition cannot fully explain these trends and thus other factors, such as declines in acid deposition, may have greater influence on terrestrial N cycling in forests. Our data also indicate that trends in wood $\delta^{15}N$ values vary among tree species and individuals, and these differences may be due to species-specific sensitivity to acid deposition and local disturbance. Finally, decreased acid deposition and declining $\delta^{15}N$ trends in tree rings do not necessarily translate into decreased NO_3-N export in streams, as evidenced by the divergent trends in the North and South. The variable changes in ecosystem N cycling in the North and South highlight the need to further integrate terrestrial and stream datasets to comprehensively assess forest responses to decreased atmospheric pollution and other ongoing environmental changes.

Acknowledgements

I thank Robin Paulman, Michael Satchwell, Andrew Tichensky, and Jasmin Zvornicanin for assistance in the field and with stable isotope analyses. I also thank my fellow coauthors: Dr. Sara E. Scanga, Dr. Gregory B. Lawrence, Dr. David M. Nelson, Dr. Keith N. Eshleman, Gabriel A. Zabala, Alexandria A. Alinea, and Charles D. Schirmer. This research was made possible through the support of an Environmental Protection Agency Science to Achieve Results Graduate Fellowship (#FP-91749901-0, to RDS), Utica College grants for students and faculty (to S. Scanga, G. Zabala, A. Alinea),

and a teaching assistantship through the Marine-Estuarine-Environmental Sciences (MEES) Graduate Program (to RDS). This research was also supported in part by an appointment to the Research Participation Program for the U.S. Environmental Protection Agency, Office of Research and Development, administered by the Oak Ridge Institute for Science and Education through an inter-agency agreement between the U.S. Department of Energy and EPA. The views presented here are those of the authors and do not represent official views or policy of the U.S. Environmental Protection Agency (EPA) or any other U.S. federal agency, except the U.S. Geological Survey. Any use of trade, firm, or product names is for descriptive purposes only and does not imply endorsement by the U.S. Government.

Chapter 3: Drivers of wood $\delta^{15}N$ decline, temporal variability, and correlation with stream nitrate in two temperate deciduous forests over a twenty-five-year period

Abstract

Productivity and export of nutrients from forested catchments may be constrained or enhanced by the influence of recent changes in climate, atmospheric chemistry, and disturbance on terrestrial nitrogen availability. A limitation to understanding drivers of long-term trends in terrestrial N availability and its subsequent influence on stream nitrate export is a general lack of long-term data on terrestrial and aquatic N cycling at comparable spatial scales. Here we analyze relationships between stream nitrate concentrations and wood $\delta^{15}N$ records (n = 96 trees) across five neighboring headwater catchments in the Blue Ridge physiographic province and within a single catchment in the Appalachian Plateau physiographic province. Climatic, acidic deposition, and forest disturbance datasets were developed to elucidate the influence of these factors on terrestrial nitrogen availability through time. We hypothesized that spatial and temporal variation of terrestrial N availability, for which tree-ring $\delta^{15}N$ records serve as a proxy, affects the variation of stream nitrate concentration across space and time. Across space at the Blue Ridge study sites, stream nitrate concentration increased linearly with increasing catchment mean wood $\delta^{15}N$. Over time, stream nitrate concentrations decreased with decreasing wood $\delta^{15}N$ in five of the six catchments. Stream nitrate concentrations were also more responsive to changes in terrestrial nitrogen availability through time at more N-rich sites, likely due to the fact that the more N-limited sites had little to no nitrate present in the streams. Wood $\delta^{15}N$ showed a significant negative relationship with disturbance and acidic deposition. Disturbance likely exacerbated N limitation by inducing nitrate leaching and enhancing vegetative uptake. As observed

elsewhere, lower rates of acidic deposition and subsequent deacidification of soils may be increasing terrestrial N availability. Despite the ephemeral modifications of terrestrial N availability by these two drivers and climate, long-term declines in terrestrial nitrogen availability were robust and have likely driven much of the declines in stream nitrate concentration throughout the central Appalachians.

Introduction

Recent changes in climate, atmospheric chemistry, and disturbance have the potential to influence the productivity and export of nutrients from forested catchments by either constraining or enhancing nitrogen (N) availability (Elmore et al. 2016, McLauchlan et al. 2017, Peñuelas et al. 2017). For example, N availability could be enhanced from warming soils increasing mineralization rates, atmospheric N deposition adding N to soils, or changes in microbial communities increasing mineralization rates as acidified soils recover from decades of elevated acidic deposition (Aber et al. 1989, Rustad et al. 2001, Sinsabaugh et al. 2004, Sinsabaugh 2010, Brookshire et al. 2011, Oulehle et al. 2011, Lawrence et al. 2015b, Oulehle et al. 2017). On the other hand, greater N demand resulting from factors such as longer growing seasons or elevated atmospheric CO_2 concentrations could reduce N availability (Ollinger et al. 2002, Norby et al. 2016). The latter is supported by evidence that N availability has declined in temperate forests during the past three decades inferred from foliar and wood chemistry and net mineralization and nitrification rates in North American forests (McLauchlan et al. 2010, Durán et al. 2016, Elmore et al. 2016, McLauchlan et al. 2017, Groffman et al. 2018). Stream nitrate export has also declined since the mid-1990s throughout many forests of the eastern United States (Eshleman et al. 2013), which could result from declines in terrestrial nitrogen availability. However, few studies have co-located records

of terrestrial N availability and stream water chemistry with which to assess this hypothesis.

A limitation to understanding drivers of long-term trends in terrestrial N availability and its subsequent influence on stream nitrate export is a general lack of long-term data on terrestrial and aquatic N cycling at comparable spatial scales. For example, stream nutrient data are often only obtained for limited periods or measured only periodically (Argerich et al. 2013, Durán et al. 2016), and such snapshots may not be adequate for comparison with longer-term indicators of terrestrial N cycling, such as deduced from tree-ring δ^{15}N records (Gerhart and McLauchlan 2014). While streamwater nutrient data are generally considered integrative of an entire watershed (Likens 2017), in-stream processing could lead to an incongruity between stream and terrestrial N datasets (Scanlon et al. 2010). Finally, long-term records of terrestrial N availability preserved in tree-ring δ^{15}N data are typically normalized to the mean δ^{15}N value of tree-ring time series to focus on temporal patterns (McLauchlan et al. 2007), but doing so masks potential information about spatial variation in terrestrial N availability contained in non-normalized δ^{15}N values. Catchments where long-term records of stream nutrient export exist and multiple tree-ring δ^{15}N records of multiple species can be obtained represent promising locations for assessing the relationship between, and drivers of, stream nitrate export and terrestrial N availability. For example, Sabo et al. (2016) observed higher mean (non-normalized) δ^{15}N tree-ring values across a catchment in the Adirondack Mountains with higher mean annual flow-weighted nitrate concentrations relative to an adjacent catchment with lower nitrate concentrations (n = 20 tree-ring δ^{15}N records per catchment), as well as declines in δ^{15}N values of tree rings and stream nitrate

concentrations for one of two subcatchments. However, a limitation of that study was that the water chemistry data spanned a period of only 11 years and that the most important tree species in one of the study catchments (*Fagus grandifolia*; American beech) could not be cored because it suffered from extensive disease and mortality (Sabo et al. 2016b). Thus, uncertainty remains about whether tree-ring $\delta^{15}N$ records are representative of the relationship between terrestrial N availability and stream nitrogen export (Sabo et al. 2016b).

To assess the relationship between terrestrial N availability and stream nitrogen export and to identify candidate drivers of the temporal variability of wood $\delta^{15}N$, we assembled dendroisotopic records for 96 trees and stream nitrate records for six small forested catchments in the central Appalachian Mountains. Rather than restricting our efforts to describing the temporal variability of $\delta^{15}N$ for specific tree species, which may not ultimately be representative of catchment-wide changes in terrestrial nitrogen availability (Burnham et al. 2016), we used a randomized sampling design to capture forest wide changes in wood $\delta^{15}N$. Furthermore, we used absolute non-normalized $\delta^{15}N$ values to explore the spatiotemporal variation in terrestrial nitrogen availability and its relationship with stream nitrate. Our objective was to test the hypothesis that spatial and temporal variation in terrestrial N availability observed in tree-ring $\delta^{15}N$ records is associated with the spatial and temporal variation of stream nitrate concentration, respectively. To elucidate some of the potential drivers of terrestrial N availability, relationships among acidic deposition (nitrogen (N) + sulfur (S) deposition), precipitation, temperature, and forest disturbance on wood $\delta^{15}N$ were also assessed.

Methods

Site Description

The Upper Big Run catchment (UBR, 1.63 km^2) is located within the Appalachian Plateau physiographic province in the western panhandle of Maryland, USA (Figure 10, Figure S1). The underlying geology within the watershed consists of folded sedimentary rocks of Devonian through Mississippian age (Eshleman et al. 1998). Soils (Ultisols and Inceptisols) are primarily composed of stony loams of the Dekalb/Gilpin and Meckesville series (NRCS 2009). According to the National Vegetation Classification System, the two primary ecological forest systems that occur within the catchment are Northeastern Interior Dry-Mesic Oak Forest and Appalachian Hemlock-Hardwood Forest (GAP 2011). The watershed is 91% forested with the remainder consisting of meadows, roads, cropland, and a power-line right-of-way. Various silvicultural activities have been carried out in Upper Big Run since the 1970s and multiple insect defoliation events have been observed in the late-1980's and mid-2000's (Figure S1; Eshleman et al. 1998, Townsend et al. 2012).

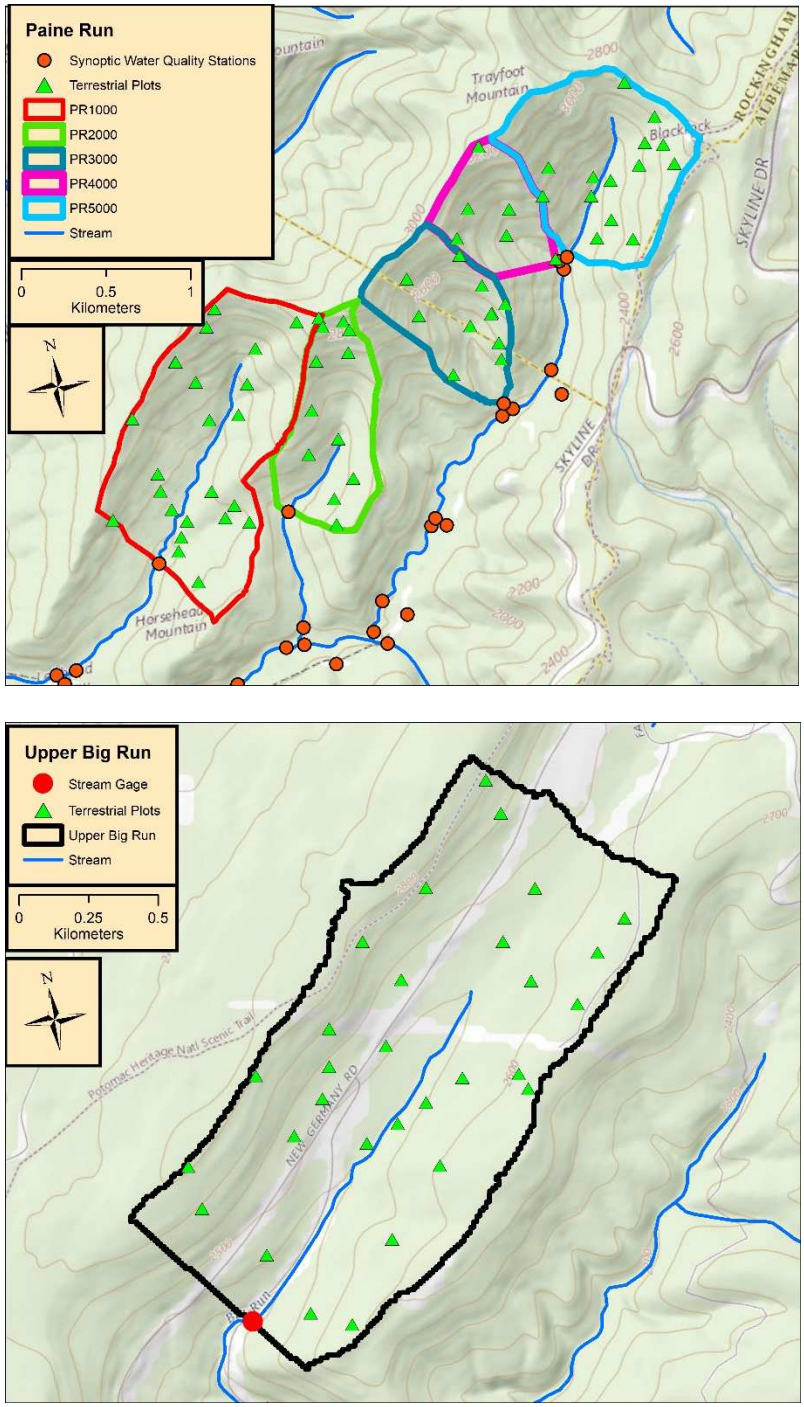

Figure 10. Maps of Upper Big Run and the five headwater catchments of Paine Run subjected to tree coring. The five headwater catchments were labeled PR1000, PR2000, PR3000, PR4000, and PR5000 from west to east since they contain unnamed tributaries, and these site IDs corresponded with individual trees sampled in the respective catchments (Table S5).

The Paine Run catchment (PR, 12.7 km^2) is located on the Blue Ridge in Shenandoah National Park, Virginia (Figure 10, Figure S1). The watershed falls within a

designated wilderness area. Surficial geology of Paine Run is composed of phyllite, quartzite, and metasandstone. Soils (Ultisols and Entisols) are primarily composed of channery or stony loams of the Hartleton or Drall soil series. Numerous rubble islands are scattered throughout the catchment (NRCS 2009). Paine Run is composed of secondary growth forests that have not been logged since the early 20th century. Vegetation surveys from the 1980's show that chestnut oak (*Quercus prinus*) and pine (*Pinus* spp.) were the dominant species. Widespread oak mortality in the early 1990's was associated with repeated gypsy moth defoliation in the upper elevations of the watershed (Scanlon et al. 2010). Today, common forest types that occur within the catchment are Southern and Central Appalachian Oak Forest and Southern and Central Appalachian Cover Forest along with scattered North-Central Appalachian Circumneutral Cliff and Talus systems (GAP 2011). The five headwater catchments of Paine Run subjected to study each contain unnamed tributaries to the mainstem. As such, the catchments were labeled PR1000, PR2000, PR3000, PR4000, and PR5000 from west to east. These labels corresponded to the individual trees sampled in the respective catchments (Table S5).

Dendroisotopic records

Thirty trees at UBR and 66 trees at PR were cored at randomly located plots (Figure 10). In the field, 706.86 m^2 circular plots were established at the sampling points at UBR, and 225 m^2 square plots were established within the five PR subcatchments (e.g., PR1000, PR2000, etc.). Tree species composition surveys were completed during the fall and winter of 2014; all stems >5 cm diameter at breast height (dbh) within each plot were measured and identified. The bole of one individual of the species with the highest summed dbh in each plot was cored twice using a 5.15 mm incremental borer. The cores

were returned to the lab, dried in an oven at 60°C, sanded, and stored until ring widths were identified using CooRecorder software (Larsson 2009). Two to three-year increments were generally cut from one bore per tree using a razor blade and stored in 96-well plates prior to $\delta^{15}N$ analysis. Rings were cut along the grain in slices to ensure weighted sampling across years, thus representing a true weighted-average across each increment.

Approximately 10 mg of wood from the two to three-year increments for the 1980-2013 period was subsampled and used for $\delta^{15}N$ and %N analysis. The midpoint of the aggregated range (e.g., 2003) was identified, and the preceding even year increment assigned, and results falling within 1986 to 2010 period were reported. Following the exact procedures described in Sabo et al. (2016), prepared samples (n = 1322) were analyzed for $\delta^{15}N$ using a Carlo Erba NC2500 elemental analyzer (CE Instruments, Milano, Italy) interfaced with a Thermo Delta V+ isotope ratio mass spectrometer (Bremen, Germany). Following combustion in an elemental analyzer, a Carbosorb trap was used to remove CO_2 and a magnesium perchlorate trap was used to remove water vapor. The $\delta^{15}N$ data were normalized to the AIR scale using a two-point normalization curve with internal standards calibrated against USGS40 and USGS41 (Qi et al. 2003, Brand et al. 2014). The analytical precision among runs (1σ) of an internal wood standard was 0.3‰. Catchment-scale tree ring $\delta^{15}N$ values were estimated by taking the arithmetic mean of all tree ring $\delta^{15}N$ values in a given time period for all trees within a watershed (Sabo et al. 2016b).

Atmospheric deposition, water quality, disturbance, and climatic data

Stream chemistry and discharge have been monitored at UBR and PR since 1990 and 1992, respectively (Eshleman et al. 1998, Scanlon et al. 2010, Eshleman et al. 2013). Synoptic spring baseflow sampling in each of the five PR subcatchments was conducted from 1992-1994 period and, after a long cessation, was restarted in 2007 and repeated annually through 2016. All water samples were analyzed for nitrate concentrations using ion chromatography. The spatial relationship between mean catchment-scale $\delta^{15}N$ and mean spring baseflow nitrate concentrations at PR for the period of observation was explored using linear regression. At UBR, mean annual flow-weighted concentrations, estimated using a multi-parameter loading model (Eshleman et al. 2013), were compared against one year lagged catchment-scale $\delta^{15}N$ values at the UBR site using simple linear regression. The one year lagged values were used because there was an assumed lag between N available in a given growing season and subsequent flush in the following dormant season. Other lags were explored, but did not provide more robust relationships. Likewise, linear regression was used to test the relationship between spring baseflow nitrate concentrations and one year lagged catchment-scale $\delta^{15}N$ values at UBR and the PR headwater catchments. Linear interpolation between catchment-scale $\delta^{15}N$ time periods (e.g., between 1992 and 1994) was used to provide an annual record of catchment-scale $\delta^{15}N$ values that is directly comparable to stream records since tree rings were analyzed in 2-3 year increments. For the Paine Run sites, this allowed three additional spring baseflow concentrations to be compared against catchment-scale $\delta^{15}N$ (i.e., 1993, 2007, and 2009) and 10 additional spring baseflow and mean annual flow-weighted concentration values at Upper Big Run. To clarify, the difference in the number

of spring baseflow samples between UBR and PR was due to the hiatus in sampling at PR. It should be further noted that the development of an observed annual catchment scale-δ^{15}N time series would unlikely contain much value considering evidence that nitrogen translocates between adjacent growth rings (Burnham et al. 2016). Thus, the interpolated time series are likely representative of the true trajectory of terrestrial N availability akin to that of mean annual flow-weighted or spring baseflow concentration being ideal metrics for tracking changes in nitrogen loss to streams (Eshleman et al. 2013, Kline et al. 2016). Regardless, a parallel regression analysis was also carried out using non-interpolated data to confirm that the sign and magnitude of the slope estimates were consistent with the calibration using the interpolated time series (results reported in supplemental).

Disturbance within 45m of the center of individual plots was described using the Disturbance Index (DI, (Healey et al. 2005) applied to Landsat 5, 7 and 8 (TM/ETM+/OLI) data. As such, disturbance was quantified in 8 to 12% of the area in each catchment. All available tier I surface reflectance and quality assurance quality control (QAQC) data for Landsat 5, 7, and 8 were extracted for each cored plot and downloaded using the Google Earth Engine. Using the provided QAQC information, surface reflectance observations collected under suboptimal conditions (cloudy, cloud shadow, snow and ice, etc.) were removed from the data set. From the data that passed quality control, the six Landsat multispectral bands were reduced to three orthogonal indices of brightness (B), greenness (G), and wetness (W) through the tasseled cap transformation (DeVries et al. 2016). The Disturbance Index (DI) is a simple linear combination of these indices (DI = B-(G+W)), where greener and wetter pixels indicate

less disturbance and brighter, dryer, and browner pixels indicate greater disturbance. A continuous stable forest period (~5 to 15 years) for each individual plot was identified by referencing local logging maps provided by the Maryland State Forest Service and the North American Forest Dynamic data product, "Forest Disturbance History from Landsat, 1986-2010" (Figure S1). To standardize for sun-canopy-sensor geometry, we organized all "stable forest" DI observations by day of year and used locally weighted regression models (i.e., LOESS) to model the average DI phenology. From the LOESS fit, expected DI for each day of year was estimated that account for canopy phenology and sun angle effects that reoccur each growing season. The difference between the observed and modeled DI values (ΔDI) was calculated for all observations, representing disturbance above (positive values) or below (negative values) the mean DI during the stable period for any given day of year. A mean growing season (May 1st to September 30th) ΔDI value was calculated using all Landsat observations that fell within the years corresponding to the cut tree ring segments. Similar approaches using various empirical models to describe Landsat phenology in forests have been applied elsewhere (e.g., (Zhu et al. 2012, Elmore et al. 2016) with the overall goal being to normalize for intra-annual variation so that inter-annual variation can be quantified. It should be clarified that mean catchment ΔDI was not quantified at the catchment scale (i.e., sampling all pixels within a watershed) and related to stream nitrate concentrations. This relationship has already been demonstrated in multiple studies (Townsend et al. 2004, McNeil et al. 2007, Eshleman et al. 2009, Townsend et al. 2012). My interest was ascertaining the effect of ΔDI on wood δ^{15}N.

Annual wet deposition of inorganic N (IN) and sulfur (S) and precipitation for UBR and the PR sub-catchments was extracted for the locations of individual trees. Data sets used included wet deposition annual gradient maps published by the National Atmospheric Deposition Program for the 1980-2015 period and climate data published by the PRISM Climate group (Latysh and Wetherbee 2012). Annual temperature values were determined by averaging extracted monthly temperatures from PRISM climatic maps. Little to any intra-site variation at UBR and PR in the climatic and deposition variables was observed due to the coarse spatial resolution (~ 4 km), so only the site averages were reported. Annual values of temperature, precipitation, and wet deposition of N and S deposition corresponding with the cut tree ring segments were averaged by taking the simple arithmetic mean, and used in later statistical analyses to predict the inter-annual variation in tree-ring δ^{15}N.

Annual inorganic S and N wet deposition, ΔDI, mean annual temperature, and mean annual precipitation were used as predictor variables to explain the inter-annual variation in tree ring δ^{15}N. To avoid multicollinearity and to gain greater confidence in causal relationships, the linear effect of time was assessed first, and then removed from both predictor and response variables associated with each individual tree. Thus, the residuals from the suite of predictor variables were leveraged to explain detrended tree-ring δ^{15}N residuals using multiple linear regression in SigmaPlot 14.0. Multicollinearity among the predictor variables was assessed using variance inflation factor (VIF; Graham 2003).

Results

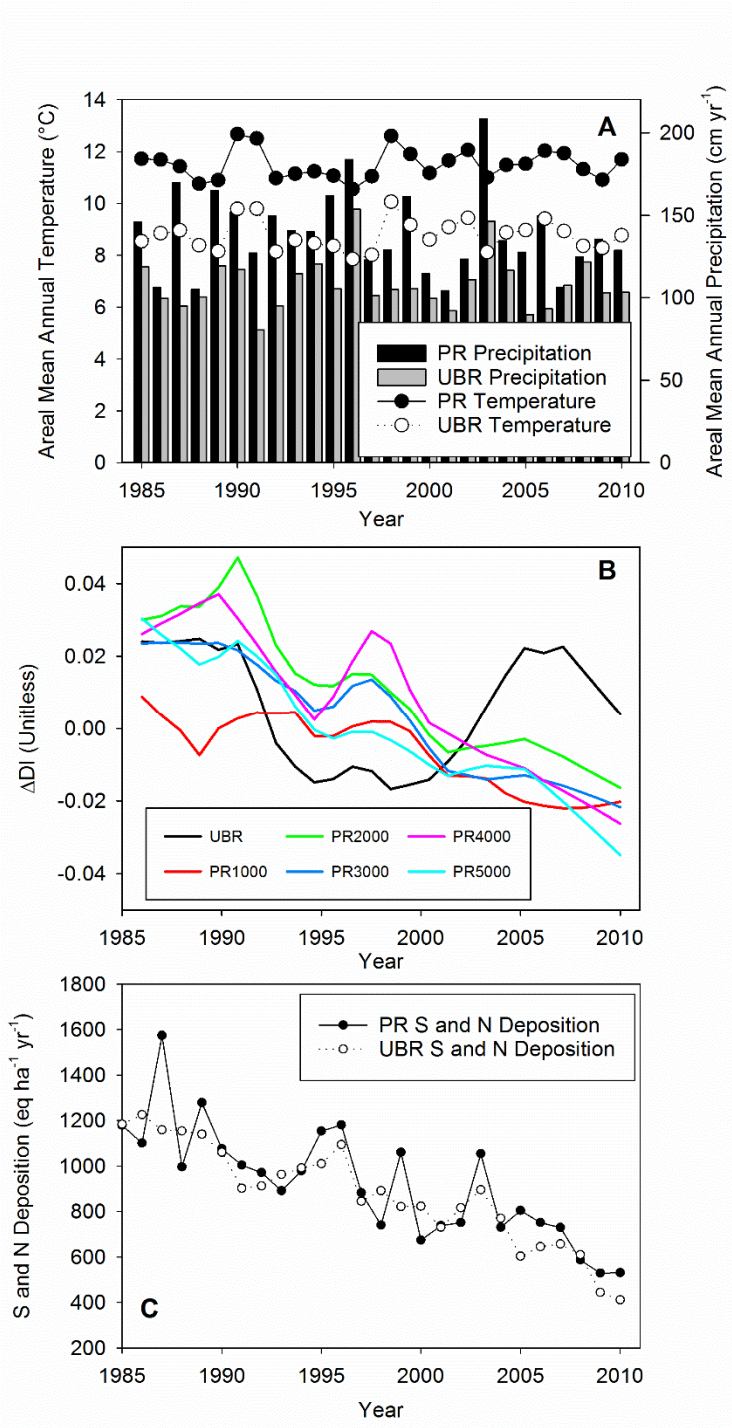

Figure 11. Time series of (A) annual temperature, precipitation, (B) mean disturbance index (ΔDI) for the population of sampled trees in individual catchments, and (C) annual S and N deposition at Paine Run (PR) and Upper Big Run (UBR). For (B) only, the LOESS functions fit to all ΔDI observations that corresponded to individual tree ring segments within a catchment are shown (raw ΔDI data illustrated in Fig. S2-S7 in Appendix).

No long-term trends in annual precipitation or temperature were observed at our study catchments over the 25-year analysis period (Figure 11A). LOESS curves of the annual change in disturbance index (ΔDI) of individual tree time series at UBR and PR suggested a period of disturbance from the mid-1980s to early 1990s for our population of trees (Figure 11B, Figure S1). ΔDI generally declined after the late 1980s and early 1990s at all PR headwater catchments, which is consistent with remote sensing based disturbance classification products (using different methodologies) detecting disturbance in the late 1980s and early 1990s (Figure 11B, Figure S1). ΔDI at UBR declined throughout the 1990s following logging then increased after 2000, coincident with another round of logging activities and reported incidents of gypsy moth defoliations (Figure 11B, Figure S1; Townsend et al. 2012). S and N deposition declined nearly 50% throughout the period of record at both sites (Figure 11C). During this period, catchment-scale δ^{15}N significantly decreased ($p<0.01$) at all headwater catchments at PR and UBR throughout the period of record except for PR4000 (Figure 12, Table S1). Consistent with these aggregated values, 80 of the 96 individual trees showed linear declines in tree-ring δ^{15}N of which twenty were significant ($p < 0.05$, Table S4-S5). Only 11 of the remaining 16 trees with positive linear increases in tree ring δ^{15}N were significant ($p < 0.05$).

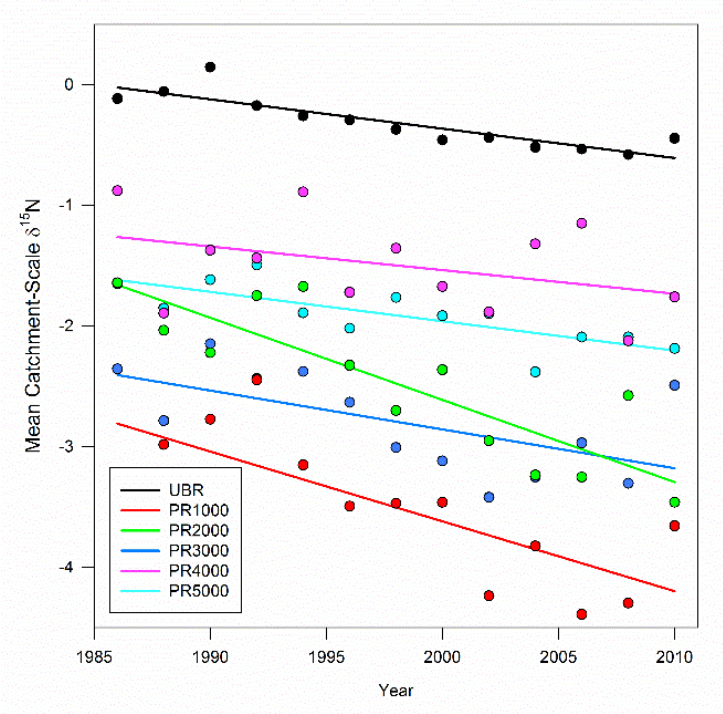

Figure 12. Time series of catchment-scale $\delta^{15}N$ for Upper Big Run (UBR) and the five Paine Run (PR) sub-catchments and associated regression lines. Simple linear regression results indicated significant declines in catchment-scale $\delta^{15}N$ for all catchments except for PR4000(UBR: $y = -0.017 + 33.86$, $R^2 = 0.65$, $p < 0.001$; PR1000: $y = -0.056 + 107.86$, $R^2 = 0.68$, $p < 0.001$; PR2000: $y = -0.055 + 107.57$, $R^2 = 0.70$, $p < 0.001$; PR3000: $y = -0.032 + 60.48$, $R^2 = 0.47$, $p = 0.003$; PR4000: $y = 0.013x - 26.65$, $R^2 = 0.06$, $p = 0.35$; PR5000: $y = -0.023 + 43.81$, $R^2 = 0.60$, $p < 0.001$). Raw tree-ring $\delta^{15}N$ time series illustrated in the supplemental (Figure S2-S7).

Across basins and over time at individual basins, catchment mean wood $\delta^{15}N$ values were observed to have positive linear relationships with stream nitrate concentrations. Across 5 sub-basins at PR, mean spring baseflow nitrate concentrations (averaged across all years) increased linearly with increasing catchment mean wood $\delta^{15}N$ ($R^2 = 0.86$; $P = 0.023$, Table 6). The slope of this relationship equates to a gradient in spring base flow nitrate concentration from 0.09 to 0.73 mg N/L being associated with a gradient in catchment mean wood $\delta^{15}N$ from -3.6 to -1.5 ‰ (Figure 13A). The portion of variance in nitrate concentration explained by the spatial gradient in mean wood $\delta^{15}N$ observed at PR was removed by taking the difference between the mean predicted stream nitrate concentration from the observed nitrate concentration value in a given year.

Temporal variation in wood $\delta^{15}N$ was a significant model effect on nitrate concentrations (Figure 13B), with a positive effect of catchment wood $\delta^{15}N$ observed through time at four of the five Paine Run catchments (Table 7). The results from this analysis were consistent with the coefficient estimated using the non-interpolated catchment-scale $\delta^{15}N$ data (Table S2). While the variance in stream nitrate concentrations explained was generally similar, the relationships were only significant in two of the four Paine Run catchments using the non-interpolated catchment-scale $\delta^{15}N$ time series (Table S2). Estimates of slope coefficients generally increased with increasing mean wood $\delta^{15}N$ ($p > 0.05$, Figure 13C). Therefore, stream nitrate concentrations were least sensitive to annual variation in wood $\delta^{15}N$ at sites with low wood $\delta^{15}N$ (e.g., PR1000) and were most sensitive at sites with high wood $\delta^{15}N$ at Paine Run (e.g., PR5000, Figure 13C). Like the findings from PR, mean annual flow-weighted nitrate and spring baseflow nitrate concentrations at UBR were positively correlated with catchment wood $\delta^{15}N$ ($R^2=0.88$; $P < 0.0001$ and $R^2=0.43$; $P = 0.0017$, respectively Figure 13B); and these relationships were robust when using the non-interpolated catchment-scale $\delta^{15}N$ time series with equivalent, significant slope estimates (Table S2).

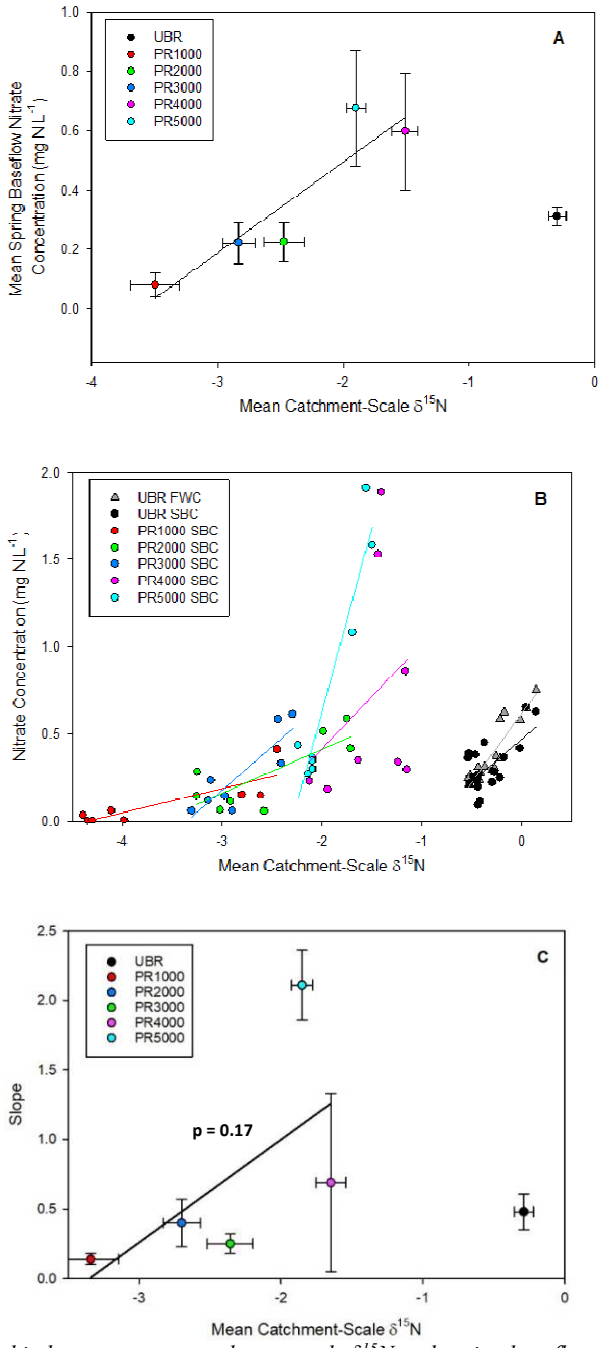

Figure 13. A), Relationship between mean catchment-scale $\delta^{15}N$ and spring baseflow nitrate concentrations across space over the period of record among the Paine Run (PR) and Upper Big Run (UBG) headwater catchments ($y = 0.35x + 1.29$, $R^2 = 0.86$, $p = 0.023$ for data from PR). The error bars illustrate the standard error of the mean. B) Relationships between 1-year lagged catchment scale $\delta^{15}N$ and nitrate concentrations at individual PR headwater catchments and UBR; all regressions were significant except for PR4000 (UBR FWC: $y = 0.79x + 0.62$, $R^2 = 0.85$, $p < 0.01$; UBR SBC: $y = 0.48x + 0.47$, $R^2 = 0.40$, $p < 0.01$; PR1000: $y = 0.14x + 0.55$, $R^2 = 0.67$, $p < 0.01$; PR2000: $y = 0.25x + 0.53$, $R^2 = 0.67$, $p < 0.01$; PR3000: $y = 0.40x + 1.05$, $R^2 = 0.45$, $p = 0.04$; PR4000: $y = 0.69x + 0.94$, $R^2 = 0.14$, $p < 0.32$; PR5000: $y = 2.11x + 4.23$, $R^2 = 0.91$, $p < 0.01$). C) The linear relationship between mean catchment-scale $\delta^{15}N$ and slope estimates based on the relationship between 1-year lagged catchment scale $\delta^{15}N$ and nitrate concentrations for the PR catchments ($y = 0.74x + 2.48$, $R^2 = 0.19$, $p = 0.17$).

Using the simple linear regression models (Table 7), catchment-scale $\delta^{15}N$ was used to model the temporal variability in spring baseflow and mean annual flow-weighted nitrate concentrations from 1990 to 2010 for UBR and 1992 to 2010 for PR. The 1-year lagged catchment-scale $\delta^{15}N$ regression models were effective in capturing peak nitrate concentrations in the early 1990s followed by a decline to the 2000s in five of the six catchments (Figure 14). Furthermore, the models were successful in generating the generally stable stream nitrate concentrations at UBR during the 2000s. Predicted nitrate concentration time series were generally smoother than the observed spring baseflow nitrate concentration time series (one sample per year), likely reflecting the interpolation of wood $\delta^{15}N$ values between the measured 2 to 3-year increments, wood $\delta^{15}N$ values being minimally affected by annual discharge, and the fact the nitrogen has the potential to translocate between adjacent tree rings.

Table 6. Results from the linear regression analysis of 1-year lagged catchment-scale wood $\delta^{15}N$ as a predictor of spring baseflow nitrate concentrations over the period of record among the five Paine Run (PR) headwater catchments.

PR Spatial Model	*Coefficients*	*Standard Error*	*P-value*	R^2
Intercept	1.29	0.21	<0.01	0.86
Slope	0.35	0.08	0.02	

Table 7. Results from the linear regression analyses modeling the effect of 1-year lagged catchment scale wood $\delta^{15}N$ on (1) observed mean annual flow-weighted and spring baseflow nitrate concentrations at Upper Big Run (UBR), (2) spring baseflow nitrate concentrations at individual Paine Run (PR) headwater catchments after factoring out the influence of the spatial gradient.

UBR Mean Annual Flow-Weighted Concentration	*Coefficients*	*Standard Error*	*P-value*	R^2
Intercept	0.62	0.03	<0.01	0.85
Slope	0.79	0.07	<0.01	
UBR Spring Baseflow Concentration				
Intercept	0.47	0.05	<0.01	0.40
Slope	0.48	0.13	<0.01	
PR1000				
Intercept	0.55	0.14	<0.01	0.67
Slope	0.14	0.04	<0.01	
PR2000				
Intercept	0.53	0.18	0.03	0.67
Slope	0.25	0.07	<0.01	
PR3000				
Intercept	1.05	0.46	0.06	0.45
Slope	0.40	0.17	0.04	
PR4000				
Intercept	0.94	1.01	0.38	0.14
Slope	0.69	0.64	0.32	
PR5000				
Intercept	4.23	0.50	<0.01	0.91
Slope	2.11	0.25	<0.01	

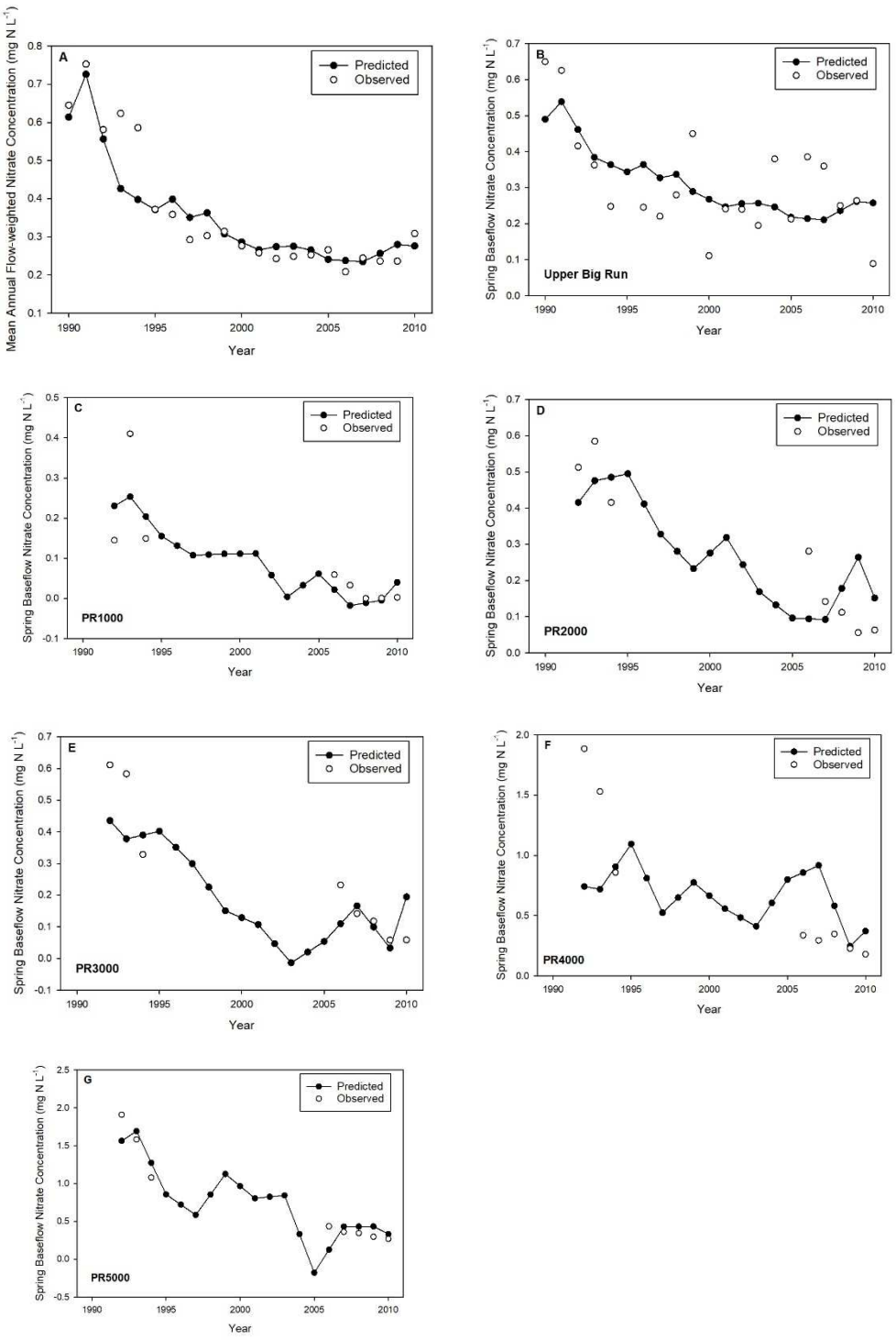

Figure 14. Predicted and observed mean annual flow-weighted nitrate concentrations at Upper Big Run (UBR) (panel A) along with predicted and observed spring baseflow nitrate concentrations for the five Paine Run (PR) headwater catchments and UBR (panel B-G).

After removing the linear effect of time, all predictor variables except for temperature were significant in explaining the inter-annual variation in residual tree ring

$\delta^{15}N$ (Table 8). Residual tree-ring $\delta^{15}N$ increased with increased residual precipitation ($P < 0.001$), but decreased with increased S and N deposition ($P < 0.001$) and ΔDI residuals ($P = 0.016$). As such, higher rates of disturbance and acidic deposition decreased tree-ring $\delta^{15}N$, whereas higher rates of precipitation increased tree-ring $\delta^{15}N$. Of the significant predictor variables and after accounting for trends over time, S and N deposition was the most influential with the highest sum of squares, whereas ΔDI had the lowest sum of squares (Table 8). The multiple linear regression model, though significant ($P < 0.001$), explained very little of the inter-annual variation of detrended tree-ring $\delta^{15}N$ ($R^2=0.041$). If using non-detrended data in a generalized linear model with a categorical variable of a tree identification code (i.e., the factor), the suite of predictor variables plus time explained upwards of 90% of the variance with similar slope coefficients as predicted by the multiple linear regression model (Table S3), but multi-collinearity amongst the predictor variables was identified (VIF > 14 for year and S and N deposition).

Table 8. Results from the multiple linear regression analysis assessing the effects of detrended annual S and N deposition, disturbance (ΔDI), annual precipitation, and annual temperature on detrended tree ring $\delta^{15}N$ (n =973).

	COEFFICIENT	STANDARD ERROR	SUM OF SQUARES	P	STANDARDIZED COEFFICIENT	VIF
INTERCEPT	0.0154	0.0317		0.628		
S AND N DEPOSITION RESIDUAL	-0.00352	0.00056	37.97	<0.001	-0.27	1.901
ΔDI RESIDUAL	-2.247	0.935	5.55	0.016	-0.077	1.046
PRECIPITATION RESIDUAL	0.0145	0.0032	19.59	<0.001	0.201	2.004
TEMPERATURE RESIDUAL	0.0503	0.0815	0.37	0.537	0.021	1.165
REGRESSION				P <0.001	$R^2 = 0.041$	

Discussion

Our results strongly suggest that spatiotemporal variability in stream nitrate concentrations is strongly correlated with a widely-used proxy for terrestrial N availability: wood δ^{15}N. Positive relationships between catchment-scale δ^{15}N and stream nitrate concentrations are consistent with our understanding that wood, foliar, and soil δ^{15}N records are indicators of terrestrial nitrogen availability (Craine et al. 2009, Gerhart and McLauchlan 2014). Across space at the PR headwater catchments, those catchments with higher mean wood δ^{15}N exhibited higher stream nitrate concentrations. This result suggests that catchments with higher terrestrial N availability (i.e., N supply greater than plant demand) will have greater nitrate export. A similar observation was made in a comparative watershed study comparing mean annual flow-weighted nitrate concentrations and non-normalized catchment-scale δ^{15}N values in the Adirondacks, but this analysis was not considered conclusive since one of the predominant species was not sampled due to disease (Sabo et al. 2016b). Moving beyond dendroisotopic records, forested catchments with corresponding lower foliar and soil C:N ratios also typically have higher stream nitrate concentrations throughout the Northeast (Aber et al. 1989, Aber et al. 1998). Further expanding this spatial analysis to include other catchments with stream nitrate and dendroisotopic records is needed to see if broader positive spatial relationships between stream and terrestrial nitrogen availability emerge (akin to global foliar [N] and δ^{15}N gradient relationships, Craine et al. 2009). Such a relationship would be surprising to observe beyond localized scales due to differences in the underlying geology, forest management strategies, species composition, successional status, and topography among forest, however.

Over time, periods with higher wood $\delta^{15}N$ were associated with periods of higher stream nitrate concentrations. Catchment-scale $\delta^{15}N$ regression models also successfully described the decadal stability of mean annual flow-weighted nitrate concentrations at UBR and were generally predictive of spring baseflow nitrate concentrations in five of the six catchments. A similar linear model using a single species, tulip poplar (*Liriodendron tulipifera*), wood $\delta^{15}N$ record was also recently used to explain the inter-annual variation of stream nitrate concentrations at a catchment in Fernow Experimental Forest (Burnham et al. 2016). Other observational studies have suggested similar relationships through time (McLauchlan et al. 2007, Sabo et al. 2016b). In combination, our results and previous studies provide evidence that wood $\delta^{15}N$ models can be used to fill in temporal gaps in, and potentially extend, water quality records back in time.

At our sites, it was also observed that the sensitivity of stream nitrate concentrations to wood $\delta^{15}N$ was not stable across space. Lower significant slope coefficient estimates (slope < 0.4) corresponded to catchments with lower mean catchment-scale $\delta^{15}N$ (< -2.5‰) and nitrate concentrations over the period of record, suggesting the sensitivity of stream nitrate concentrations to changes in catchment-scale $\delta^{15}N$ through time is partly a function of the amount of N available relative to plant demand at a site. This insight is consistent with evidence that forested catchments that retain minimal amounts of atmospherically deposited nitrogen (i.e., the most N rich sites) have the greatest absolute reduction in stream nitrate yields and flow-weighted concentrations following declines in atmospheric N deposition (Eshleman et al. 2013). As such, forested areas with higher nitrogen availability relative to plant demand will demonstrate a greater per unit decline in nitrate concentrations as wood $\delta^{15}N$ declines,

evaluated on an annual basis. Whether this linear relationship holds outside the range of $\delta^{15}N$ values observed at these catchments (-2.5 to 0‰) or reaches an inflection point (i.e., a phase shift) should be pursued in future research (Aber et al. 1989).

Throughout the period of record, catchment-scale $\delta^{15}N$ suggests that terrestrial nitrogen availability relative to plant demand generally declined through time, but trends at the scale of an individual tree were more variable. These clear declines in terrestrial nitrogen availability at the scale of the catchment and associated variability in individual tree-ring $\delta^{15}N$ trends are consistent with other dendroisotopic studies reporting over a similar period throughout the eastern United States (Burnham et al. 2016, Elmore et al. 2016, Sabo et al. 2016b, Mathias and Thomas 2018). While species specific sensitivities to atmospheric N and S deposition (Horn et al. 2018), soil acidification status (Sabo et al. 2016b), and disturbance (Howard and McLauchlan 2015) may modify the trajectory of N availability, it is clear that N availability for forest in general has declined. This decline in terrestrial nitrogen availability, described as "oligotrophication" (Elmore et al. 2016, McLauchlan et al. 2017, Groffman et al. 2018), may contribute to future declines in forest productivity, especially as atmospheric N deposition continues to decline and CO_2 concentrations continue to rise (Eshleman et al. 2013, Lloret and Valiela 2016, Wang et al. 2017). Although it is uncertain what the ultimate impacts of declining nitrogen availability will be on the terrestrial compartment, it is clear that less and less of the terrestrial nitrogen is reaching the already oligotrophic streams of Upper Big Run and Paine Run (Dodds et al. 1998).

Our water quality analysis demonstrated that stream nitrate concentrations are largely driven by changes in terrestrial nitrogen availability, but what is driving longer-

term trends and the general inter-annual variation in terrestrial nitrogen availability? Recent studies have applied a suite of statistical approaches to explain $\delta^{15}N$ through time (Elmore et al. 2016, Mathias and Thomas 2018), but collinearity issues amongst potential predictor variables and time make it difficult to statistically attribute the influence of various environmental drivers on wood $\delta^{15}N$. We applied a conservative approach in which the linear correlation with time was removed from both the response and predictor variables to (1) better identify causal relationships between predictor and response variables by actually comparing unique information in the time series and (2) gain greater confidence in the sign and error of coefficient estimates by eliminating multicollinearity. Our resulting regression model was significant, but only explained a small portion (4%) of the detrended residual $\delta^{15}N$ of the 96 trees. This low explanatory power speaks to the complexity of statistically modeling individual tree-ring $\delta^{15}N$ responses using spatially coarse environmental datasets, particularly when trends over time are evaluated separately and removed from the time series. Furthermore, our decision to sample wood in 2-3 year segments rather than annual increments reduced our ability to explain variation at higher temporal frequencies. Leveraging sub-annual datasets like identifying maximum disturbance in a given year (Townsend et al. 2004) or spring timing (Elmore et al. 2016) or collapsing the variance of the detrended residual $\delta^{15}N$ into catchment-scale $\delta^{15}N$, might improve the explanatory power, but generally would require data with higher temporal frequency or spatial density.

Despite the aforementioned limitations, the significant coefficient estimates offer some insights into forest-wide drivers of terrestrial nitrogen availability. After removing the long-term trend of declining S and N deposition and declining wood $\delta^{15}N$, S and N

deposition exhibited a negative relationship with wood $\delta^{15}N$ (Table 8), suggesting that lower rates of acidic deposition are associated with enhanced nitrogen availability on inter-annual scales. It has been observed in the lab and in the field that decreased soil pH and aluminum mobilization can lead to increased retention of soil organic matter and shifts in microbial activities (Sinsabaugh et al. 2004, Sinsabaugh 2010, Oulehle et al. 2011, Oulehle et al. 2017). The predominantly deciduous forests of UBR and PR lie on poorly buffered, infertile soils and are likely experiencing deacidification as the soils regain base cations and limit toxic aluminum mobilization after decades of elevated rates of acidic deposition (Lawrence et al. 2015b, Kline et al. 2016, Groffman et al. 2018). Studies that have observed deacidification suggest that organic pools of carbon and nitrogen are now being mineralized and lost to streams at both experimentally manipulated and reference catchments (Oulehle et al. 2011, Johnson et al. 2014, Rosi-Marshall et al. 2016, Oulehle et al. 2017). Ultimately, the magnitude and duration of this release of legacy nitrogen and its impact on terrestrial nitrogen availability and stream nitrate loss is likely conditional on forest growth responses to increased base cation availability (Battles et al. 2013), longer growing seasons (Elmore et al. 2016), increased CO_2 (Norby et al. 2016), and improved air quality (Mathias and Thomas 2018).

At first it seems paradoxical that the net effect of increased S and N deposition would result in decreased terrestrial N availability relative to plant demand. Total nitrogen deposition directly contributes to labile nitrogen in forests (Lovett and Goodale 2011) and rapid decreases in stream nitrate concentrations in many forested catchments throughout North America and Europe have been observed following decreases in atmospheric N and S deposition (Rogora et al. 2012, Eshleman and Sabo 2016). These

observations would create the expectation that the S and N deposition model effect on wood $\delta^{15}N$ should be positive rather than negative (Sabo et al. 2016b). In regards to the declines in stream nitrate, it should be kept in mind that the greatest observed decreases in stream nitrate concentrations have occurred during the dormant season when only soil sinks (though minimal) would be active to process atmospheric inputs and regenerated NH_3 (Eshleman et al. 2013). Tree ring and catchment scale $\delta^{15}N$ records may not necessarily capture this "bypass" of atmospheric and microbial nitrate inputs, which can be processed and leached during the dormant season (Sabo et al. 2016a).Therefore the rapid decline in nitrate in many forested catchments following declines in atmospheric N deposition are not necessarily contradictory to the current parameterization.

Wood $\delta^{15}N$ also declined in response to disturbance, suggesting that ephemeral disturbances (McNeil et al. 2007), consisting mainly of defoliation events and selective silvicultural activities, act to reduce N availability in these systems over the long-term. While it is apparent short-lived pulses are often observed immediately after a disturbance (Eshleman 2000), the loss of this nitrate may be insufficient to increase the isotopic signature of plant available nitrogen pools in the soils and it is unclear if this pulse of N is even available to defoliated plants. Furthermore, the enhancement of a long-term growth sink ultimately reduces N availability in the ecosystem. This speculation is consistent with a study carried out in UBR and the surrounding Savage River State Forest which reported that the nitrogen content of leaves was lower at sites that had experienced disturbance relative to undisturbed sites (McNeil et al. 2007). Similar conclusions have also been reported based on soil $\delta^{15}N$ data from forests of the Pacific Northwest (Perakis et al. 2015). In contrast to the negative effects of acidic deposition and disturbance on

wood δ^{15}N, precipitation had a positive relationship. Increased precipitation likely helps maintain soil moisture throughout the growing season thereby promoting greater N mineralization rates throughout the summer (Rustad et al. 2001). Thus, increased precipitation may have promoted greater N supply relative to plant demand (Durán et al. 2016, Sabo et al. 2016a).

Declines in terrestrial nitrogen availability over the past 30 years drove reductions in stream nitrate concentration and loss at our study sites, consistent with reported declines in nitrate export from forested catchments throughout the mid-Atlantic and the Northeast over a similar time period (Kothawala et al. 2011, Eshleman et al. 2013). The impacts of decreased nitrate loss to streams may help diminish the occurrence of episodic acidification in headwater systems and chronic eutrophication in downstream rivers, lakes, and estuaries—welcomed improvements to these chronically impaired aquatic ecosystems. Overall, it's clear that forest nitrogen availability has and will continue to impact downstream nitrogen availability, and that these trends can be monitored through dendroecological evaluation of wood δ^{15}N.

Acknowledgements

I thank Robin Paulman, Joshua Tabora, Susan Snow, Ian Cheek, Vanessa Cunningham, Stephanie Siemek, Ian Smith, and Michael Furlong for assistance in the field and with stable isotope analyses. I also thank Jim Garlitz and Katie Kline along with other personnel of the Appalachian Laboratory water chemistry lab for carrying out water quality analyses. This research was made possible through the support of an Environmental Protection Agency, Science to Achieve Results Graduate Fellowship (#FP-91749901-0, to RDS), National Geographic Young Explorer's Grant (to RDS), and

a teaching assistantship through the Marine-Estuarine-Environmental Sciences (MEES) Graduate Program (to RDS). This research was also supported in part by an appointment to the Research Participation Program for the U.S. Environmental Protection Agency, Office of Research and Development, administered by the Oak Ridge Institute for Science and Education through an inter-agency agreement between the U.S. Department of Energy and EPA. The views presented here are those of the authors and do not represent official views or policy of the U.S. Environmental Protection Agency (EPA) or any other U.S. federal agency. Any use of trade, firm, or product names is for descriptive purposes only and does not imply endorsement by the U.S. Government.

Chapter 4: Point source loading and cleaner air decreases total nitrogen export from the Potomac to the Chesapeake Bay

Abstract

Future development of catchment-wide strategies to effectively reduce nitrogen loss to surface water is hampered by uncertainty over the effectiveness of specific management actions in contributing to water quality restoration. Recent emergence and compilation of annual long-term terrestrial, atmospheric, and aquatic datasets allowed for a novel, empirical approach in assessing the relative effects of cropland nitrogen use efficiency, NO_x emission controls, and wastewater treatment plant upgrades on stream total nitrogen (TN) export in three mixed land use catchments of the Chesapeake Bay—Potomac River at Chain Bridge (POTW) and the North and South Fork Shenandoah Rivers. Parsimonious statistical models were constructed to explain the temporal variation in TN export with the effect of discharge removed to identify likely drivers of TN export for the 1986-2012 period. A simple **l**umped, **l**and **u**se **s**pecific **n**itrogen loading (LLUS-N) model was also used as a means of attributing catchment TN export to point and non-point sources through time. Statistical analysis of the residual time series from the statistical model suggested that changes in point source loads and agricultural surpluses were the best predictors of temporal changes in TN export in all three catchments. These statistical insights were corroborated by modeled changes in point and non-point source loads using LLUS-N. Decreased non-point source loads from forested and agricultural areas of POTW, likely driven by decreasing atmospheric N deposition, explained the majority (60%) of the modeled improvement in water quality. Reductions in point source loads were responsible for 40% of the modeled declines in TN export rates in POTW over the period of record and declines in point source loading were the primary offsets to other

increasing sources of N inputs (e.g., manure) in the Shenandoah catchments. Based on these statistical and empirical modeling insights, management efforts should prioritize limiting the accumulation of surplus nitrogen in terrestrial compartments of the catchment and decrease point source loading to surface water to achieve future water quality restoration goals.

Terminology

Catchment export- The mass of total nitrogen (TN, kg N yr^{-1}) discharged at the catchment outlet ($E_{w,t}$).

Yields- Catchment export normalized by catchment area (kg N ha^{-1} yr^{-1})

Net Inputs/Surpluses- The surplus anthropogenic nitrogen active in the terrestrial compartments after accounting for anthropogenically driven removal processes (e.g., crop removal on agricultural land)

Retention- The proportion of agricultural surplus, urban N inputs, forest N inputs, point source loads not reaching the catchment outlet over a given time period.

Introduction

Eutrophication of lakes and estuaries is caused by anthropogenically driven increases in riverine nutrient loads, particularly nitrogen (N), throughout the world (Vitousek et al. 1997, Galloway et al. 2008). Rapid urbanization and subsequent increases in human and industrial waste along with increased N inputs into agricultural systems and associated inefficiencies in its use have amplified point and non-point source loading to river and streams (Galloway et al. 2003). Furthermore, the release of N oxides and other reduced forms of N mainly through the combustion of fossil fuels or volatilization following application of synthetic fertilizers and excretion of livestock waste has also resulted in an unintentional redistribution of N across the landscape through atmospheric deposition (Shcherbak et al. 2014, van Grinsven et al. 2015, Lloret and Valiela 2016, Griffis et al. 2017). This input pathway appears to be a major driver of non-point source loads from urbanized and natural areas (Eshleman et al. 2013, Bettez et al. 2015). In China, point source loads, agricultural inputs, and atmospheric deposition have generally risen over the past three decades with corresponding increases in riverine N export (Gao et al. 2014, Chen et al. 2016a). In contrast, areas of western Europe and North America have begun to slowly reverse previous increases in N inputs/surpluses by increasing N use efficiency (NUE) in agricultural production, upgrading wastewater treatment plants with enhanced nutrient removal technologies, and enacting regulations to decrease NO_X emissions from stationary and mobile sources (Doering et al. 2011, Sutton et al. 2011, Zhang et al. 2015b). Following these parallel efforts, riverine N export from many catchments in these regions has either stabilized or decreased (Garmo et al. 2014, Hale et al. 2015, Oelsner et al. 2017). Attributing the role of decreased atmospheric N deposition, agricultural surpluses, and point source loading to improvements in water quality, while

also accounting for potential changes in catchment-wide retention due to the implementation of other best management practices (e.g., stream restoration, riparian buffer planting, etc.), would provide valuable information to managers developing strategies to minimize N loss to downstream ecosystems (Keisman et al. 2015).

Application of lumped, input-output models could be a simple and effective method for attributing the influence of management actions on annual changes in water quality (Caraco and Cole 1999, Howarth et al. 2012, Chen et al. 2016b, Eshleman and Sabo 2016). Regardless of the specific formulation of equations or N input/surplus variables used, these models are fundamentally related in their implicit assumption of steady state where parameters are calibrated by linking N inputs/surpluses with observed catchment N export values (Dupas et al. 2017). The models have demonstrated strong, positive relationships between N export and N inputs/surpluses across space and time (Howarth et al. 2012, Chen et al. 2016b, Sinha and Michalak 2016, Hong et al. 2017), but catchment N export in each year was also found to be strongly dependent on discharge. Researchers have developed model structures that incorporate an interactive dependence of catchment N export on: 1) N inputs accounted via various budgeting techniques; and 2) discharge by either directly incorporating observed discharge values or relevant climatic variables (e.g., annual precipitation) that are highly correlated with annual discharge (Sinha and Michalak 2016, Sinha et al. 2017).

A commonly applied budgeting approach, the net anthropogenic N input (NANI), sums the contribution of agricultural N fixation, atmospheric deposition, fertilizer application, and net N import/export of food and feed in a catchment (Boyer et al. 2002, Sinha et al. 2017, Chen et al. 2018). The incorporation of NANI into various empirical

models has helped explain most of the spatiotemporal variation in dissolved inorganic N and total N (TN) export throughout the Yangtze river basin (Chen et al. 2016b), Europe (Howarth et al. 2012, Hong et al. 2017), and the contiguous United States (Howarth et al. 2012, Sinha and Michalak 2016). Furthermore, these studies offered insight into what sources of anthropogenic N are driving increased N inputs and subsequent export in a catchment. However, NANI-based models are limited in their ability to attribute the role of changing non-point source N loads from specific land uses and point source loads (Chen et al. 2018).

It may be possible to apply NANI-based models or some other input-output models to catchments with homogenous land use (e.g., forest, urban) and subsequently use the results of such models to parameterize more complex models that can attribute TN export to specific land uses. However, this ideal approach is likely untenable considering the rather extreme differences in the input, retention, and loss of N in catchments with equivalent land use (Howarth et al. 2012, Argerich et al. 2013, Adams et al. 2014, Bettez et al. 2015). For example, in the central Appalachians of the United States, regional retention efficiencies of atmospheric N deposition in forested catchments range from close to 0% to near 95% (Eshleman et al. 2013, Sabo et al. 2016a). The degree to which the N-retentiveness of a single forested or urban catchment could adequately represent the mean retention of a particular land use across a region is unknown. While similar in principle, other research groups trying to develop moderately-disaggregated, process-based models have instead relied on the literature to constrain the potential range of parameters during calibration. Following model optimization, the next step is to evaluate the uncertainty of the parameter estimates and the sensitivity of the

model to specific parameterizations in order to identify processes likely driving the inter-annual variation in catchment TN export (Van Meter et al. 2017, Chen et al. 2018, Hu et al. 2018).

Other empirical models more rooted in the conceptual model of kinetic N saturation have relied solely on using atmospheric N deposition as the N input variable and assumed that non-atmospheric inputs are static through time in mixed land use catchments (Lovett and Goodale 2011, Eshleman et al. 2013). This assumption allowed estimates of unique retention factors of atmospheric deposition and baseline loading factors (i.e., N load not influenced by atmospheric deposition) for both forest and non-forested portions of 18 mixed land use catchments within the Chesapeake Bay watershed (Eshleman et al. 2013, Eshleman and Sabo 2016). Findings from these kinetic N saturation studies suggest that decreased atmospheric deposition, particularly onto non-forested areas, was the primary driver of water quality improvement in the region (Eshleman and Sabo 2016). More deterministic modeling studies have suggested that increases in N use efficiency (NUE) in agricultural lands and wastewater treatment plant upgrades may have also driven water quality improvements during the same time in the Chesapeake region (Linker et al. 2013, Shenk and Linker 2013). However, the current suite of kinetic N saturation and NANI-based models in their current forms are incapable of testing such an assertion without further refinement since they do not simultaneously account for parallel changes in other N inputs onto specific land uses, point source loads, and/or N loads from specific land uses through time.

To address these limitations, I: 1) explored a suite of statistical models; and 2) developed a lumped conceptual model capable of examining the potential roles of

hydroclimate and implementation of management actions on observed TN export variations. The first approach involved constructing parsimonious statistical models to explain temporal variations in TN export (with the effect of discharge removed) as a way of identifying likely drivers of TN export. The possible drivers evaluated included point source N loads, urban N inputs, agricultural N surpluses, and atmospheric N deposition onto forested land. Building on past NANI and kinetic N saturation studies, the lumped conceptual model developed in this study was fundamentally based on the idea that different land use contributions (i.e., agriculture, forest, urban) to catchment TN export can be modeled using land use-specific average N retention factors and N budgets, with the overall catchment TN response assumed to be additive across the different land uses. Like other lumped conceptual models, retention was allowed to vary as function of annual discharge so as to further explore the influence of both hydroclimate and N inputs and surpluses on the inter-annual variability of catchment TN export. In contrast to the statistical analysis, the lumped conceptual model was not constrained by a need for parsimony. Rather, the model put forward was considered a realistic, yet simple, conceptualization of the catchment capable of exploring the potential impact of varied inputs and N surpluses on observed catchment TN export through time. The parameterization of this model was subjected to further uncertainty and sensitivity analysis as a way of evaluating the primary drivers of modeled catchment TN export.

Terrestrial N budgeting, catchment TN export, discharge, and land use data were acquired for the Upper Potomac River at Chain Bridge near Washington, D.C. (POTW) and two of its rural sub-catchments, North Fork Shenandoah (NFSR) and South Fork Shenandoah (SFSR), for the 1986-2012 period (Homer et al. 2015, Chanat et al. 2016).

POTW, the second largest tributary to the Chesapeake Bay, displayed significant declines in TN export during a period when fertilizer, point source loading, and atmospheric N deposition all decreased (Shenk and Linker 2013). The rural, contiguous sub-catchments of NFSR and SFSR offered an intriguing comparison because SFSR displayed declines in TN export, whereas the adjacent catchment of NFSR displayed an increase during the period despite similar agricultural practices and land use (Chanat et al. 2016, Eshleman and Sabo 2016, Oelsner et al. 2017). Ultimately, the objectives of this study were to: 1) examine if N retention has substantially changed over the period of record in the study catchments, 2) statistically identify the likely drivers of temporal trends in catchment TN export, and 3) attribute changes in catchment TN export to specific N sources and land uses.

Methods

Study sites: Site description and water quality data

The POTW is situated within four physiographic provinces (Piedmont, Blue Ridge, Ridge and Valley, and Appalachian Plateau). The majority of the human population is located near the catchment outlet (Figure 15), but scattered urban centers are located throughout the catchment. Generally, POTW contains an urban, agricultural to forest gradient from east to west with distinct forested areas occurring in the mountains (Figure 15). SFSR and NFSR are predominantly located within the Ridge and Valley physiographic province, but the eastern boundary of the SFSR is made up of the Blue Ridge. SFSR and NFSR have similar proportions of forest within their catchments (~56%, Table 9), with the forested land generally situated along ridgelines in the Shenandoah, Massanutten, and Blue Ridge mountain ranges (Figure 15). The broad Shenandoah Valley itself is dominated by agriculture with dispersed urban centers

(Figure 15). Significant amounts of poultry production via concentrated animal feeding operations (CAFOs) and processing also occur in the valleys within NFSR and SFSR (Keisman et al. 2018). Only ~2 and ~3% of the agricultural land is cultivated cropland in SFSR and NFSR (i.e., non-pasture or hayfields), whereas ~7% of agricultural land is cultivated cropland in POTW (Homer et al. 2015).

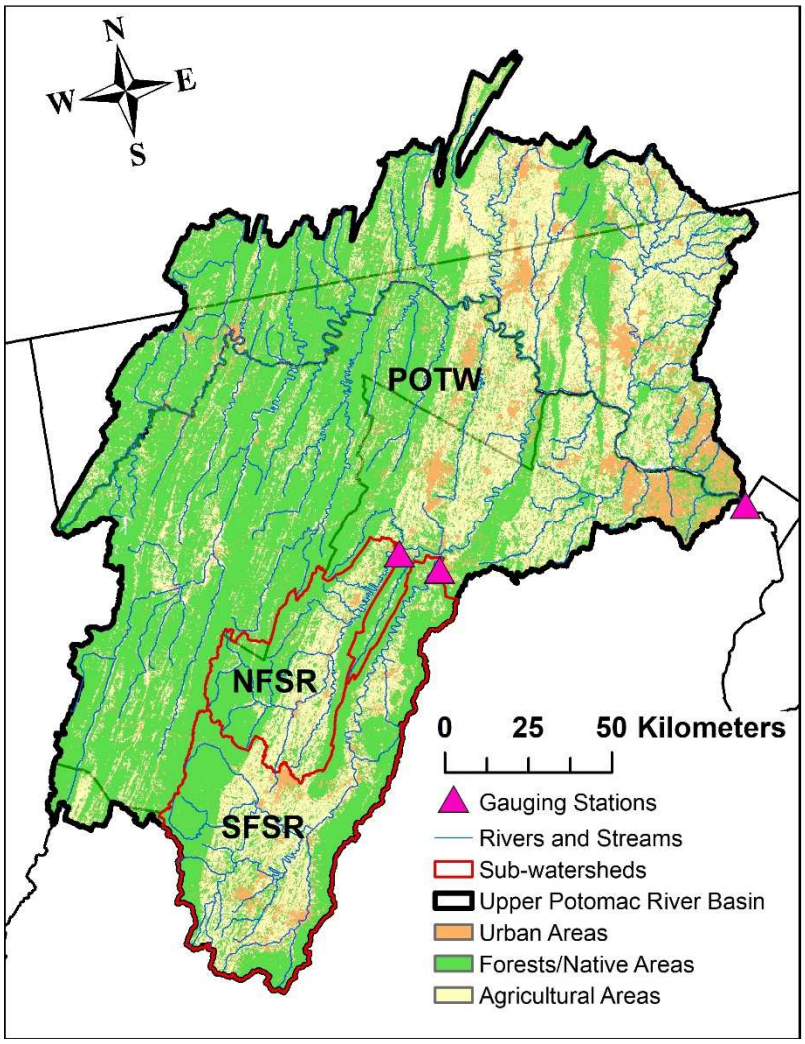

Figure 15. Map displaying the study catchments (Homer et al. 2015, Chanat et al. 2016).

Table 9. Site information for the study catchments. Land use data extracted from 2011 National Land Cover Dataset (Homer et al. 2015).

Station	USGS Station ID	Area (km^2)	Forests/ Native Areas (%)	Urban (%)	Cropland (%)	Pasture (%)	Open Water (%)
South Fork Shenandoah River at Front Royal, VA (SFSR)	01631000	4231	55.6	10.8	2.9	29.9	0.6
North Fork Shenandoah River near Strasburg, VA (NFSR)	01634000	1998	58.5	7.0	2.3	31.8	0.4
Potomac River at Chain Bridge, Washington, D.C. (POTW)	01646580	29930	59.0	10.5	6.5	22.7	1.3

Annual discharge and TN export values (1986-2012 water years) were acquired from the "Water Quality Loads and Trends at Non-Tidal Monitoring Stations in the Chesapeake Bay Watershed" data platform. Catchment TN export estimates were generated using the "**W**eighted **R**egressions on **T**ime, **D**ischarge, and **S**eason" statistical load model (WRTDS; Hirsch et al. 2015). Outputs from WRTDS are considered the best estimates of the "true condition" export rates for evaluating long-term and short-term trends in water quality in the Chesapeake Bay due to lower bias and greater explanatory power for stations with longer water quality records (Chanat et al. 2016, Moyer 2016). Furthermore, the USGS and Bay managers have adopted WRTDS as their primary tool to evaluate long and short-term trends in water quality in the Chesapeake Bay region (Keisman et al. 2015, Chanat et al. 2016).

Point and non-point source input datasets

Monthly TN load and discharge data for wastewater treatment plants (WWTPs) in Virginia, West Virginia, Maryland, and Pennsylvania were acquired from the database developed for Bay Program Nutrient Point Source Data platform (CBP 2016). This database contains both modeled and monitored effluent discharge data for all facilities in

possession of a National Pollutant Discharge Elimination System (NPDES) permit. Monthly loads were extracted from the database and summed to calculate annual point source loads for each of the study catchments for calendar years 1986, 1990, 1995, 2000, 2005, 2010, and 2012 to assess potential changes in point source N loads within the period of record. Linear interpolation was applied to fill in temporal gaps to generate a continuous annual time series for later modeling efforts (calendar year). Point source loads into stream networks are generally independent of climatic variation, so this interpolation scheme was assumed representative of the trajectories in point source loads as characterized by this database (CBP 2016). As such, the effects of combined sewage overflows, which do occur in certain jurisdictions in parts of POTW where sewer and storm drains are not separated, are not explicitly described in this research. It was decided to aggregate monthly point source loads by calendar year to ensure consistency with other non-point source input datasets described below. This introduces a three-month incongruency with WRTDS annual export values based on water years (October to September) and the input datasets (January to December).

Agricultural fertilizer N application, manure N application onto cropland and pasture, excreted N, cultivated biological N fixation, and harvested crop N removal rates were extracted from the International Plant Nutrition Institute's Nutrient Use Geographic Information System (Fixen et al. 2012). This dataset depends heavily on a combination of United States Department of Agriculture Agricultural Census, Association of American Plant Food Control Officials, and National Agricultural Statistic Service data, which provide raw data to estimate annual, county level fertilizer and manure N production rates along with crop harvest data. Annual N input and crop N removal rates have been

estimated for five separate years centering on the Agricultural Census with additional data coming from the National Agricultural Statistics Service (1987, 1992, 1997, 2002, 2007, 2008, 2009, 2010, 2011, 2012) at the county and HUC-8 scale (Fixen et al. 2012). Linear interpolation was applied to fill in temporal gaps to generate a continuous time series for later modeling efforts (i.e., 1987-2012). Ideally, agricultural N flux data would be available on an annual basis, but no dataset currently exists. Thus, interpolated time series are assumed to follow the general trajectories of agricultural N fluxes through the different Agricultural Census sampling periods.

Both NFSR and SFSR are HUC-8 catchments, so the data were directly extracted from the tabulated database. POTW consisted of nine HUC-8 drainages. Thus, agricultural fertilizer application, manure N application onto cropland and pasture, excreted N, cultivated biological N fixation, and harvested crop N removal rates from all nine HUC-8 basins were summed by mass for POTW. There is some additional uncertainty in the distribution of these application rates. Though these fluxes are restricted to agricultural areas throughout each county (Fixen et al. 2012, Homer et al. 2015), watersheds do not always align with county boundaries. This misalignment may result in some of the agricultural fluxes being misattributed. However, issues of misattribution for our study sites would likely be minimal considering the size of POTW and the fact that the Shenandoah watersheds generally align with the county boundaries.

Fertilizer application rates onto urban land were acquired from a USGS data platform that estimates county urban and agricultural fertilizer application rates across the country for the 1987 to 2012 period (Gronberg and Spahr 2012, Brakebill and Gronberg 2017). This database relies on state reported sales data from the Association of American

Plant Food Control Officials (AAPFCO). State estimates are then allocated to the county level and are differentiated into farm and non-farm application in a weighting scheme using a combination of expenditure data from the Census of Agriculture and effective population densities. It should be noted agricultural fertilizer N application estimates from the IPNI NuGIS are equivalent to USGS estimates since both use the same data sources and allocation schemes (Fixen et al. 2012).

Total atmospheric N deposition estimates have been previously reported (Eshleman and Sabo 2016) and are based on wet nitrate and ammonium deposition gradient maps published by the National Atmospheric Deposition Program (NADP 2015). The explicit assumption that "total N deposition = 2 x annual wet deposition" was used because the most recent and advanced total (i.e., wet + dry) deposition estimates (TDEP) that explicitly include dry N deposition only go back to 2000 (Eshleman and Sabo 2016). This assumption typically estimates total atmospheric N deposition (including organic N species) by 20 to 50% lower than TDEP in POTW, but the direction and magnitude of change in deposition using either dataset is equivalent (Figure S8). Estimates of uncertainty, especially of modeled dry deposition which is thought to be high (Bash et al. 2013), are currently lacking, however. In light of the incomplete record, uncertainty in total deposition estimates, and strong linear relationships between the 2x wet deposition and total deposition estimates, the 2x annual wet deposition assumption was used. Total N deposition onto agricultural, urban, surface water, and forested land uses was estimated by apportioning catchment total deposition (kg N yr^{-1}) according to the proportion of each land use in the catchment.

Agricultural fertilizer application, manure N application onto cropland and pasture, cultivated biological N fixation, and harvested crop N removal rates extracted from the NuGIS database were used to calculate an annual partial N surplus (i.e., inputs (excluding N deposition) – outputs) on agricultural land. The total annual N surplus in agricultural lands includes 2x wet atmospheric N deposition. Thus, this surplus metric is calculated by taking the difference between the summed NuGIS inputs plus estimated atmospheric deposition and NuGIS outputs (crop N removal). Nitrogen use efficiency was calculated by dividing the annual crop N removal value by the summed NuGIS and atmospheric deposition input. It could be suggested that manure inputs should not be considered inputs in various mass balances since it is likely that some of the N requirement of the animal population is satisfied by sources internal to the catchment (Jordan and Weller 1996, Russell et al. 2008). It should be clarified that I am not seeking to calculate net catchment inputs, rather the amount of anthropogenically-mediated N remaining in fields and pasture in a given year (lumped). To further assuage concerns of double counting (though not completely eliminate the issue), the manure N application rate onto cropland and pasture is the estimated amount of N recovered from intensive livestock production operations (e.g., animal feedlots) and also accounts for losses during transport and volatilization. Ultimately, accounting for the manure input is imperative for accounting of agricultural surpluses and NUE (Sutton et al. 2011, Billen et al. 2013, Shenk and Linker 2013, Zhang et al. 2015b).

Long-term linear trends in N export, atmospheric N deposition, fertilizer N application, manure N application, excreted N, cropland N fixation, crop N removal, and point source N loading rates were assessed through simple linear regression. Absolute

and relative changes in these individual N inputs/surpluses were then calculated to provide a summary assessment of how terrestrial N fluxes have generally shifted through time (Eshleman et al. 2013). If it was determined that linear regression was an inappropriate approach to deriving the best linear estimate of absolute and relative change for a specific N input/surplus, then a non-linear regression procedure was applied to confidently ascertain long-term linear changes (Hu et al. 2015, Chen et al. 2016b). As done in other catchment mass balance studies, 1000 values for each year of given input variable were generated using a Monte Carlo simulation assuming a normal distribution with a predefined coefficient of variation of 30% if no reliable estimates of uncertainty were reported (Sobota et al. 2013, Chen et al. 2016a, Chen et al. 2016b, Van Meter et al. 2017). A distribution of linear slope and associated y-intercept estimates were determined by evaluating the 1000 unique time series. The 2.5, 50.0 and 97.5% intervals of the slope and intercept were identified to determine the upper, median, and lower estimates of change throughout the period of record (Hu et al. 2015).

Factoring out the influence of annual discharge on catchment TN export and retention

The relationship between annual discharge and catchment TN export was explored using simple linear regression. Time series of the model residuals (discharge model) were then visually assessed for temporal structure and were used later in the statistical modeling analyses described below (section Approach #1). Discharge is also known to influence the retention of N inputs and surpluses in a given year (Sinha and Michalak 2016, Chen et al. 2018). I specifically define retention as the proportion of agricultural surplus ($I_{a,t}$), urban N inputs ($I_{u,t}$), forest N inputs ($I_{f,t}$), and, point source loads ($I_{p,t}$) not exported ($E_{w,t}$) at the catchment outlet over a given time period (i.e.,

$\frac{\sum I_{a,t},I_{u,t},I_{f,t}I_{p,t}-E_{w,t}}{\sum I_{a,t},I_{u,t},I_{f,t}I_{p,t}}$, Table 10). In addition, the relationship between catchment retention and annual discharge was assessed using simple linear regression. Residual time series were then generated to visually assess if retention (after removing the effect of annual discharge) was increasing, decreasing, or remaining constant through time.

Approach #1: Statistical modeling of discharge model residuals

The influence of potential drivers on the temporal variation in the discharge model residuals was explored using correlation and non-linear regression analyses. As described above, the linear effect of discharge was removed from WRTDS TN export values to explore the inter-annual variation in export independent of discharge. The Pearson correlation of all predictor variables, including urban nitrogen inputs ($I_{u,t}$, Table 10), forest nitrogen inputs ($\boldsymbol{I_{f,t}}$, Table 10), annual N surplus in agricultural lands ($I_{a,t}$, Table 10), and annual discharge ($\boldsymbol{R_{w,t}}$, Table 10) to the response variable, residual catchment TN export, was constructed and the significance of the associations was tested using the Pearson Product Moment Correlation tool in SigmaPlot 14.0 (SigmaPlot). A complete parallel correlation matrix of all variable combinations using non-interpolated time series was also constructed to evaluate the robustness of the correlation using non-interpolated time series.

The linear effect of annual discharge was first removed from all predictor variables before proceeding with the residual catchment TN export analysis by generating the residual time series using the simple linear regression model. This allowed the model to be fully specified with the mean value of all predictor variables centering on zero (same as the discharge model residual) and removing any linear correlation with discharge, thus allowing any variation independent of discharge to be compared. In

addition to reporting the standard statistical outputs, the Akaike information criterion (AICc) was also determined as a means of model selection (Akaike 1998). More parsimonious models that maximize goodness-of- fit relative to other models will have lower AICc; thus a model's quality was ranked by their absolute difference to the model with the lowest AICc (ΔAICc). All linear combinations of predictor variables were evaluated using SigmaPlot 14.0. All model combinations that provided positive slope coefficient estimates and produced a $\Delta AICc < 2$ were reported. Any models with $\Delta AICc > 2$ were not considered meaningful and were not reported (Aho et al. 2014), while negative slope coefficients were considered spurious because the logic implies that increased inputs resulted in decreased catchment TN export.

Table 10. Reference table listing the parameters and the input, state, and output variables of the statistical model developed to explain the discharge model residuals (approach #1) and LLUS-N (approached #2) along with a summary of the method of determination. The definition and mathematical derivation of catchment retention is also described.

Output Variable	**Description**	**Determination**
$E_{w,t}$ *(kg N yr^{-1})*	Catchment TN export as modeled by LLUS-N	$\boldsymbol{E_{w,t} = I_{p,t} * B_p R_{w,t} + I_{a,t} * B_a R_{w,t} + I_{u,t} * B_u R_{w,t} + I_{f,t} * B_f R_{w,t}}$
Input and State Variables		
$I_{p,t}$ *(kg N yr^{-1})*	Point source TN loading within a catchment in a given year	Estimates acquired from *Bay Program Nutrient Point Source Data Platform*
$I_{u,t}$ *(kg N yr^{-1})*	Summed fertilizer application and total atmospheric deposition rates onto urban lands within a catchment in a given year	1. Extracted urban fertilizer application rates from the USGS "County-Level Estimates of Nitrogen and Phosphorus from Commercial Fertilizer for the Conterminous United States, 1987-2012" database 2. Apportioned total deposition onto specific land uses based on the proportion of each land use in each catchment
$I_{f,t}$ *(kg N yr^{-1})*	Total atmospheric deposition rates onto forested lands within a catchment in a given year	1. Apportioned total deposition onto specific land uses based on the proportion of each land use in each catchment
$I_{a,t}$ *(kg N yr^{-1})*	Annual N surplus in agricultural lands within a catchment in a given year	1. Manure application, agricultural fertilizer application, cultivated biological N fixation, and harvested crop N removal estimates were extracted from the International Plant Nutrition Institute's Nutrient Use Geographic Information System 2. Apportioned total deposition onto specific land uses based on the proportion of each land use in each catchment 3. Annual N surplus in agricultural lands is calculated by taking difference between the inputs (manure application, agricultural fertilizer application, cultivated biological N fixation, and total deposition) and outputs (crop N removal).
$R_{w,t}$ *(m yr^{-1})*	Annual discharge within a catchment in a given year, normalized by area	Annual discharge estimates provided by the *Chesapeake Bay Program Loads and Trends* database
Catchment Retention (unitless)	The proportion of agricultural surplus, urban N inputs, forest N inputs, point source loads not reaching the catchment outlet over a given time period.	$\frac{\sum I_{a,t}, I_{u,t}, I_{f,t} I_{p,t} - E_{w,t}}{\sum I_{a,t}, I_{u,t}, I_{f,t} I_{p,t}}$
Parameters		
B_p *(yr m^{-1})*	Scaling factor of the point source loading export coefficient (e.g., $B_p R_{w,t}$)	Simultaneously determined along with parameters of other export coefficients via nonlinear regression on SigmaPlot 14.0, constraints to parameterization defined by literature
B_f *(yr m^{-1})*	Scaling factor of the forest export coefficient (e.g., $B_f R_{w,t}$)	Simultaneously determined along with parameters of other export coefficients via nonlinear regression on SigmaPlot 14.0, constraints to parameterization defined by literature
B_a *(yr m^{-1})*	Scaling factor of the agricultural export coefficient (e.g., $B_a R_{w,t}$)	Simultaneously determined along with parameters of other export coefficients via nonlinear regression on SigmaPlot 14.0, constraints were solved by difference based on observed retention values for the catchment and literature reported retention values for other N sources.
B_u *(yr m^{-1})*	Scaling factor of the urban export coefficient (e.g., $B_u R_{w,t}$)	Simultaneously determined along with parameters of other export coefficients via nonlinear regression on SigmaPlot 14.0, constraints to parameterization defined by literature

Approach #2: Lumped conceptual model of catchment TN export

The statistical analysis described above was complimented by the construction of a simple lumped conceptual model, the **L**ump **L**and **U**se **S**pecific **N**itrogen (LLUS-N) export model. Conception of this model was partly inspired by efforts to determine the importance of point source loads, atmospheric deposition, and fertilizer use on nitrate export in catchments across the globe (Caraco and Cole 1999). It was conceptualized that a fraction of watershed inputs ($\boldsymbol{I_{w,t}}$) and point source loads ($\boldsymbol{I_{p,t}}$) are exported from the catchment ($\boldsymbol{E_{w,t}}$) in a given year (all in kg N yr^{-1}), but the retention of watershed inputs is a non-linear function of area-normalized discharge ($\boldsymbol{R_{w,t}}$, in m yr^{-1}, referred to as annual discharge throughout). This can be mathematically described as:

$$\boldsymbol{E_{w,t} = D_w * I_{p,t} + I_{w,t} * D_w * B_w R_{w,t}}^{\boldsymbol{C_w}} \quad \textbf{1)}$$

where $\boldsymbol{D_w}$, $\boldsymbol{B_w}$, and $\boldsymbol{C_w}$ are (constant) model parameters (Caraco and Cole 1999). In-stream retention processes were conceptualized to be captured by the $\boldsymbol{D_w}$ parameter and was assigned a literature value of 0.7 (Billen 1991), whereas the $\boldsymbol{B_w}$, and $\boldsymbol{C_w}$ parameters were used to represent the sensitivity of non-point source loads to annual discharge. These values were calibrated through optimization (Caraco and Cole 1999). Building on this conceptual framework, LLUS-N attempts to apportion the inter-annual variation in catchment TN export to changes in point and non-point source loads from urban, forested, and agricultural areas within the catchment—thus requiring a slightly more complex model than Eq. 1) to represent land use-specific average N retention and non-point source loads:

$$\boldsymbol{I_{w,t} * D_w * B_w R_{w,t}{}^{C_w} = I_{a,t} * B_a R_{w,t}{}^{C_a} + I_{u,t} * B_u R_{w,t}{}^{C_u} + I_{f,t} * B_f R_{w,t}{}^{C_f}}$$

2)

The $\boldsymbol{I_{a,t}}$, $\boldsymbol{I_{u,t}}$, and $\boldsymbol{I_{f,t}}$ terms represent annual time series of anthropogenic N inputs or surpluses (**kg N yr^{-1}**) onto agricultural, urban, and forested areas within a catchment, respectively (Table 10) with the respective land-use specific scaling factors (i.e.,***B's)*** and exponents (i.e., ***c***'s) effectively replacing the $\boldsymbol{B_w}$ and $\boldsymbol{C_w}$ parameters in Eq. 1). The term, $\boldsymbol{I_{a,t}}$, is the annual N surplus onto agricultural lands which is the difference between N inputs onto agricultural land (atmospheric deposition, synthetic fertilizer, applied manure, cultivated biological N fixation) and N removed from the field following harvest. Annual urban inputs, $\boldsymbol{I_{u,t}}$, include lawn fertilizer and total atmospheric N deposition, whereas the forest N input term, $\boldsymbol{I_{f,t}}$, represents total atmospheric N deposition onto forest. The in-stream retention term, $\boldsymbol{D_w}$, is not explicitly listed in this derivation due to the fact that in-stream retention varies as a function of discharge (Beaulieu et al. 2011, Miller et al. 2016), thus making the assignment of a fixed value suspect. The estimated net effect of in-stream retention would still be captured in the calibration of the scaling factors and exponents, but it ultimately cannot be separated from other retention processes through optimization, however. Along a similar line, the $\boldsymbol{D_w}$ interaction with point source loading inputs ($\boldsymbol{I_{p,t}}$) was substituted with a parallel non-linear export function to allow the retention of point source loads to vary with discharge (i.e., $\boldsymbol{B_p R_{w,t}{}^{C_p}}$). Annual point source load estimates, $\boldsymbol{I_{p,t}}$, were extracted from Bay Program Nutrient Point Source Data platform as described above. Substituting equation 2) and the non-linear export function for the point source loading interaction into equation 1 results in:

$$E_{w,t} = B_p R_{w,t}^{C_p} * I_{p,t} + I_{a,t} * B_a R_{w,t}^{C_a} + I_{u,t} * B_u R_{w,t}^{C_u} + I_{f,t} * B_f R_{w,t}^{C_f}$$

3)

I preliminarily explored the use of the full power function representations of non-point loads (e.g., $B_a R_{w,t}^{C_a}$, $B_u R_{w,t}^{C_u}$) in LLUS-N, but encountered issues with equifinality (the number of model parameters increased from 4 to 8); in addition, these models increased AICc (> 2). Therefore, I simplified Eq. 3) by assuming all of the exponents were equal to unity. As such, the final LLUS-N model formulation was:

$$E_{w,t} = I_{p,t} * B_p R_{w,t} + I_{a,t} * B_a R_{w,t} + I_{u,t} * B_u R_{w,t} + I_{f,t} * B_f R_{w,t}$$

4)

Catchment TN export attributable to specific point and non-point sources was thus assumed to vary as a linear function of annual normalized discharge, $R_{w,t}$ (assumed nonvariant across the three land uses within each basin) Corresponding source specific scaling factors (B's, n = 4) were simultaneously calibrated in SigmaPlot 14.0 using the custom equation non-linear regression tool (e.g., B_a, B_u, B_f, and B_p, Table 10). Ranges of scaling factors that could be used for parameterization were constrained by the literature (described in a paragraph below). Another major assumption of LLUS-N was that there is no carryover of inputs from one year to the next. Some have reported that modeling legacy sources of N may be important for modeling the inter-annual variation in catchment TN export and forecasting future trajectories of TN export. However, others have concurrently developed models of similar predictive skill relying solely on annual N inputs within the same regions (Chen et al. 2016a, Van Meter et al. 2017, Chen et al.

2018, Hu et al. 2018). A final implicit assumption of LLUS-N worth noting is that the modeled retention of each land use to different inputs of N will be exactly the same, as have other lumped empirical models (Howarth et al. 2012, Chen et al. 2018). It has been suggested that the retention of atmospherically deposited N may differ from retention of other N sources (Jaworski et al. 1992, Eshleman and Sabo 2016, Sabo et al. 2016a), but empirical data to constrain such factors are currently unavailable.

Rather than assume that a constant fraction of an input is exported in a particular year (Eshleman et al. 2013), N retention in LLUS-N varies as a function of annual discharge (Chen et al. 2016b, Chen et al. 2018). The unitless product of the scaling factor and annual discharge (e.g., $\boldsymbol{B_u R_{w,t}}$, units are yr m^{-1} and m yr^{-1}, Table 10**)** determines the proportion of the input/surplus exported from a specific land use or point source in a given year. As such the retention (***A***) of inputs/surpluses can be calculated by subtracting the proportion exported in each year from 1 (e.g., $\boldsymbol{A_u}$ = 1 - $\boldsymbol{B_u R_{w,t}}$). Since I am assigning constraints on the mean retention efficiencies to specific land uses and point sources for the period of record (listed below), the mean export efficiency ($\overline{\boldsymbol{B_u R_{w,t}}}_{\boldsymbol{,1986-2012}}$) can also be calculated (e.g., 1 – $\boldsymbol{A_u}$= $\overline{\boldsymbol{B_u R_{w,t}}}_{\boldsymbol{,1986-2012}}$). The mean annual discharge is known for all three catchments, so the scaling factor can be solved by rearranging the equation (e.g., $\frac{1-\overline{A_u}}{\mathbf{R_{w,1986-2012}}} = \boldsymbol{B_u}$, Table 11). In the mid-Atlantic, $\boldsymbol{B_a}$ is far less constrained, but this parameter was effectively estimated by difference since we relied on the literature to constrain retention of other sources of N in the catchment.

Long-term catchment input-output budgets along with other empirical modeling studies were used to constrain retention for urbanized areas ($\boldsymbol{A_u}$**,** 60-85%, Groffman et al. 2004, Kaushal et al. 2008, Buda and DeWalle 2009, Bettez et al. 2015, Groffman et al.

2017, Hobbie et al. 2017) and forests ($\boldsymbol{A_f}$, 75-95% Eshleman et al. 2013, Eshleman and Sabo 2016). Recent work quantifying the role of in-stream processing in attenuating nitrate loads to stream network in the mid-Atlantic (specifically POTW) was used to constraint retention rates for point source loads ($\boldsymbol{A_p}$, 10-30%, Beaulieu et al. 2011, Miller et al. 2016).

Parameter uncertainty for all model coefficients was also estimated in SigmaPlot 14.0 concurrent with non-linear regression by first identifying the asymptotic standard error for the best-fit parameters and calculating 95% confidence intervals through the reduced chi-square method (all part of the SigmaPlot 14.0 non-linear regression tool). Model sensitivity to parameterization was evaluated by calculating the change in the Nash-Sutcliffe Coefficient (ΔNSE) and the proportional change in catchment TN export to proportional change in an individual scaling factor. Similar to other modeling studies (Chen et al. 2018, Hu et al. 2018, Sha et al. 2018), model performance was primarily evaluated using the NSE, but model residual time series were visually compared with the residual time series of the linear discharge model.

Table 11. Pre-defined maximum and minimum scaling factor constraints (yr m^{-1}) for the point source loading, urban, and forest (B_p, B_u, and B_f) based on literature reported retention values (%, A_u, A_p, A_f) . The agricultural scaling factor (B_a) and retention value (A_a) was solved by difference (since agriculture is the remaining source of N export).

	POTW	**SFSR**	**NFSR**	**REFERENCES**
$\boldsymbol{B_u}$ $\boldsymbol{A_u}$	0.41-1.10 85-60%	0.43-1.15 85-60%	0.52-1.38 85-60%	Groffman et al. 2004, Kaushal et al. 2008, Buda and DeWalle 2009, Bettez et al. 2015, Groffman et al. 2017, Hobie et al. 2017
$\boldsymbol{B_p}$ $\boldsymbol{A_p}$	1.66-2.49 30-10%	1.73-2.59 30-10%	2.07-3.11 30-10%	Beaulieu et al. 2011, Miller et al. 2016
$\boldsymbol{B_f}$ $\boldsymbol{A_f}$	0.14-0.69 95-75%	0.14-0.72 95-75%	0.17-0.86 95-75%	Eshleman et al. 2013, Eshleman and Sabo 2016
$\boldsymbol{B_a}$ $\boldsymbol{A_a}$	1.07-1.55 61-44%	0.32-0.55 88-80%	0.54-0.77 85-78%	NA, solved by difference

Results

Changes in the inputs, transformations, and surpluses of N

Fertilizer N, manure N, and total atmospheric N deposition were consistently the largest sources of N inputs in all three catchments (Figure 16). Agricultural surpluses increased 51% and 66% from 1986 to 2012 at NFSR and SFSR, respectively. This increase in surplus N was primarily driven by increased manure application rates that exceeded increased crop harvest rates by >100% in both catchments over the period (Table 12, Figure 16). Declines in atmospheric N deposition and increased crop harvest resulted in nutrient use efficiency (~40%) remaining approximately constant throughout the period of record, however (Figure 16). While shifts in agricultural fluxes and surpluses were similar among the two adjacent Shenandoah catchments, differences in point source loads were apparent (Figure 17). Point source loads were three to four times larger at SFSR at the beginning of the record and dramatically declined (63% ±4%) over the period of record to 0.6 kg N ha^{-1} yr^{-1} (Figure 17), whereas point source loads actually increased at NFSR until the early 2000s before beginning to decline to rates lower than those observed in the 1980s.

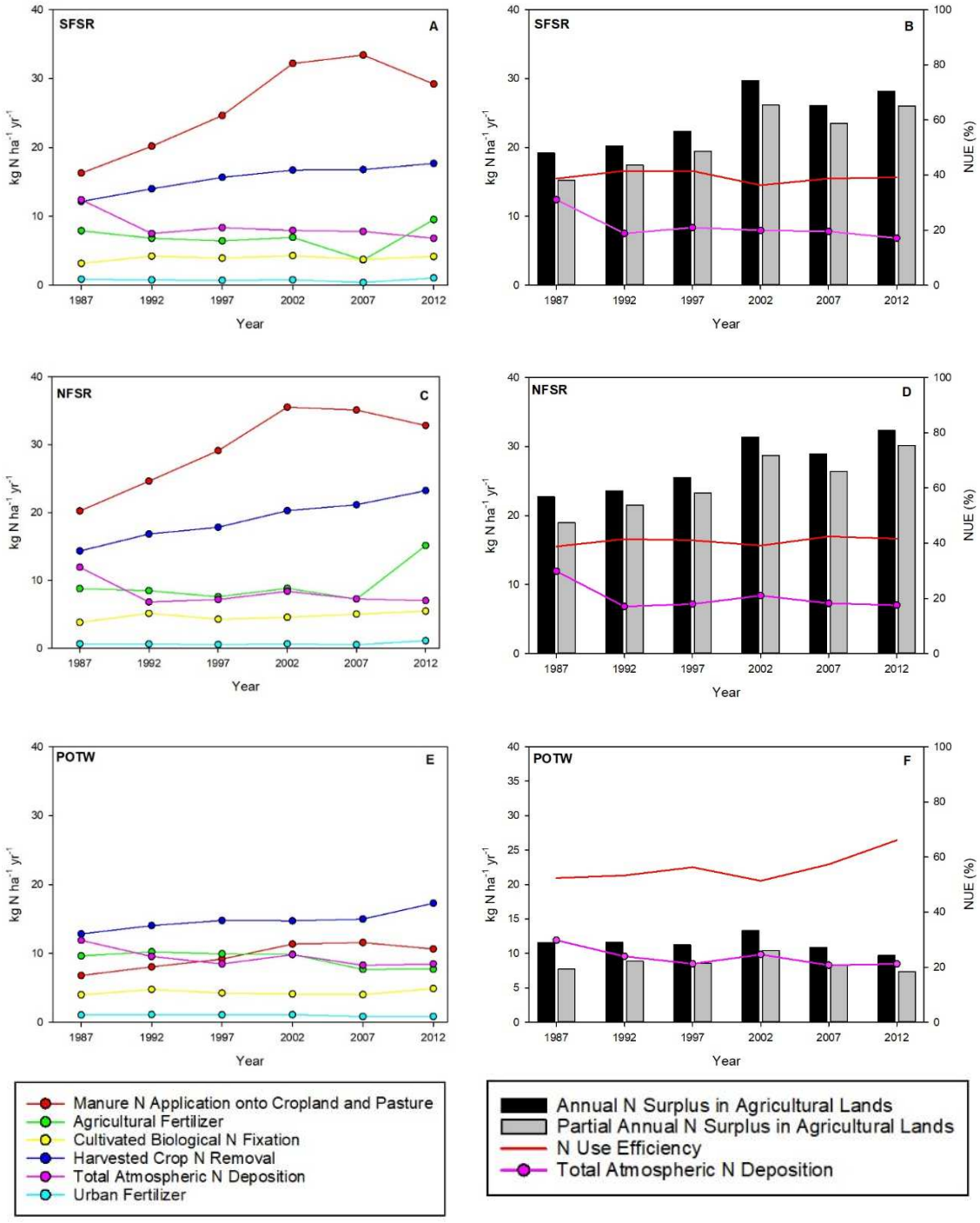

Figure 16. Annual N input and crop N removal rates along with associated changes in agricultural surplus and nitrogen use efficiency for North Fork Shenandoah River (NFSR), South Fork Shenandoah River (SFSR), and Potomac River at Chain Bridge (POTW). For illustrative purposes, only data centering on the Agricultural Census are plotted. Partial Annual N Surplus excludes N deposition as an input into agricultural lands.

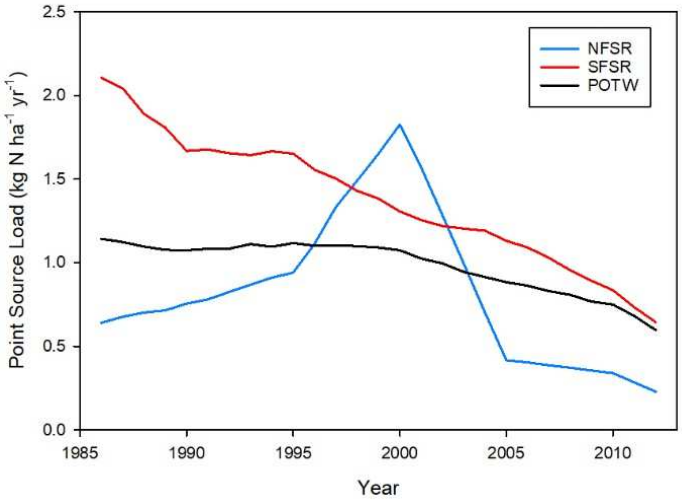

Figure 17. Time series of annual point source loading rates normalized by catchment area for North Fork Shenandoah River (NFSR), South Fork Shenandoah River (SFSR), and Potomac River at Chain Bridge (POTW).

Total atmospheric N deposition and agricultural fertilizer application each declined by ~30% in POTW, whereas manure N applied to pastures and cropland, as well as urban fertilizer use, increased dramatically (i.e., 72% and 66%, respectively, Table 12). The increase in manure and urban fertilizer application offset the decline in agricultural fertilizer use and atmospheric N deposition in POTW, resulting in total inputs being essentially equivalent in 1986 and 2012. However, harvested crop N removal increased 19% (±9.1%) in POTW. Annual N surplus on agricultural lands in POTW declined over the period of record (Table 12), but NUE increased by ~60% between 2002 and 2012 (Figure 16). Generally, annual N surpluses and partial annual N surpluses (excluding N deposition as an input) in agricultural lands were increasing until ~2002, but declined throughout the latter part of the record--a period when atmospheric N deposition was also declining. While annual N surpluses on agricultural lands declined coincident with decreased atmospheric N deposition (Figure 16), partial annual N surpluses in agricultural lands in POTW did not change from 1987 to 2012 and remained

at ~7.5 kg N ha^{-1} yr^{-1} (Table 12). Point source loading strongly decreased by 39% (±7.8%), with declines beginning in the late 1990s (Figure 17, Table 12). Although this relative decline is impressive on a percentage basis, point sources loads are 5 to 10 times smaller than other nitrogen inputs onto the catchment (Figure 16 and Figure 17).

Table 12. Linear estimates of absolute and relative changes for agricultural mass balances, N input, point source loading, and crop N removal rates during the 1986-2012 period along with associated 95% confidence intervals. Bold text indicates significant changes through time using simple linear regression ($p<0.05$) unless indicated otherwise.

	NFSR		**SFSR**		**POTW**	
	Absolute Change (95% C.I.) (kg N ha^{-1} yr^{-1})	Relative Change (95% C.I.) (%)	Absolute Change (95% C.I.) (kg N ha^{-1} yr^{-1})	Relative Change (95% C.I.) (%)	Absolute Change (95% C.I.) (kg N ha^{-1} yr^{-1})	Relative Change (95% C.I.) (%)
Annual N Surplus in Agricultural Lands	**11.1 (9.2-13.0)**	**50.8 (42.2 – 59.5)**	**12.0 (9.9-14.1)**	**65.6 (54.4-77.0)**	**-1.2 (-2.8 – -0.4)**	-9.9 (-23.2 – 3.3)
Partial Annual N Surplus in Agricultural Lands	**12.1 (10.4 – 13.9)**	**64.8 (55.3 – 74.3)**	**13.2 (11.3 – 15.1)**	**88.7 (76.0 – 101.4)**	0.0 (-1.3 – 1.3)	-0.4 (-15.5 – 14.7)
Manure N Applied to Pasture and Cropland	**15.8 (12.7 -18.9)**	**72.8 (58.5-87.2)**	**17.8 (14.6 – 21.0)**	**105.2 (86.2 – 124.2)**	**5.1 (4.1 – 6.0)**	**72.0 (58.3 – 85.7)**
Agricultural Fertilizer Application	**2.6 (0.5 – 4.7)**	**34.2 (6.1 – 62.3)**	-0.6 (-2.2 – 1.0)	-8.7 (-31.4 -14.0)	**-3.4 (-4.5 - -2.3)**	**-31.7 (-42.2 - -21.2)**
Cultivated Biological N Fixation	0.5 (-0.1 – 1.2)	12.0 (-2.9 – 27.0)	0.1 (-0.5 – 0.7)	2.4 (-13.3 – 18.0)	-0.2 (-0.74 – 0.28)	-5.3 (-17.1 – 6.4)
Harvested crop N removal	**6.9 (4.9 – 8.9)**	**46.2 (32.6 – 59.8)**	**4.1 (2.3 – 6.0)**	**31.9 (17.8 – 46.0)**	**2.5 (1.3 – 3.7)**	**19.0 (9.9 – 28.1)**
Point Source TN loading	**-0.51*** **(-0.7 – -0.3)**	**-43.6*** **(-23.2 – 64.8)**	**-1.3 (-1.4 - -1.2)**	**-63.1 (-59.1 - -67.0)**	**-0.5 (-0.6 - -0.4)**	**-37.7 (-45.5 - -29.9)**
Total Atmospheric N Deposition	**-3.7 (-5.9 - -1.5)**	**-38.2 (-60.8 - -15.7)**	**-3.8 (-5.8 - -1.9)**	**-37.3 (-56.0 - -18.5)**	**-3.6 (-5.7 - -1.6)**	**-32.0 (-50.0 - -14.0)**
Urban Fertilizer Application	**0.3 (0.2 – 0.4)**	**115.1 (71.8 – 158.3)**	**0.3 (0.1 – 0.5)**	**70.4 (32.7 – 108.2)**	**0.7 (0.3 -1.1)**	**65.5 (26.0 – 105.1)**

***** *Linear estimates of absolute and relative changes were calculated using a non-linear regression procedure to better constrain uncertainty estimates for this more complex time series (Hu et al. 2015, Van Meter et al. 2017, Chen et al. 2018).*

The relationship of observed catchment retention and export with annual discharge

Catchment N export, illustrated as yield to facilitate comparison among all three catchments, increased with increased discharge (Figure 18). Annual discharge was observed to explain most of the inter-annual variation in catchment export in the three catchments. Further inspection of the residual time series revealed distinct temporal structures that could be potentially explained by other drivers (explored in sections below). Ignoring the 1986 data point (a very high flow year at the beginning of the WRTDS calibration dataset) at POTW, catchment yield residuals were generally constant from the mid-1980s through the mid-1990s, then steadily declined post-1996. My interpretation is that a process independent of discharge appears to be driving declines in TN export at POTW after the mid-1990s. Likewise, residuals were consistently positive at SFSR from 1987 to 1994. Thereafter, residuals were generally more negative at SFSR. Residuals became progressively more positive until the early 2000s at NFSR and began to decline after 2004. It should be noted, after evaluating the standardized residuals from the regression analysis, the TN export values from 1986 at POTW and from 2012 at SFSR were flagged as outliers and are not representative of their respective population trends. This was not entirely unexpected, since interpreting the tail ends of WRTDS runs should be done with caution. Both residual values (i.e., 1986 for POTW and 2012 for SFSR) were excluded from subsequent statistical analysis.

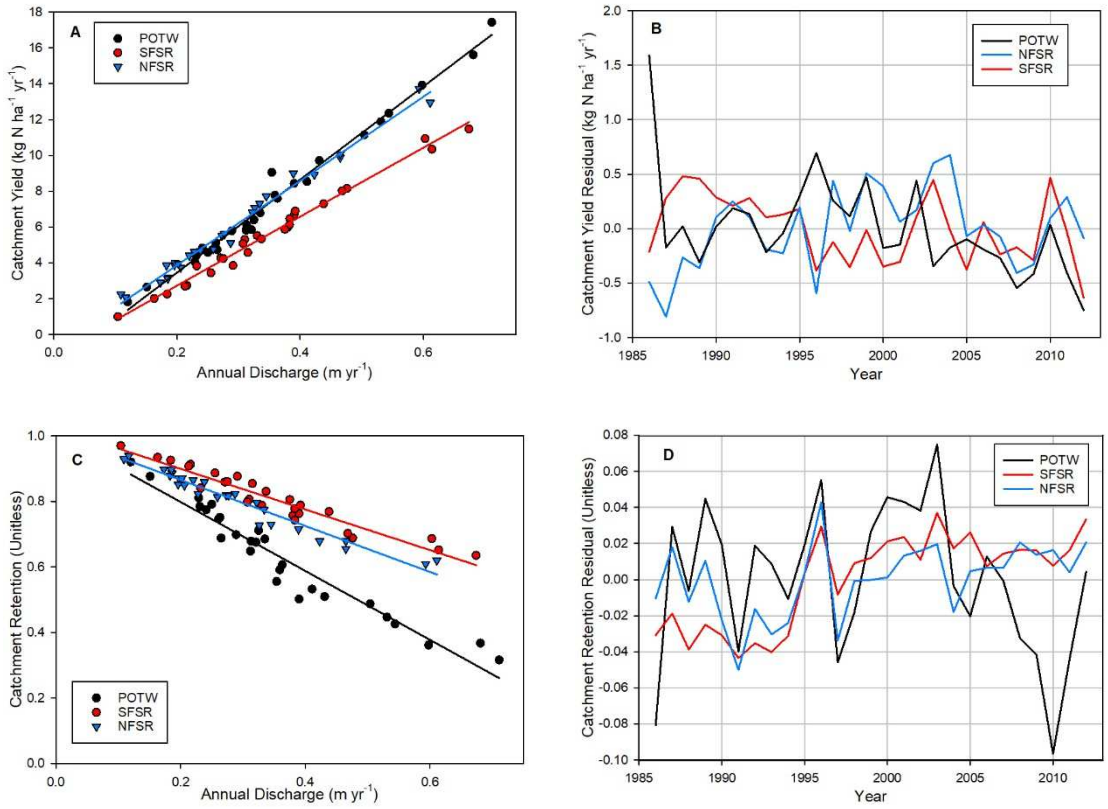

Figure 18. A) Scatterplot displaying the relationship between annual discharge ($R_{w,t}$) and catchment yield ($\frac{E_{w,t}}{Area}$, catchment export normalized by catchment area). This is the discharge model. Catchment export increased with increased discharge in all three catchments (for Potomac River at Chain Bridge (POTW): y = 26.0x -1.7, r2=0.99, p <0.01; for North Fork Shenandoah River (NFSR): y = 23.5x -0.8, r2=0.98, p <0.01; for South Fork Shenandoah River (SFSR): y = 19.3x – 1.1, r2=0.98, p <0.01). B) Residual time series of catchment yield after removing the linear effect of annual discharge. C) Scatterplot displaying the relationship between annual discharge and retention (i.e., $\frac{\sum I_{a,t},I_{u,t},I_{f,t}I_{p,t}-E_{w,t}}{\sum I_{a,t},I_{u,t},I_{f,t},I_{p,t}}$) of nitrogen inputs ($I_{a,t}$, $I_{u,t}$, and $I_{f,t}$) and point source loading ($I_{p,t}$). Retention decreased with increased discharge (For POTW: y = -1.1x + 1.01, r2=0.93, p <0.01; for NFSR: y = -0.7x + 1.01, r2=0.95, p <0.01; for SFSR: y = -0.6x + 1.02, r2=0.91, p <0.01). D) Residual time series of catchment retention after removing the linear effect of annual discharge.

Using the observed terrestrial N flux, point source loading, and WRTDS export time series, I assessed the inter-annual variation in observed retention efficiencies after removing the linear effect of discharge. From 1986 to 2012, POTW retained 62% of net inputs and point source loads, whereas NFSR and SFSR had retention values of 80 and 81%, respectively. Retention decreased with increased discharge, however (Figure 18). After removing the linear effect of discharge, retention efficiencies in POTW generally

varied ± 10% through time (note that retention values are shown in unitless proportions). POTW demonstrated a sudden negative shift in retention efficiency of 10% from 2009 to 2010 (a particularly wet year with a major rain on snow driven flood in late winter), however (Figure 18). This negative residual was not present after 2010. Outside of 2010, retention is mostly stable over the period of record at POTW. In contrast, retention was consistently lower at SFSR and NFSR from 1986 to 1994. It should be noted that only the population of negative residuals for the 1986 to 1994 period were considered significantly different from 0 only for SFSR ($p<0.01$, one tailed t-test), however. After 1994, retention residuals stabilized at NFSR (bounced around zero) but became consistently positive at SFSR. These results suggest that retention was 3 to 4% higher post-1995 relative to the 1986-1994 period at SFSR.

Approach #1: Potential drivers of discharge model residuals

Time series of the discharge model residuals were further examined to elucidate the drivers of catchment TN export. Through time, residual catchment export was observed to be positively correlated with point source loading in all three catchments, but this correlation was only significant in POTW (Table 13). Significant positive correlations ($p < 0.05$) between annual N surplus in agricultural lands and residual catchment export were detected in both NFSR and POTW. Positive correlations between predictor and response variables leveraging the interpolated time series were consistent with correlations using non-interpolated time series (Table S6). Furthermore, forest inputs, annual N surplus in agricultural lands, and point source loads were highly correlated, but not statistically significant ($r > 0.5$, Table S6). Negative correlations between predictor and response variables suggest a negative relationship between inputs and residual catchment export through time. These negative correlations likely capture

input and export residual trends moving in opposite direction (e.g., forest N inputs going down but export residuals increasing at NFSR) and likely indicates the input variable does not greatly influence the inter-annual variability in catchment N export residuals.

Table 13. Pearson correlation coefficients between predictor variables and the discharge model residuals. Bold indicates a significant correlation ($p < 0.05$). Correlation among predictor variables and the discharge model residuals using non-interpolated time series is reported in the Appendix (Table S6).

	Catchment Export Residuals POTW	Catchment Export Residuals SFSR	Catchment Export Residuals NFSR
Urban Inputs ($I_{u,t}$)	-0.05	-0.36	-0.15
Annual N Surplus in Agricultural Lands ($I_{a,t}$)	**0.54**	-0.26	**0.41**
Forest Inputs ($I_{f,t}$)	0.34	0.16	-0.35
Point Source Loading ($I_{p,t}$)	**0.58**	0.30	0.35

After removing the linear effect of discharge from the predictor variables, all linear combinations of predictor variables explaining residual catchment export were evaluated using ΔAICc. All model combinations generating positive slope coefficients and ΔAICc < 2 were reported (Table 14). At NFSR and POTW, the "agricultural surplus and point source model" were identified as effective models in explaining residual catchment export from the discharge model (Table 14). Slope coefficients of annual N surplus in agricultural lands ($I_{a,t}$) were similar in both catchment (~0.06), but coefficient estimates for point source loading varied three-fold between the catchments (0.33 vs. 1.04, Table 14). The slope coefficient estimates for point source loading were consistently greater than 1.0 for POTW in both the point source and agricultural surplus and point source models. Parameter values greater than 1.0 means that the change in total catchment export exceeded the change in point source load. As such, another source of N to catchment export covaries with point source loads. This parameterization suggests that, while the statistical correlation between point sources loads and catchment TN export is strong, the decline in point source loading cannot fully account for the decline in

catchment TN export at POTW on a per-unit-mass basis. The top performing models for NFSR and POTW were highly effective in modeling the trajectory of catchment TN export (Figure 19) and explained a moderated amount of the variance ($R^2 > 0.3$, Table 14). Furthermore, they were generally found to be unbiased as R^2 and NSE were found to be equivalent. In contrast, the best model for SFSR (i.e., the "point source model") explained little of the variance in catchment export residuals (Table 14, $R^2 = 0.09$) and was unable to model the sudden negative shift in residuals after 1995 (Figure 19). It should be noted that identified predictor variables and their sign were similar using the same model selection procedure and the non-interpolated time series centered on the Agricultural Census (Table S7).

Table 14. For all model combinations generating ΔAICc < 2 and positive slope coefficients, statistical outputs of the exploratory modeling analysis used to explain temporal patterns in the discharge model residuals (kg N ha^{-1} yr^{-1}) as a function of inputs (kg N ha^{-1} yr^{-1}). Coefficient estimates along with 95% C.I. were reported. Bolded text indicates coefficient estimate was significantly different from zero, a blank indicates the parameter was not included in the model.

Catchment	Model Reference	Urban Inputs ($I_{u,t}$)	Annual N Surplus in Agricultural Lands ($I_{a,t}$)	Forest Inputs ($I_{f,t}$)	Point Source Loading ($I_{P,t}$)	ΔAICc	R^2	NSE
NFSR	Agricultural Surplus and Point Source		**0.05 ± 0.04**		**0.33 ± 0.28**	0.00	0.30	0.30
SFSR	Point Source				0.25 ± 0.31	0.00	0.09	0.08
	Forest			0.06 ± 0.12		1.72	0.03	0.02
POTW	Point Source				**1.38 ± 0.69**	0.00	0.38	0.38
	Agricultural Surplus and Point Source		0.07 ± 0.11		**1.04 ± 0.85**	0.63	0.40	0.39

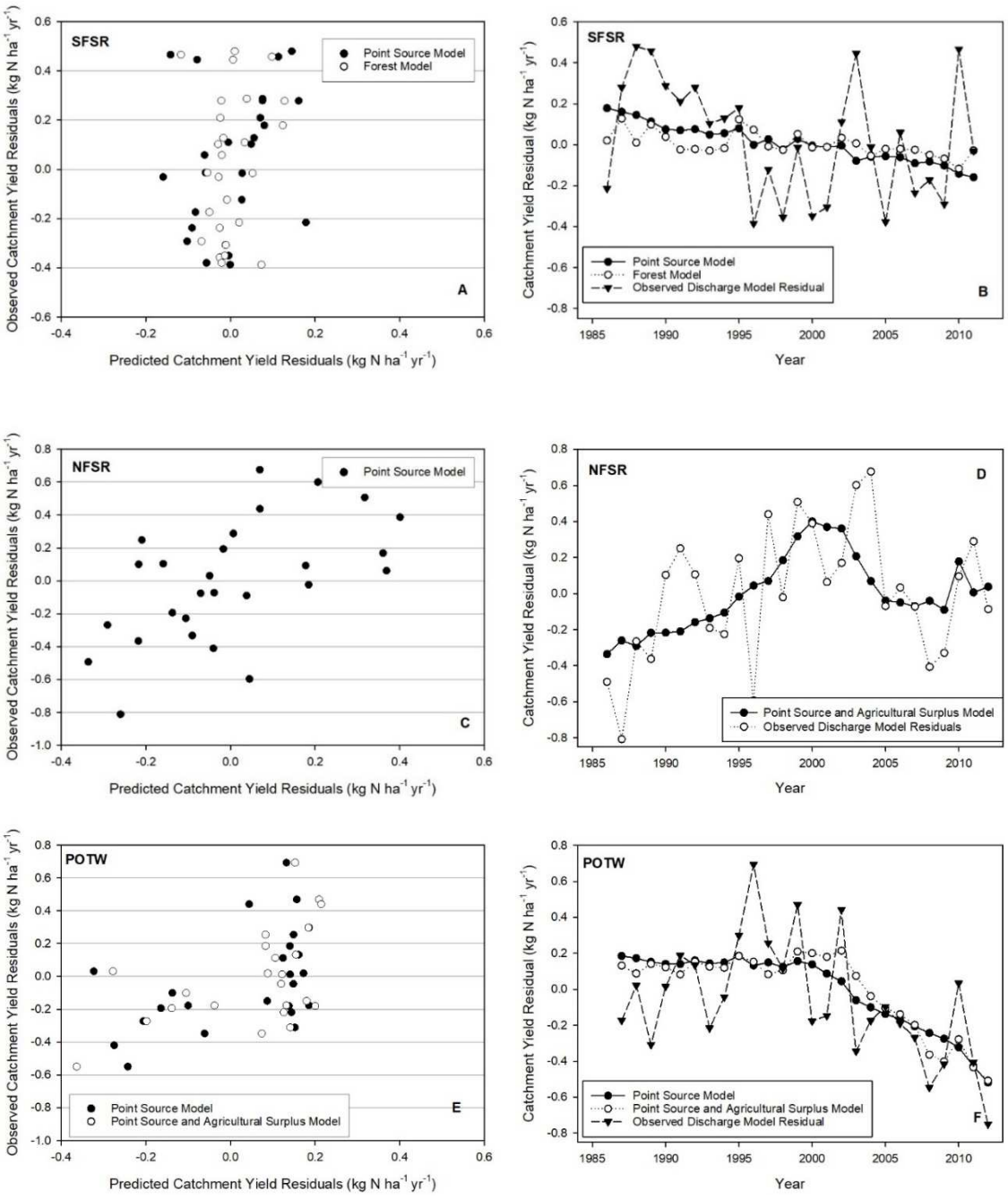

Figure 19. Scatterplots of predicted vs. observed catchment export residuals (A, C, E) along with time series of export residuals and predicted export from the most efficient models as identified by ΔAICc (B, D, F).

Approach #2: LLUS-N Results

Literature values for N retention were used to constrain point source export and non-point source exports from forested and urban lands. By difference, the range of agricultural retention was then predefined to fully constrain all the individual scaling factors in LLUS-N, and these parameters along with associated uncertainty were evaluated through non-linear regression. All model iterations successfully converged and best model fit solutions explained 96% of the variance in catchment TN export using the custom non-linear regression tool in SigmaPlot 14.0. Issues of equifinality were highlighted in the parameter uncertainty analysis since all possible parametrizations fell within the 95% confidence intervals (Table 15), thus indicating that a variety of parametrizations within the predefined parameter constraints were possible at generating similarly performing models.

In order to then better elucidate the sensitivity of the model to parameterization, scaling factors were individually adjusted ±50% to determine the proportional impact of parameterization on catchment export (S) and model performance as measured by the difference in the best fit model NSE (Nash-Sutcliffe efficiency) and the adjusted model (ΔNSE, Table 16). Catchment export was most sensitive to the retention of annual N surplus in agricultural lands with a 10% change in $\boldsymbol{B_a}$ resulting in a >7.5% change in catchment export in POTW and NFSR. While catchment export was most sensitive to changes in $\boldsymbol{B_a}$ at SFSR (41%, Table 16), $\boldsymbol{B_u}$ and $\boldsymbol{B_f}$ were also influential. This greater influence was likely reflective of SFSR having the highest point source loads (after normalizing by area) for most of the record among the three catchments (Figure 17). Changes in $\boldsymbol{B_a}$ consistently produced the greatest changes in NSE (0.4 – 0.79, Table 16).

Thus, constraining the retention of agricultural surpluses in all three catchments was imperative for limiting bias and maintaining explanatory power.

Table 15. Resulting parameterization and long-term retention values along with predefined constraints for individual sources of catchment TN export of LLUS-N using non-linear regression. After evaluating the parameter uncertainty, all possible parameterizations within the predefined range of parameter constraints were within 95% confidence bounds thus indicating issues of equifinality.

		Urban (B_u)	**Agriculture (B_a)**	**Forest (B_f)**	**Point (B_p)**	**NSE**
NFSR	Parameter	0.52 (0.52 – 1.38)	0.69 (0.54 – 0.77)	0.32 (0.17 – 0.86)	2.58 (2.07 – 3.11)	0.96
	Retention	85% (60 – 85%)	80% (78 – 85%)	91% (75 – 95%)	26% (10 – 30%)	
SFSR	Parameter	0.43 (0.43-1.15)	0.41 (0.32-0.55)	0.62 (0.14 – 0.72)	2.59 (1.73 – 2.59)	0.96
	Retention	85% (60 – 85%)	86% (80 – 88%)	78% (75 – 95%)	10% (10 – 30%)	
POTW	Parameter	0.62 (0.41–1.10)	1.42 (1.07–1.55)	0.16 (0.14–0.69)	2.49 (1.66–2.49)	0.96
	Retention	78% (60 – 85%)	49% (44 – 61%)	94% (75 – 95%)	10% (10 – 30%)	

Table 16. The proportional change in catchment TN export relative to the proportional change in individual parameterization (S) along with the absolute change in model performance as measured by the difference in Nash-Sutcliffe coefficient between the originally calibrated models and models with individual parameters adjusted ±50% (ΔNSE).

	POTW		SFSR		NFSR	
	S*	**ΔNSE**	**S***	**ΔNSE**	**S***	**ΔNSE**
B_p (±50%)	0.14	-0.01	0.34	-0.08	0.10	-0.02
B_f (±50%)	0.05	-0.002	0.21	-0.06	0.10	-0.01
B_u (±50%)	0.04	-0.002	0.04	-0.001	0.04	-0.001
B_a (±50%)	0.78	-0.793	0.41	-0.40	0.76	-0.74

**Sensitivity is proportional change of variable y, relative to baseline y_b, divided by the proportional change in parameter x, relative to the baseline value x_b (i.e., when simplified $S = \left|\frac{(y-y_b)*x_b}{(x-x_b)*y_b}\right|$). As such, if a 10% change in x results in a 10% change in y then S = 1.*

LLUS-N explained much of the inter-annual variation in catchment TN export (Figure 20). This result was not unexpected considering the strong linear correlation between catchment export and annual discharge (Figure 18A). All observed WRTDS catchment export values fell within the 95% prediction intervals of LLUS-N. This observation is somewhat impressive, considering the discharge-concentration relationships in WRTDS can vary through time (Zhang 2018), whereas the LLUS-N is a fixed effect model (akin to LOADEST). As such, it seems likely the discharge-

concentration relationships have not substantially changed at POTW, NFSR, and SFSR for the period. Further inspection of the residual time series revealed short periods of consistent over- or under-prediction during the record, however. The most apparent among all three catchments is during the 1999-2002 drought period where LLUS-N consistently overpredicted catchment TN export (negative residuals, Figure 20). Likewise, LLUS-N generally underpredicted catchment export in the late 1980s and early 1990s in SFSR and NFSR that was followed by a period of overprediction that generally decayed towards the end of the record.

After model calibration and evaluation, LLUS-N was leveraged to attribute trends in catchment TN export by modeling catchment export along with point and non-point source export contributions to TN export under mean discharge conditions (Figure 21). Linear slope and intercept estimates of individual point and non-point source loads were then used to estimate linear changes in catchment TN export along with point and non-point source export over the period of record. Consistent with insights from the statistical analysis of the discharge model residuals, declines in agricultural N surpluses and point source loads were the primary drivers of decreased catchment TN export at POTW (Figure 21B). Even relying on the maximum range of the parameter constraints in LLUS-N, modeled declines were different from zero in POTW, with a TN export decline of 11 to 17% over the period of record. Also, consistent with insights from the statistical analysis, point source loads and increases in agricultural surpluses were primarily responsible for the 24% increase in TN export at NFSR (15 to 24% increase overall if relying on the max and minimum parameter range). SFSR displayed little to no change in TN export over the period of record, however, with observed declines in the point source

load and non-point source load from forested areas just offsetting increases in export associated with an increase in the agricultural N surplus.

The modeled net effect of NO_x emission controls on improving catchment TN export was also further explored. I applied a scenario where the observed declines in atmospheric N deposition did not occur in all three catchments (Figure 21). If the mean atmospheric deposition rate for the 1986 to 1996 period is used to replace all observed annual values to all land uses for the 1997 to 2012 period, the 13% modeled decline in catchment TN export (Figure 21) would have been reduced by ~75% at POTW (i.e., only a 3% decline, Figure 21). Likewise, the modeled increase in catchment TN export at NFSR would have increased from 24 to 40%. Rather than experiencing a weak decline in export, catchment TN export would have actually increased 10% at SFSR if not for reductions in atmospheric N deposition.

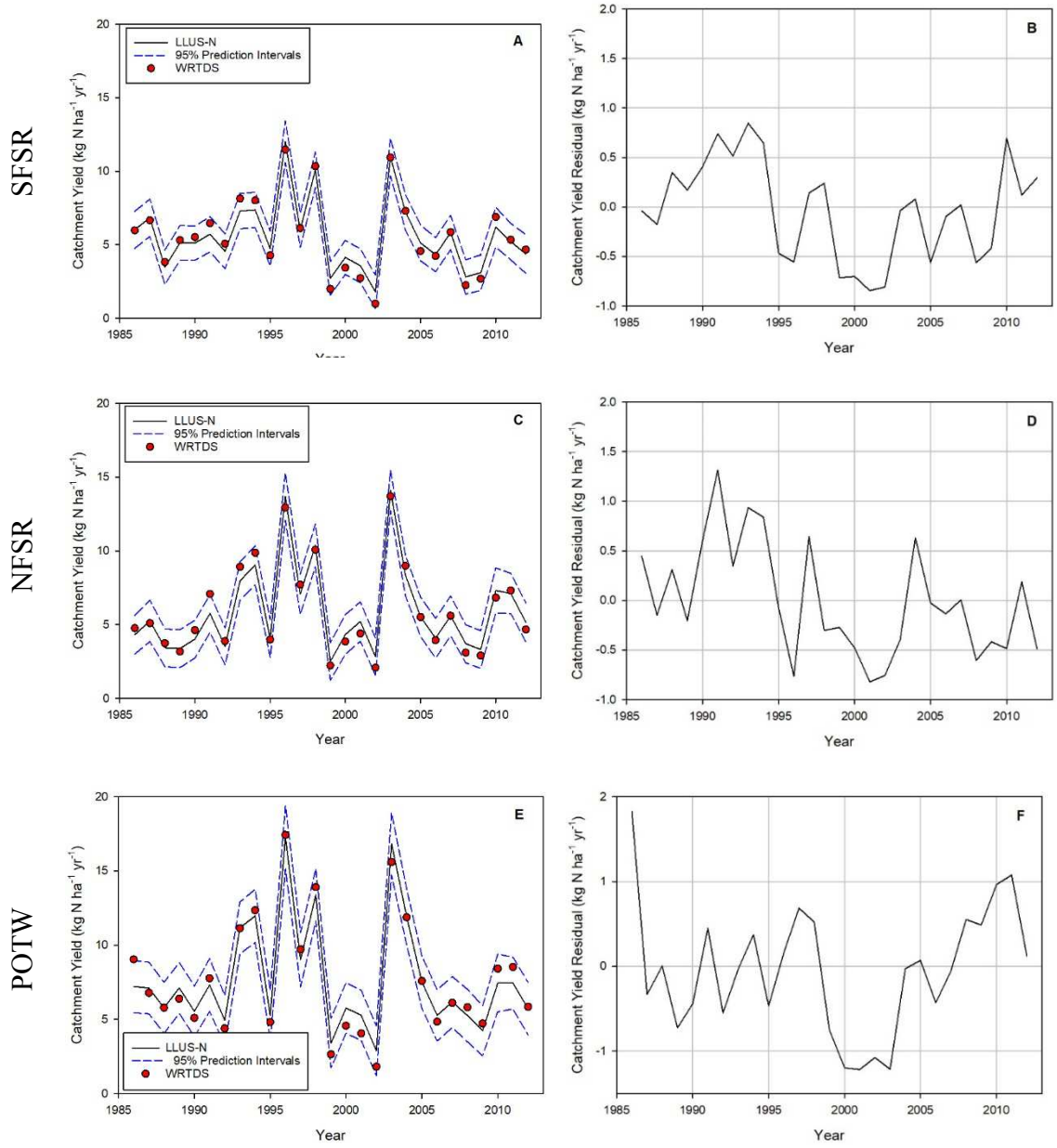

Figure 20. Time series of predicted (black line) and observed WRTDS (red dots) catchment export values (reported as yield) along with a time series of LLUS-N model residuals.

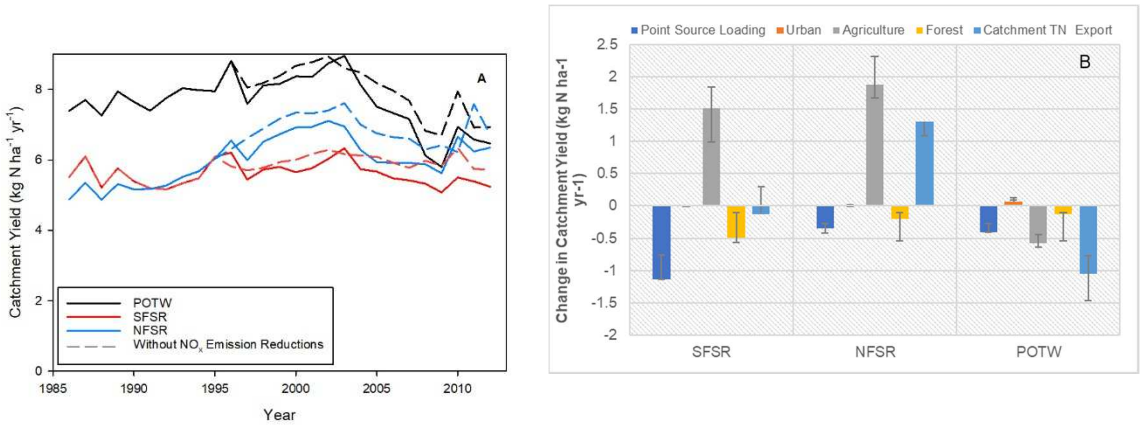

Figure 21. A) Time series of predicted catchment TN export (illustrated as yield to facilitate comparison among catchments) under mean annual discharge conditions, along with an applied scenario where observed declines in atmospheric N deposition did not occur (dashed lines). The mean atmospheric N deposition for the 1986 to 1996 period replaced all observed values from 1997 to 2012. B) Linear change estimates in point and non-point source load contributions to catchment TN export (illustrated as yield), asymmetric error bars represent the range of change if relying on the range of maximum and minimum scaling factors of LLUS-N.

Discussion

Both the statistical and lumped conceptual modeling analyses provide new support for the interpretation that declining atmospheric N deposition was likely the primary cause of declining catchment TN export in POTW (Eshleman and Sabo 2016). This inference is based on the following observations from the modeling work: 1) declining atmospheric N deposition was the primary driver of decreasing N export from urban, forested, and agricultural areas; 2) partial annual N surpluses in agricultural lands were equivalent in 1986 and 2012 (~7.5 kg N ha yr^{-1}, grey bars in Figure 16F) due to increases in crop removal and decreases in fertilizer inputs being largely offset by increased manure inputs; and 3) despite the observation of partial annual N surpluses remaining constant in POTW, agricultural N surpluses declined by 1.2 kg N ha^{-1} yr^{-1} due mostly to corresponding reductions in atmospheric N deposition decreasing agricultural inputs by 3.6 kg N ha^{-1} yr^{-1} (black bars and pink line in Figure 16F). From a kinetic N saturation perspective (Lovett and Goodale 2011), a decline in N input would result in a corresponding decrease in catchment TN export if discharge-retention relationships are

constant through time (Zhang 2018). Thus, based on simple accounting from the model, the reductions in atmospheric deposition decreased inputs and surpluses across the POTW thereby decreasing modeled non-point source loads across the catchment. This principle is clearly illustrated in the "without NO_X emission reductions" scenario that essentially eliminated modeled declines in non-point source loads in POTW (dashed black lines, Figure 22). While reductions in non-point source loads were the primary driver of water quality improvement, reduction in point source loads was also an important factor for POTW (~40%).

The importance of atmospheric N deposition in offsetting further degradation of modeled water quality at NFSR and SFSR is apparent (Figure 22). Declining atmospheric N deposition was the primary driver of decreasing modeled N export from forested and urban portions of these basins. It also offset modeled water quality degradation brought about by increased agricultural surpluses by decreasing inputs by 3.8 kg N ha^{-1} yr^{-1}. The influence of atmospheric N deposition on catchment TN export is not as large as it is in POTW for LLUS-N, however, due to the high retentiveness of agricultural lands (~80%) and extremely high annual agricultural surpluses in the Shenandoah catchments (40 to 90 kg N ha^{-1} yr^{-1} if normalized by agricultural area). Also unlike in POTW, declines in atmospheric N deposition, even if diminished to background levels (< 2 kg N ha^{-1} yr^{-1}), would not have been capable of offsetting increases in agricultural surpluses brought about increased fertilizer/manure inputs. The magnitude of difference in N sources within these catchments highlight that further efforts to attenuate atmospheric N deposition will have minimal impact unless catchment NUE dramatically increases or manure transport programs are implemented to reduce N inputs (Keisman et al. 2018, Swaney et al. 2018).

These modeling insights are admittedly rooted in a simple model relying on coarse, catchment-scale nitrogen budgets that likely cannot be corroborated with observations at the field scale. In order to conclusively state that reductions in atmospheric deposition were instrumental in decreasing agricultural surpluses and subsequent contributions to catchment TN export, long-term field monitoring data documenting changes in N pools along the hydrologic continuum are needed (e.g., trends in soil NO_3, groundwater NO_3, to tile line drainage NO_3). To my knowledge, the availability of such time series capable of capturing catchment-wide changes in NO_3 levels and leaching rates from agricultural areas do not exist across POTW. Furthermore it is uncertain even if small changes in annual N surpluses relative to the large legacy N pool present in soils could even alter catchment TN export (Sanford and Pope 2013, Chen et al. 2018). Many recently forwarded empirical models have indicated that catchments would rapidly respond to changes in N inputs and surpluses at the catchment scale (Stets et al. 2015, Chen et al. 2016b, Eshleman and Sabo 2016, Sinha and Michalak 2016, Sinha et al. 2017), while other empirical modeling work highlights the importance of capturing legacy N effects in soils and groundwater in explaining catchment TN export trends (Chen et al. 2014, Chen et al. 2016a, Van Meter et al. 2017, Chen et al. 2018, Hu et al. 2018). Deploying a probabilistic sampling design and implementing experimental reductions of N inputs and surpluses to assess field response times is likely not feasible (at the scale of the catchment). Thus, future modeling and catchment monitoring work should prioritize comparing catchment wide responses to changes in N inputs and surpluses across many sites to better inform management strategies and set expectations

for the public when setting water quality goals (Keisman et al. 2015, Keisman et al. 2018).

Catchment-wide retention at POTW was observed to be 18% lower and more sensitive to discharge than its nested sub-catchments of NFSR and SFSR. This observation indicates that other areas in the POTW must have retention values less than 66% and have even greater sensitivity to increased discharge (i.e., slopes > 1.01, Figure 18). This inference is consistent with the observations of northern sub-catchments (e.g. Antietam, Upper Monocacy) having reported mean TN yields at least twice as large as those in SFSR and NFSR despite similar or sometimes even lower agricultural N surpluses (Chanat et al. 2016). This lower retention and greater yield is likely due to the fact that there is a much larger proportion of agricultural land being cultivated for crops in the Great Valley and Piedmont regions of POTW (primarily in Maryland and Pennsylvania) compared to the Shenandoah sub-catchments in Virginia (Table 9). At the field scale, retention of N surpluses on cropland are significantly lower than pasture (Billen et al. 2013). Other studies have also reported that more cropland dominated catchments have lower retention than other mixed land use catchments (David et al. 1997, Hong et al. 2013). Since grazing land is less likely to be tilled, it's possible that greater amounts of soil carbon and microbial/root biomass along with greater cover of the grass forage throughout the year promote greater retention of nitrogen inputs (Billen et al. 2013). Another reason why retention is significantly higher in the Shenandoah catchments may be due to that the fact the primary source of N comes from manure. Some have speculated that the increased availability of carbon from manure application may enhance denitrification (Weier et al. 1993), but other field studies comparing the

influence of manure vs. inorganic nitrogen fertilizer on nitrate and ammonium loss in cropland report more variable findings, however (Jokela 1992, Smith et al. 2007).

Based on visual inspection, retention of N inputs and point source loads were found to be generally stable throughout the period of record after removing the effect of annual discharge in two of the three catchments. This finding provides general support of the steady state assumption for calibration procedures of lumped empirical models parameterizing a single catchment retention factor (Dupas et al. 2017). Furthermore, the general stability of retention at NFSR and POTW suggests that best management practices designed to attenuate non-point source pollution did not have an apparent catchment-wide effect over the period. This finding does not necessarily dismiss the effectiveness of BMPs specifically designed to attenuate surplus nitrogen (e.g., stream restoration, riparian buffer planting, cover cops, etc.), but it does emphasize that the major drivers of TN export in larger catchments were likely driven more by high order input and removal processes during the observation period as well as climate in our study catchments (Howarth et al. 2012, Sinha and Michalak 2016).

Retention was consistently 3 to 4% lower at SFSR over the 1986-1994 period relative to the latter part of the record. As such, a catchment-wide retention factor cannot be confidently calibrated and applied throughout the period of record (Dupas et al. 2017). A more complex model would be needed. It is possible that the sudden change in catchment retention may have responded to forest N retention being compromised by acute and widespread disturbance brought about by gypsy moth (*Lymantria dispar dispar*) in the late 1980s and early 1990s (Eshleman et al. 1998, Eshleman 2000). The latter explanation is particularly relevant in SFSR (and partly in NFSR) because it

suggests that some of the perceived improvement in water quality attributable to management actions may be partly an artifact of increased forest loads to stream networks due to disturbance-induced N leakage near the beginning of the record. Disturbance-induced N leakage typically dissipates within five to seven years of peak disturbance for catchments in the Blue Ridge (Eshleman 2000), thus the disturbance signal may have mostly ended around the mid-1990s. Another possible explanation for the shift in retention is that the predominant N source in the catchment has changed, which would ultimately modify mean catchment retention. This mechanism was further explored in the statistical and LLUS-N analyses discussed further below.

Catchment TN export was highly correlated with annual discharge, but subsequent statistical analysis of the discharge model residual time series suggested that changes in point source loads and agricultural surpluses were the best predictors of temporal trends in all three catchments when using both interpolated and non-interpolated predictor variable datasets (as assessed by AICc). This responsiveness was not surprising considering point source and agricultural loading have been identified as two of the primary drivers of catchment TN export in mixed land use catchments of the Chesapeake region and elsewhere (Shields et al. 2008, Shenk and Linker 2013, Hale et al. 2015). In addition, the strong influence of point source loads and agricultural surpluses on variation in catchment TN export was also reflected in the parameter sensitivity analysis of LLUS-N, which indicated that point source loading and non-point source loads from agricultural lands had the highest relative influence on TN export (Figure 18).

This statistical analysis identified likely drivers of TN export at sites with only small incremental changes in point source loads and N inputs/surpluses through time.

Others have reported significant linear and non-linear relationships without removing the effect of discharge on export when both N inputs and TN export have greatly increased (>100% in some cases) (Chen et al. 2014, Chen et al. 2016b), but removing the linear effect of discharge on export and subsequent analysis of residuals is a simple and intuitive method for evaluating trends and identifying likely drivers of those trends through time at sites with less dramatic changes in inputs and export. This analysis provided evidence that a signal from management actions can be detected following removal of the effect of discharge and provided confidence that changes in agricultural surpluses and point source loads are influencing trends in catchment TN export.

The statistical insights into possible drivers of water quality trends in POTW and the Chesapeake Bay region at large further support conclusions of other empirical and more deterministic modeling efforts in the basin. Modeled reductions in TN loading to the Chesapeake Bay between the 1985 and 2009 scenarios of the Chesapeake Watershed Model (Phase 5.3) were mainly attributed to 1) regulated sources of atmospheric deposition and wastewater and 2) reductions in agricultural loading (Shenk and Linker 2013). However, there was uncertainty over the potential driver of decreased agricultural loading between the different scenarios since combined inputs of fertilizer and manure were generally constant from 1985 to 2009. Similar reductions in loading to the Chesapeake Bay have been suggested using statistical, NANI based models (Sinha and Michalak 2016), but it was unclear whether or not decreased NANI or lower precipitation rates were driving the decline. Past research in POTW suggested that the majority of the observed decrease in TN export could be attributed to reductions in atmospheric N emissions and subsequent declines in atmospheric deposition using a modified kinetic N

saturation model (Eshleman and Sabo 2016, Lloret and Valiela 2016). This study did not explore parallel changes in other N sources (e.g., increased manure production) or N removal (e.g., wastewater treatment plant upgrades or increased crop N removal) that may have also driven water quality trends, thus further work was needed to address these uncertainties.

Before expounding on insights provided by LLUS-N, it should be acknowledged that LLUS-N was not capable of eliminating all temporal patterns in the residual time series. LLUS-N performance was particularly poor 1) during the 1999-2002 drought period where it consistently overpredicted catchment TN export and 2) consistently underpredicted export in early 1990s in the Shenandoah catchments. Whether or not the inter-annual variation in yield residuals are ultimately meaningful is unclear, however, considering that the slightly shifting discharge-concentration relationships of WRTDS are only beginning to be explored (Zhang 2018).

The importance of annual discharge in driving the inter-annual variability in catchment TN export was instrumental in maintaining LLUS-N model performance. Discharge primarily determines the transport of terrestrial nitrogen pools into the stream network, in turn altering the residence time and flow paths of nitrogen and other elements traveling to the catchment outlet (Kirchner et al. 2000, Kirchner and Neal 2013). Discharge is also important in the fact that it carries the "memory" of climatic conditions of previous years, so the response of annual discharge to a given year's precipitation is variable given antecedent moisture conditions and the slow input of older groundwater (Kirchner et al. 2000, Kirchner and Neal 2013). Ultimately discharge or relevant variables to model discharge are keys to modeling the inter-annual variation in TN

export, but discharge alone was incapable of explaining reported trends in TN export at our sites.

LLUS-N performed well in modeling catchment TN loads and generated similar estimates of long-term changes in catchment TN export compared to other flow-based statistical loading models designed to remove the effect of discharge (Zhang et al. 2015a, Chanat et al. 2016). LLUS-N catchment TN export rates declined ~13% during the 1986-2012 period in POTW, respectively. This decline is within the confidence limits of the 11% decrease in POTW reported from a WRTDS flow-normalized TN trends analysis (Hirsch et al. 2015, Chanat et al. 2016). The modeled increase of TN export at NFSR (24%) was also equivalent to the increase in TN export reported in other USGS studies (Chanat et al. 2016, Oelsner et al. 2017). Modeled declines in TN export at SFSR were minimal and were consistent with weak flow-normalized trends (Chanat et al. 2016, Oelsner et al. 2017). Consistency in loading trends suggest that changes in land use specific nitrogen inputs and surpluses in each of the study catchments were capable of explaining long-term shifts in TN loading, consistent with findings from other up-scaled NANI studies (Chen et al. 2016a, Goyette et al. 2016). Furthermore, the importance of land management actions (essentially NO_x emission controls) and declining point source loads can be interpreted as one of the more likely drivers of TN export trends in these catchments due to the fact that no long-term trend in discharge has been observed over the study period (Eshleman and Sabo 2016).

In order to attribute catchment TN loading from forests, urban areas, and point sources in LLUS-N, best available estimates of retention available from the literature were leveraged to constrain model parameterization. Following calibration, it was found

that individual scaling factors for these N sources were highly uncertain and that any values within the predefined range of scaling factors would have been sufficient to maintain model performance (i.e., equifinality). Similar parameter dependency and equifinality issues have been highlighted for other more deconvolved semi-empirical models (Chen et al. 2014, Chen et al. 2018, Hu et al. 2018). It is possible that a larger calibration dataset could have yielded more constrained parameter estimates, but more than likely, the signal of these individual N sources is too small relative to the inter-annual variability in TN export to overcome parametrization dependencies during calibration. Further supporting this concern, modeled catchment TN export was much less sensitive to relative changes in $\boldsymbol{B_p}$, $\boldsymbol{B_u}$, and $\boldsymbol{B_f}$ with a 1% change in these individual scaling factors resulting in less than 0.15% shift in catchment TN export at NFSR and POTW. The uncertainty in parameterization and general insensitivity speaks to the relatively low importance of point source loads and non-point source loads from urban and forest areas in explaining the inter-annual variation of catchment TN export at POTW and NFSR. As such, non-point source loads from agricultural areas in both POTW and NFSR, modeled by capturing the agricultural surplus and annual discharge interaction, is likely the predominant driver of the inter-annual variation in catchment TN export. It should be noted, however, that the weak influence of non-agricultural sources on the inter-annual variation in TN export does not justify dropping these factors from LLUS-N. The small incremental changes in modeled N loads from urban, forest, and wastewater treatment plants played an instrumental role in generating modeled trends. Furthermore, modeled fluxes from these sources provide a reasonable approximation of

the potential influence of these sources on catchment TN export and are thus valuable to watershed management strategies (Keisman et al. 2015).

The importance of point and non-point source load contributions to catchment TN export varied as nitrogen inputs and surpluses changed through time. As such the mean retentiveness and loading rates of a catchment shifted in response to changing N inputs/surpluses across the landscape. Through time, catchment retention at SFSR, as modeled by LLUS-N under mean discharge conditions, increased from 78 to 83% over the period due to the sources of N shifting more towards agricultural surpluses rather than point source loads. Similarly, retention decreased from 81 to 78% from the mid-80s to early 2000s at NFSR and then recovered as point source loads began to decrease. Even though point source loads are small relative to the agricultural surplus, the low retentiveness of point source loads result in a higher per unit decline in TN loss to the stream outlet relative to N left on agricultural lands. Changes in the mean retentiveness of the catchment can help explain the observation of more negative retention residuals in the earlier part of the record shifting towards more generally positive values. Even with this change in retention, however, LLUS-N still underpredicted catchment TN export during the 1986-1994 period at NFSR and SFSR. Thus, it may be worthwhile to further incorporate the role of forest disturbance in influencing catchment TN export in future research if a basin-wide disturbance index could be incorporated as an additional interaction term for forests loss (Townsend et al. 2004).

Based on modeled insights from the LLUS-N, corroborated by the statistical analysis of the discharge model residuals, succinct narratives on the drivers of water quality improvement and degradation can be offered for each of the study catchments. I

speculate shifts or possible declines in industrial production in SFSR resulted in dramatic reductions in point source loading since the 1980s. Reductions in point source loading combined with a 41% decrease in atmospheric deposition 1) offset water quality degradation brought about by increasing agricultural surpluses (driven primarily by increased manure inputs) and 2) resulted in slightly decreased catchment TN export rates for the period of record. As discussed above, however, some of this improvement may be driven by lower catchment-wide retention in the earlier part of the record. In contrast, point source loading in NFSR was significantly smaller than SFSR and point source loading was actually increasing until the late 1990s whereupon it began to decline after the early 2000s. Increased point source loads are attributed to the growth of poultry processing and a newly launched wastewater treatment plant failing to meet discharge pollutant standards. This treatment plant progressively came into compliance throughout the 2000s and eventually reduced point source loads in the catchment to levels below those observed in the 1980s (AP 1999, Blankenship 2000). Decreases in point sources and atmospheric deposition partly counteracted water quality degradation brought about by increasing agricultural mass balances in NFSR, resulting in a modeled 24% increase in catchment TN export. In both NFSR and SFSR, insights from the nitrogen inventories and LLUS-N highlight an urgent need to increase NUE and decrease agricultural surpluses. Through time, the influence of atmospheric deposition and point source loading reductions on catchment TN export rates will wane if agricultural mass balances continue to increase in the future.

In contrast to the Shenandoah catchments, all three of the primary management actions—increased NUE, decreased NO_x emission, and point source loading

reductions—contributed to the modeled decline in catchment TN loading rates in POTW. Over the entire1986-2012 period, efforts to increase NUE have contributed little to the improvement in N loads (as evidenced by a weak decline in partial annual N surpluses). However, that is partly due to an initial rise in partial N surpluses in agricultural lands from the 1980s to the early 2000s. Since ~2002 partial annual N surpluses on agricultural lands have seemingly begun to decline alongside increased NUE, decreased atmospheric deposition, and decreased fertilizer use in POTW. The timing of this improvement coincided with the legislation of the Nutrient Management Law in Maryland (Dotterer 2017), which required all major farm operations to have certified nutrient management plans. If the trend in NUE continues, TN loading rates should continue to decline further even if decreases in point source loading and atmospheric deposition begin to taper. As mentioned at the beginning of the discussion, declines in atmospheric N deposition are potentially responsible for most of the declines in non-point source loads throughout POTW. Point source loads also declined after the late 1990s, and this decline coincides with concerted statewide efforts in Maryland to upgrade its municipal wastewater treatment facilities (Maryland 2004), but large declines in point source loads were also occurring in SFSR prior to this period.

The narratives listed above were based on the results of a simple LLUS-N model. The model can easily be operationalized in other catchments, though some adjustment of the model structure or calibration procedure may be needed based on relevant local processes. For at least two of the three study catchments, however, modeled changes in discharge, nitrogen inputs/surpluses on specific land uses, and point source loading were found to be the primary drivers of observed long-term changes in non-point and point

source TN loading. For the study period, remedial efforts to increase the retentiveness of these large catchments seem secondary to changes in terrestrial N surpluses and decreases in point source loading. Declines in annual terrestrial surplus were largely driven by decreased rates of atmospheric N deposition in POTW, but increased surpluses in SFSR and NFSR were observed due to increased manure application rates. This insight strongly suggests that management efforts should prioritize limiting the accumulation of surplus nitrogen in terrestrial compartments of the catchment and decrease point source loading to surface water where effectual to achieve future water quality restoration goals.

Acknowledgements

We thank Ning Zhou for facilitating access to the point source loading data through the Bay Program Nutrient Point Source Database. Many thanks to Drs. Andrew Elmore, David Nelson, Keith N. Eshleman, Tom Fisher and Eric Davidson of the University of Maryland Center for Environmental Science for their guidance during the project's development. This research was made possible in part through support of an Environmental Protection Agency Science to Achieve Results Graduate Fellowship (#FP-91749901-0, to RDS), teaching assistantships through the Marine-Estuarine-Environmental Sciences (MEES) Graduate Program (to RDS), and an appointment to Research Participation Program for the U.S. Environmental Protection Agency, Office of Research and Development, administered by the Oak Ridge Institute for Science and Education through an inter-agency agreement between the U.S. Department of Energy and EPA. The views presented here are those of the authors and do not represent official views or policy of the U.S. Environmental Protection Agency (EPA) or another U.S.

federal agency. Any use of trade, firm, or product names is for descriptive purposes only and does not imply endorsement by the U.S. Government.

Chapter 5: Conclusions

Long-term monitoring efforts of surface water nitrogen loading indicate dramatic shifts in the inputs, transport, and transformation of nitrogen in forested and mixed land use catchments throughout the globe (Rogora et al. 2012, Argerich et al. 2013, Chen et al. 2016a). Identifying the drivers of these changes is difficult because of the collinearity between catchment nitrogen loading and discharge along with potential lag issues associated with groundwater residence time (Hirsch et al. 2010, Chen et al. 2016a). Thus, the noise induced by climatic variation and hydrology make it difficult to ascertain proximal and distal drivers of water quality improvement and degradation. To circumvent this issue, I constructed proxy records of terrestrial N availability using either dendroisotopic records and quasi-mass balances to assess changes in terrestrial N surpluses. Assumedly, terrestrial N surpluses would not be as strongly correlated with discharge and could be related to trends in hydrologic N export. Thus, the relationships between identifiable processes that potentially increase terrestrial N surpluses like disturbance detected through remote sensing or increased manure application onto cropland based on livestock census data could be identified and related to water quality trends. This information could then be used to inform efforts looking to assess the relative influence of specific management actions and technological applications (e.g., NO_X emission controls) on observed trends in terrestrial surpluses and water quality (Doering et al. 2011, Keisman et al. 2015).

Linking changes in terrestrial N surpluses to surface water nitrogen loading can be accomplished by generating hypotheses through the lens of the kinetic N saturation conceptual model (Lovett and Goodale 2011). From the logical framework of kinetic N

saturation, I developed testable and falsifiable hypotheses to link specific processes to changes in the net atmospheric input, soil sink, vegetative uptake, and gaseous efflux rates in catchments. All three of the studies described in this dissertation accomplished this task. For example, the trends analysis of dendroisotopic and water quality records at Buck Creek provided evidence that the decline in atmospheric N deposition rates was not the predominant driver of declining terrestrial N surpluses at Buck Creek (Figure 6). In contrast to my expectations, terrestrial N surpluses were relatively constant in the North Tributary during the 1995-2010 period (Figure 5) and retention of atmospherically deposited nitrogen was actually decreasing in the South Tributary (Figure 8). These results highlight that decreased N inputs do not necessarily result in decreased terrestrial surpluses or hydrologic N export.

At Upper Big Run and Paine Run, statistical support was garnered to suggest that disturbance detected by remote sensing resulted in a decline in terrestrial N surpluses (Table 8). Changes in terrestrial N surpluses at these sites also strongly coincided with water quality changes (Figure 13). There was also statistical evidence that declining acidic deposition rates may offset general long-term declines in terrestrial N availability (Table 8). Despite the ephemeral modifications of terrestrial N availability by disturbance, acidic deposition, and climate, long-term declines in terrestrial nitrogen availability were robust and have likely driven much of the declines in stream nitrate concentration throughout the central Appalachians. Finally, I was able to identify retention values for specific land uses in the literature to calibrate a simple lumped conceptual model for three mixed land use catchments in the Chesapeake Bay (Figure 20). Leveraging quasi-mass balances and discharge, I was able to attribute shifts in

catchment TN loads to changes in the input and removal of nitrogen from the landscape (Figure 21).

Whether relying on quasi-mass balances or dendroisotopic records, my findings demonstrated the usefulness of constructing proxy datasets of terrestrial N surpluses in identifying likely processes driving changes in hydrologic N loss in forested and mixed land use catchments. Furthermore, rather than solely relying on more complex mechanistic models to attempt to explain past water quality changes, this research firmly establishes that relatively simple statistical and conceptual modeling approaches can be applied to attribute past changes in terrestrial N surpluses and water quality to specific proximal and distal drivers.

Appendix

Chapter 3: Supplementary Figures and Tables

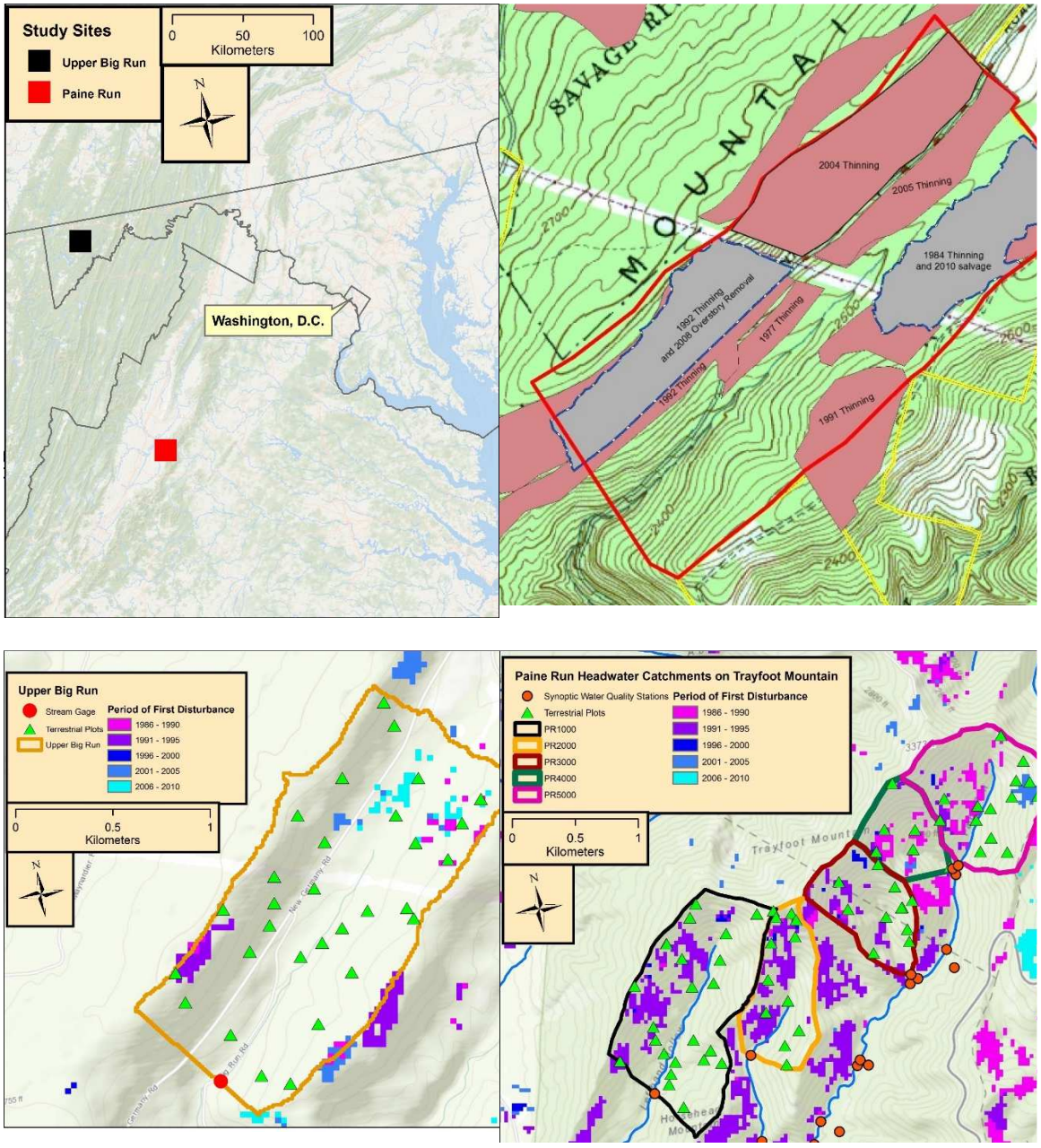

Figure S1. (A) Study site locations within the mid-Atlantic of the United States, (B) illustration of the areal extent of logging activities at Upper Big Run since 1970 (Overlapping red polygons represent more recent logging activities), (C, D) Maps of Upper Big Run and the five headwater catchments of Paine Run subjected to tree coring along with detected periods of disturbance recorded by the North American Forest Dynamic data product, "Forest Disturbance History from Landsat, 1986-2010". Logging map is courtesy of the Maryland State Forest Service.

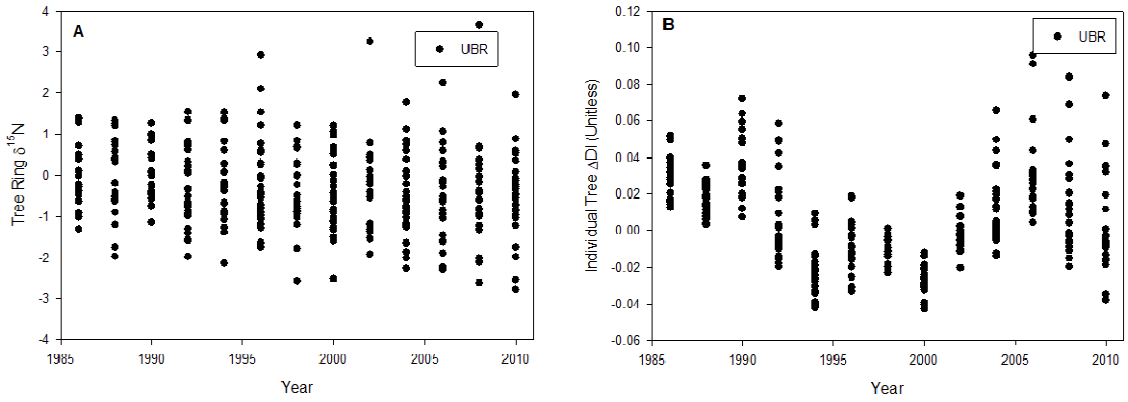

Figure S2. Mean ΔDI values corresponding to the tree-ring segments and tree-ring $\delta^{15}N$ values at UBR

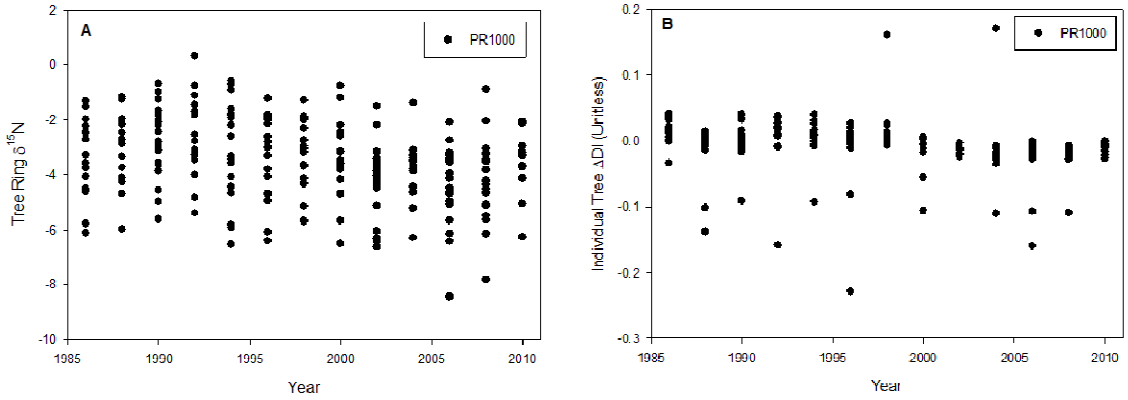

Figure S3. Mean ΔDI values corresponding to the tree-ring segments and tree-ring $\delta^{15}N$ values at PR1000.

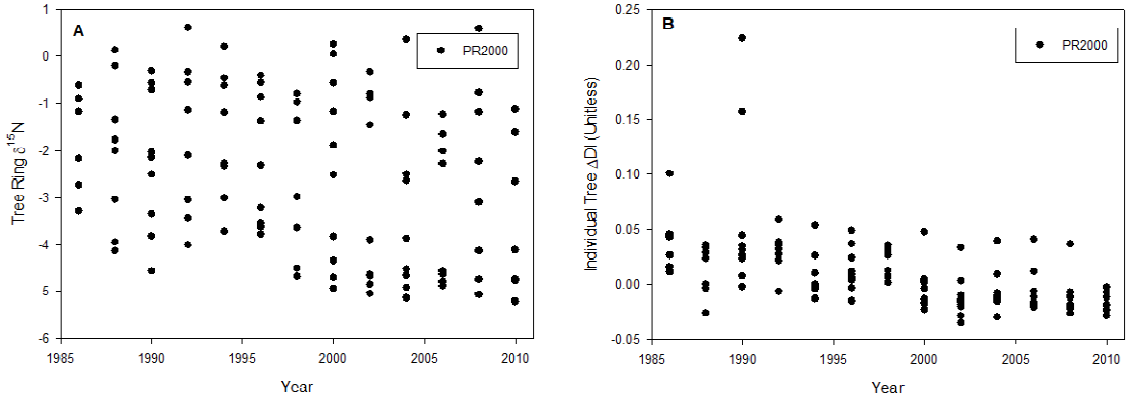

Figure S4.. Mean ΔDI values corresponding to the tree-ring segments and tree-ring $\delta^{15}N$ values at PR2000.

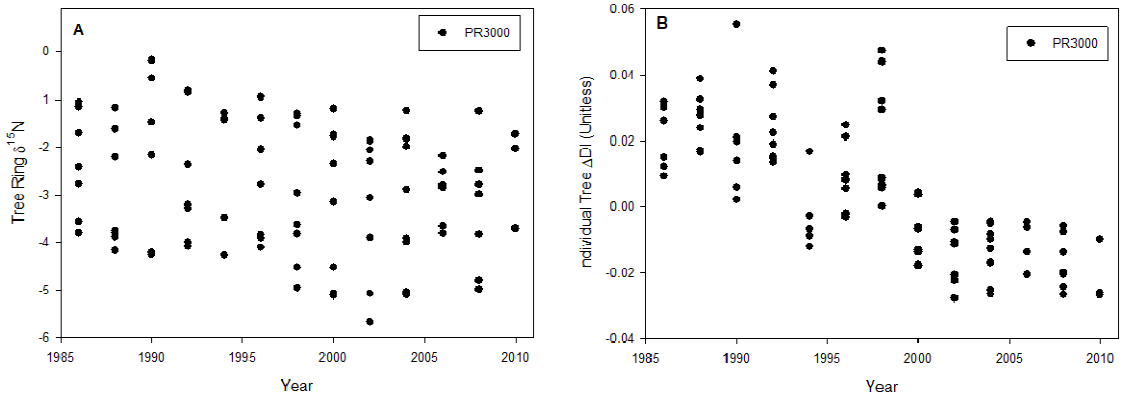

Figure S5. Mean ΔDI values corresponding to the tree-ring segments and tree-ring $\delta^{15}N$ values at PR3000.

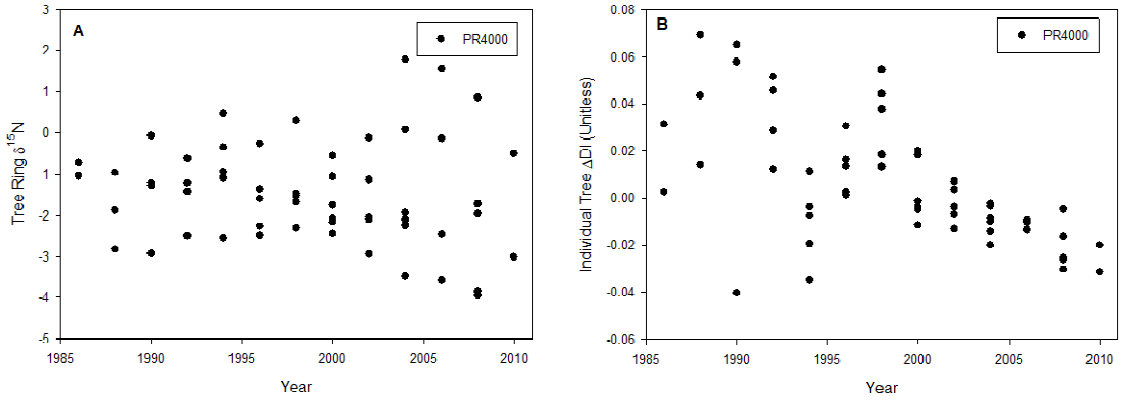

Figure S6. Mean ΔDI values corresponding to the tree-ring segments and tree-ring $\delta^{15}N$ values at PR4000.

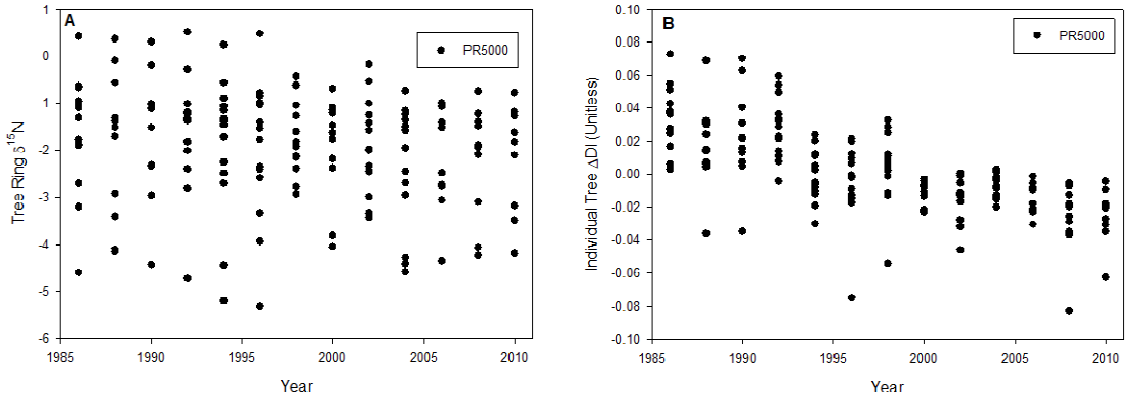

Figure S7. Mean ΔDI values corresponding to the tree-ring segments and tree-ring $\delta^{15}N$ values at PR5000.

Table S1. Statistical output of the simple linear regression analysis of the relationship between time and catchment-scale $\delta^{15}N$.

		Coefficient	Std. Error	t	P	Model R^2
UB	Constant	33.859	6.716	5.042	<0.001	0.62
	Time	-0.0171	0.00337	-5.085	<0.001	
PR1000	Constant	107.856	19.372	5.568	<0.001	0.68
	Time	-0.0557	0.00971	-5.74	<0.001	
PR2000	Constant	107.568	19.395	5.546	<0.001	0.68
	Time	-0.0551	0.00972	-5.668	<0.001	
PR3000	Constant	60.475	16.723	3.616	0.003	0.47
	Time	-0.0317	0.00838	-3.778	0.002	
PR4000	Constant	-26.651	25.945	-1.027	0.322	0.0
	Time	0.0125	0.013	0.964	0.352	
PR5000	Constant	43.81	9.336	4.692	<0.001	0.60
	Time	-0.0229	0.00468	-4.891	<0.001	

Table S2. Using the non-interpolated wood $\delta^{15}N$ dataset, results from the linear regression analyses modeling the effect of 1-year lagged catchment scale wood $\delta^{15}N$ on (1) observed mean annual flow-weighted and spring baseflow nitrate concentrations at UBR, (2) spring baseflow nitrate concentrations at individual PR headwater catchments after factoring out the influence of the spatial gradient.

UBR Mean Annual Flow-Weighted Concentration	*Coefficients*	*Standard Error*	*P-value*	R^2
Intercept	0.613	0.0295	<0.001	0.88
Slope	0.793	0.0843	<0.0001	
UBR Spring Baseflow Concentration				
Intercept	0.48	0.0593	<0.001	0.521
Slope	0.559	0.17	0.008	
PR1000				
Intercept	0.378	0.066	0.011	0.843
Slope	0.0859	0.0181	0.018	
PR2000				
Intercept	0.842	0.271	0.053	0.473
Slope	0.219	0.102	0.122	
PR3000				
Intercept	1.507	0.515	0.061	0.548
Slope	0.446	0.184	0.094	
PR4000				
Intercept	1.984	1.76	0.341	0
Slope	0.855	1.17	0.518	
PR5000				
Intercept	5.014	0.931	0.013	0.832
Slope	2.164	0.474	0.02	

Table S3. Statistical output of the general linear model analysis of the relationship among time, precipitation, disturbance temperature, and S and N deposition vs. tree ring $\delta^{15}N$.

ANALYSIS OF VARIANCE FOR THE EQUAL SLOPES MODEL

SOURCE OF VARIATION	DF	SS	MS	F	P	VIF
TREE_ID	95	2084.288	21.94	69.399	<0.001	Variable
PRECIPITATION	1	7.711	7.711	24.391	<0.001	5.6
DISTURBANCE	1	1.095	1.095	3.463	0.063	1.8
S AND N DEPOSITION	1	12.284	12.284	38.856	<0.001	16.6
YEAR	1	32.464	32.464	102.688	<0.001	14.1
RESIDUAL	872	275.676	0.316	--	--	
TOTAL	971	3190.428	3.286	--	--	
R=0.956		Rsq=0.914	Adj Rsq= 0.904			

Table S4. Statistical output of the general linear model analysis of the relationship between time and tree-ring $\delta^{15}N$.

Analysis of Variance for the Interaction Model:

Source of Variation	DF	SS	MS	F	P
Tree_ID	95	115.741	1.218	5.459	<0.001
Year	1	58.27	58.27	261.088	<0.001
Tree_ID x Year	95	117.061	1.232	5.521	<0.001
Residual	781	174.304	0.223	--	--
Total	972	3191.185	3.283	--	--
R = 0.972	Rsqr = 0.945		Adj Rsqr = 0.932		

Table S5. Slope coefficient outputs the general linear model analysis of the relationship between time and tree-ring $\delta^{15}N$.

Tree_ID	Coefficient	95%Conf-L	95%Conf-U	P	Tree_ID	Coefficient	95%Conf-L	95%Conf-U	P
BR26	-0.0368	-0.0412	-0.0323	<0.001	PR1023	-0.02866	-0.0301	0.0464	0.676
BR10I	0.0331	0.0415	0.0984	<0.001	PR1025	-0.1294	-0.137	-0.0482	<0.001
BR11II	0.0026	-0.00636	0.0852	0.091	PR1027	-0.0654	-0.0729	0.0158	0.207
BR12II	-0.0773	-0.08	-0.00087	0.045	PR1028	-0.03514	-0.0336	0.0369	0.926
BR13I	-0.0825	-0.0843	-0.00705	0.021	PR1031	-0.0511	-0.0546	0.0261	0.488
BR14I	-0.0112	-0.0131	0.0643	0.194	PR2001	-0.05	-0.0604	0.034	0.583
BR15I	-0.0668	-0.0765	0.0166	0.207	PR2003	-0.0647	-0.0701	0.0142	0.193
BR16II	-0.03592	-0.0345	0.0363	0.961	PR2004	0.0318	0.0193	0.118	0.006
BR17I	0.0272	0.0128	0.115	0.014	PR2005	-0.0674	-0.0649	0.00369	0.08
BR18I	-0.03929	-0.0297	0.0247	0.857	PR2006	0.0294	0.0125	0.12	0.016
BR19II	-0.019	-0.0183	0.0538	0.334	PR2008	-0.0774	-0.0749	-0.00631	0.02
BR20II	-0.0234	-0.0281	0.0548	0.527	PR2009	-0.0593	-0.0705	0.0256	0.359
BR21I	-0.0159	-0.0225	0.0642	0.345	PR2010	-0.0701	-0.0772	0.0106	0.137
BR22II	-0.0059	-0.023	0.0849	0.261	PR2011	-0.0088	-0.0107	0.0668	0.156
BR23II	-0.0018	-0.00185	0.0719	0.063	PR2012	-0.0327	-0.0305	0.0388	0.816
BR24II	-0.03195	-0.0307	0.0404	0.789	PR2013	-0.0885	-0.0954	-0.00805	0.02
BR25II	-0.0064	-0.0181	0.0789	0.219	PR5013	0.0579	0.0447	0.145	<0.001
BR27I	-0.03131	-0.0351	0.046	0.79	PR3003	-0.03742	-0.0451	0.0439	0.978
BR28II	-0.03582	-0.0372	0.0392	0.96	PR3004	0.0062	-0.011	0.0969	0.118
BR29II	-0.03889	-0.0448	0.0406	0.923	PR3005	-0.0618	-0.0593	0.00935	0.154
BR2I	-0.0044	0.00165	0.0632	0.039	PR3006	-0.0697	-0.0816	0.0157	0.185
BR30I	-0.0732	-0.0781	0.00538	0.088	PR3007	-0.0862	-0.0938	-0.00511	0.029
BR31I	-0.03117	-0.0322	0.0435	0.77	PR3008	-0.03292	-0.0372	0.045	0.853
BR3I	-0.03566	-0.0326	0.0349	0.947	PR3009	-0.03539	-0.0544	0.0572	0.961
BR4II	0.0032	-0.00085	0.0809	0.055	PR3010	0.0101	0.00901	0.0848	0.015
BR5I	0.0267	0.0245	0.102	0.001	PR3011	-0.0874	-0.0849	-0.0163	0.004
BR6II	-0.03848	-0.0457	0.0423	0.94	PR3012	-0.0337	-0.0757	0.0819	0.939
BR7I	-0.0595	-0.058	0.0125	0.206	PR1019	-0.1111	-0.113	-0.0356	<0.001
BR8I	-0.0436	-0.0371	0.0235	0.659	PR4001	-0.02868	-0.0458	0.0621	0.768
BR9I	-0.1162	-0.128	-0.0309	0.001	PR4002	0.2852	0.24	0.404	<0.001
PR1002	-0.0726	-0.0769	0.00535	0.088	PR4003	-0.1131	-0.113	-0.0392	<0.001
PR1003	-0.1052	-0.105	-0.032	<0.001	PR4006	-0.0808	-0.0918	0.0039	0.072
PR1005	-0.0213	-0.0311	0.0621	0.514	PR4007	0.0303	0.0254	0.109	0.002
PR1006	-0.0521	-0.0553	0.0248	0.455	PR5001	-0.1356	-0.132	-0.0655	<0.001
PR1007	-0.0841	-0.109	0.0141	0.131	PR5002	-0.0053	-0.0185	0.0815	0.216
PR1008	0.0142	0.0108	0.0912	0.013	PR5004	-0.0137	-0.0141	0.0603	0.223
PR1009	-0.04099	-0.0518	0.0434	0.863	PR5005	-0.066	-0.0683	0.00981	0.142
PR1010	-0.08	-0.0859	-0.00051	0.047	PR4000	-0.0515	-0.0578	0.0283	0.502
PR1011	-0.0839	-0.0876	-0.00668	0.022	PR5007	-0.04417	-0.0404	0.0257	0.662
PR1012	-0.1388	-0.14	-0.064	<0.001	PR5008	0.0037	-0.0111	0.0921	0.124
PR1013	-0.0612	-0.0683	0.0195	0.276	PR5009	-0.0089	-0.00798	0.0639	0.127
PR1014	-0.1121	-0.121	-0.0292	0.001	PR5010	-0.0082	-0.0154	0.0726	0.202
PR1015	0.0015	-0.00315	0.0797	0.07	PR5011	-0.0904	-0.0992	-0.00808	0.021
PR1016	-0.0226	-0.0263	0.0546	0.493	PR5012	0.0312	0.0284	0.108	<0.001
PR1017	-0.052	-0.0879	0.0575	0.681	PR5014	-0.0228	-0.0207	0.0487	0.428
PR1018	-0.0711	-0.0799	0.0113	0.14	PR5015	-0.0143	-0.0118	0.0568	0.199
PR1021	-0.0999	-0.0987	-0.0276	<0.001	PR5016	-0.0579	-0.0666	0.0245	0.364
PR1022	-0.0748	-0.0861	0.01	0.121	PR5017	-0.018	-0.0155	0.0531	0.282

Chapter 4: Supplementary Figures and Tables

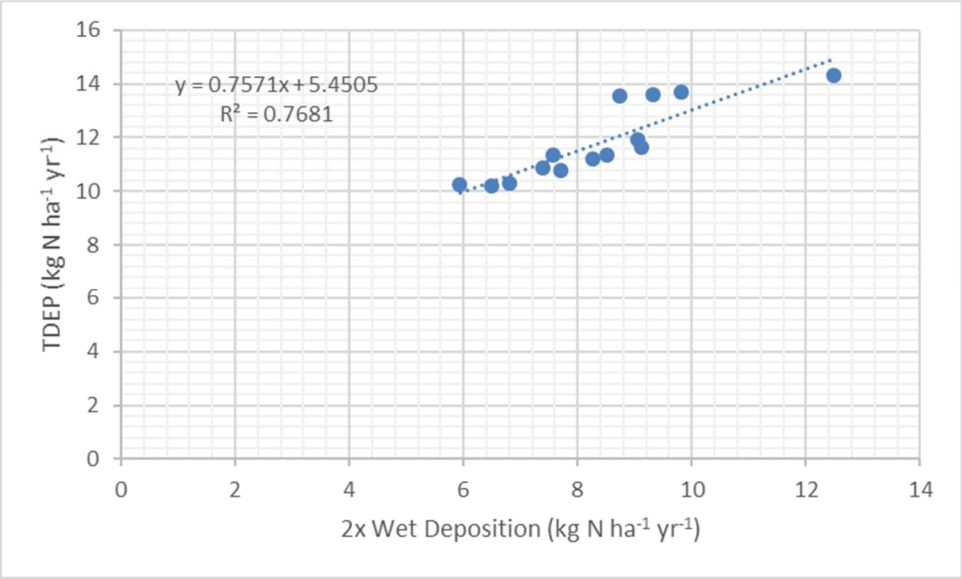

Figure S8. Linear relationship between modeled total deposition rates (TDEP, available 2000 to present) and the 2x wet deposition assumption (available, 1985 to present). During the period in which the datasets overlap, atmospheric deposition was projected to have linearly declined 26 to 29%.

Table S6. Correlation matrix displaying Pearson correlation coefficients between predictor variables and the discharge model residuals relying on non-interpolated time series. Bold indicates a significant correlation ($p < 0.05$).

		$I_{u,t}$	$I_{a,t}$	$I_{f,t}$	$I_{P,t}$	$\ddot{E}_{w,t}$
SFSR	$R_{w,t}$	-0.291	-0.668	0.374	0.329	9.25E-16
	$I_{u,t}$		0.76	-0.717	**-0.97**	**-0.926**
	$I_{a,t}$			-0.595	**-0.83**	-0.665
	$I_{f,t}$				0.784	0.594
	$I_{P,t}$					0.898
NFSR						
	$R_{w,t}$	-6.78E-02	-4.47E-01	9.61E-02	-0.583	-1.18E-15
	$I_{u,t}$		0.0946	**0.814**	0.248	-0.653
	$I_{a,t}$			-0.416	0.124	0.26
	$I_{f,t}$				0.105	**-0.827**
	$I_{P,t}$					0.305
POTW						
	$R_{w,t}$	-0.168	-0.727	-0.187	-0.103	-6.06E-16
	$I_{u,t}$		0.111	-0.546	-0.436	-0.0968
	$I_{a,t}$			0.353	0.679	0.646
	$I_{f,t}$				0.54	0.107
	$I_{P,t}$					**0.865**

Table S7. Statistical outputs of the exploratory modeling analysis looking to explain temporal patterns in the discharge model residuals. All model combinations generating ΔAICc < 2 were reported.

Catchment	Model Reference	**Urban Inputs ($I_{u,t}$)**	**Annual N Surplus in Agricultural Lands ($I_{a,t}$)**	**Forest Inputs ($I_{f,t}$)**	**Point Source Loading ($I_{P,t}$)**	ΔAICc	R2
NFSR	Agricultural Surplus		0.03 ±0.15			0	0.08
	Point Source				1.41 ±7.28	0.23	0.05
SFSR	Point Source				**0.70 ± 0.26**	0	0.9
POTW	Agricultural Surplus		**0.47 ± 0.20**			0	0.88

References

Aber, J., W. McDowell, K. Nadelhoffer, A. Magill, G. Berntson, M. Kamakea, S. McNulty, W. Currie, L. Rustad, and I. Fernandez. 1998. Nitrogen saturation in temperate forest ecosystems. BioScience **48**:921-934.

Aber, J. D., and C. T. Driscoll. 1997. Effects of land use, climate variation, and N deposition on N cycling and C storage in northern hardwood forests. Global Biogeochemical Cycles **11**:639-648.

Aber, J. D., K. J. Nadelhoffer, P. Steudler, and J. M. Melillo. 1989. Nitrogen saturation in northern forest ecosystems. BioScience **39**:378-286.

Adams, M. B., J. D. Knoepp, and J. R. Webster. 2014. Inorganic nitrogen retention by watersheds at Fernow Experimental Forest and Coweeta Hydrologic Laboratory. Soil Science Society of America Journal **78**:S84-S94.

Aho, K., D. Derryberry, and T. Peterson. 2014. Model selection for ecologists: the worldviews of AIC and BIC. Ecology **95**:631-636.

Akaike, H. 1998. Information theory and an extension of the maximum likelihood principle. Pages 199-213 Selected papers of hirotugu akaike. Springer.

AP. 1999. Shenandoah area switches to innovative wastewater treatment; VA to regulate poultry waste; EPA says VA left waterways off pollution list; Factory farm. Associated Press.

Argerich, A., S. Johnson, S. Sebestyen, C. Rhoades, E. Greathouse, J. Knoepp, M. Adams, G. Likens, J. Campbell, and W. McDowell. 2013. Trends in stream nitrogen concentrations for forested reference catchments across the USA. Environmental Research Letters **8**:014039.

Bash, J., E. Cooter, R. Dennis, J. Walker, and J. Pleim. 2013. Evaluation of a regional air-quality model with bidirectional NH 3 exchange coupled to an agroecosystem model. Biogeosciences **10**:1635-1645.

Battles, J. J., T. J. Fahey, C. T. Driscoll Jr, J. D. Blum, and C. E. Johnson. 2013. Restoring soil calcium reverses forest decline. Environmental Science & Technology Letters **1**:15-19.

Beaulieu, J. J., J. L. Tank, S. K. Hamilton, W. M. Wollheim, R. O. Hall, P. J. Mulholland, B. J. Peterson, L. R. Ashkenas, L. W. Cooper, and C. N. Dahm. 2011. Nitrous oxide emission from denitrification in stream and river networks. Proceedings of the National Academy of Sciences **108**:214-219.

Beghin, R., P. Cherubini, G. Battipaglia, R. Siegwolf, M. Saurer, and G. Bovio. 2011. Tree-ring growth and stable isotopes (13C and 15N) detect effects of wildfires on tree physiological processes in Pinus sylvestris L. Trees **25**:627-636.

Bernal, S., L. O. Hedin, G. E. Likens, S. Gerber, and D. C. Buso. 2012. Complex response of the forest nitrogen cycle to climate change. Proceedings of the National Academy of Sciences **109**:3406-3411.

Bettez, N. D., J. M. Duncan, P. M. Groffman, L. E. Band, J. O'Neil-Dunne, S. S. Kaushal, K. T. Belt, and N. Law. 2015. Climate variation overwhelms efforts to reduce nitrogen delivery to coastal waters. Ecosystems **18**:1319-1331.

Billen, G. 1991. N, P, and Si retention along the aquatic continuum from land to ocean. Ocean margin processes in global change:251-280.

Billen, G., J. Garnier, and L. Lassaletta. 2013. The nitrogen cascade from agricultural soils to the sea: modelling nitrogen transfers at regional watershed and global scales. Phil. Trans. R. Soc. B **368**:20130123.

Blankenship, K. 2000. Shenandoah treatment plant to use wastewater for irrigation. Bay Journal.

Bobbink, R., K. Hicks, J. Galloway, T. Spranger, R. Alkemade, M. Ashmore, M. Bustamante, S. Cinderby, E. Davidson, and F. Dentener. 2010. Global assessment of nitrogen deposition effects on terrestrial plant diversity: a synthesis. Ecological Applications **20**:30-59.

Boyer, E. W., C. L. Goodale, N. A. Jaworski, and R. W. Howarth. 2002. Anthropogenic nitrogen sources and relationships to riverine nitrogen export in the northeastern USA. Pages 137-169 The Nitrogen Cycle at Regional to Global Scales. Springer.

Brakebill, J., and J. Gronberg. 2017. County-Level Estimates of Nitrogen and Phosphorus from Commercial Fertilizer for the Conterminous United States, 1987-2012. US Geological Survey data release, Available at: https://doi. org/10.5066/F7H41PKX, last access **19**.

Brand, W. A., T. B. Coplen, J. Vogl, M. Rosner, and T. Prohaska. 2014. Assessment of international reference materials for isotope-ratio analysis (IUPAC Technical Report). Pure and Applied Chemistry **86**:425-467.

Brookshire, E., S. Gerber, J. R. Webster, J. M. Vose, and W. T. Swank. 2011. Direct effects of temperature on forest nitrogen cycling revealed through analysis of long□term watershed records. Global Change Biology **17**:297-308.

Buda, A. R., and D. R. DeWalle. 2009. Dynamics of stream nitrate sources and flow pathways during stormflows on urban, forest and agricultural watersheds in central Pennsylvania, USA. Hydrological processes **23**:3292-3305.

Bukata, A. R., and T. K. Kyser. 2007. Carbon and nitrogen isotope variations in tree-rings as records of perturbations in regional carbon and nitrogen cycles. Environmental science & technology **41**:1331-1338.

Burnham, M. B., B. E. McNeil, M. B. Adams, and W. T. Peterjohn. 2016. The response of tree ring δ15N to whole-watershed urea fertilization at the Fernow Experimental Forest, WV. Biogeochemistry **130**:133-145.

Burns, D. A., E. W. Boyer, E. M. Elliott, and C. Kendall. 2009. Sources and transformations of nitrate from streams draining varying land uses: evidence from dual isotope analysis. Journal of environmental quality **38**:1149-1159.

Cairney, J., and A. Meharg. 1999. Influences of anthropogenic pollution on mycorrhizal fungal communities. Environmental Pollution **106**:169-182.

Caraco, N. F., and J. J. Cole. 1999. Human impact on nitrate export: an analysis using major world rivers. Ambio **28**:167-170.

Carpenter, S. R., N. F. Caraco, D. L. Correll, R. W. Howarth, A. N. Sharpley, and V. H. Smith. 1998. Nonpoint pollution of surface waters with phosphorus and nitrogen. Ecological Applications **8**:559-568.

CBP. 2016. Bay Program Point Source Database. http://www.chesapeakebay.net/data/downloads.

Chanat, J. G., D. L. Moyer, J. D. Blomquist, K. E. Hyer, and M. J. Langland. 2016. Application of a weighted regression model for reporting nutrient and sediment concentrations, fluxes, and trends in concentration and flux for the Chesapeake

Bay Nontidal Water-Quality Monitoring Network, results through water year 2012. 2328-0328, US Geological Survey.
Chen, D., M. Hu, Y. Guo, and R. A. Dahlgren. 2016a. Modeling forest/agricultural and residential nitrogen budgets and riverine export dynamics in catchments with contrasting anthropogenic impacts in eastern China between 1980–2010. Agriculture, Ecosystems & Environment **221**:145-155.
Chen, D., H. Huang, M. Hu, and R. A. Dahlgren. 2014. Influence of lag effect, soil release, and climate change on watershed anthropogenic nitrogen inputs and riverine export dynamics. Environmental science & technology **48**:5683-5690.
Chen, D., H. Shen, M. Hu, J. Wang, Y. Zhang, and R. A. Dahlgren. 2018. Legacy nutrient dynamics at the watershed scale: principles, modeling, and implications. Pages 237-313 Advances in Agronomy. Elsevier.
Chen, F., L. Hou, M. Liu, Y. Zheng, G. Yin, X. Lin, X. Li, H. Zong, F. Deng, and J. Gao. 2016b. Net anthropogenic nitrogen inputs (NANI) into the Yangtze River basin and the relationship with riverine nitrogen export. Journal of Geophysical Research: Biogeosciences **121**:451-465.
Cleveland, C. C., B. Z. Houlton, W. K. Smith, A. R. Marklein, S. C. Reed, W. Parton, S. J. Del Grosso, and S. W. Running. 2013. Patterns of new versus recycled primary production in the terrestrial biosphere. Proceedings of the National Academy of Sciences **110**:12733-12737.
Conley, D. J., H. W. Paerl, R. W. Howarth, D. F. Boesch, S. P. Seitzinger, K. E. Havens, C. Lancelot, and G. E. Likens. 2009. Controlling eutrophication: nitrogen and phosphorus. Science **323**:1014-1015.
Corre, M. D., F. O. Beese, and R. Brumme. 2003. Soil nitrogen cycle in high nitrogen deposition forest: changes under nitrogen saturation and liming. Ecological Applications **13**:287-298.
Corre, M. D., and N. P. Lamersdorf. 2004. REVERSAL OF NITROGEN SATURATION AFTER LONG□TERM DEPOSITION REDUCTION: IMPACT ON SOIL NITROGEN CYCLING. Ecology **85**:3090-3104.
Craine, J. M., A. J. Elmore, M. P. Aidar, M. Bustamante, T. E. Dawson, E. A. Hobbie, A. Kahmen, M. C. Mack, K. K. McLauchlan, and A. Michelsen. 2009. Global patterns of foliar nitrogen isotopes and their relationships with climate, mycorrhizal fungi, foliar nutrient concentrations, and nitrogen availability. New Phytologist **183**:980-992.
David, M. B., L. E. Gentry, D. A. Kovacic, and K. M. Smith. 1997. Nitrogen balance in and export from an agricultural watershed. Journal of environmental quality **26**:1038-1048.
DeVries, B., A. K. Pratihast, J. Verbesselt, L. Kooistra, and M. Herold. 2016. Characterizing forest change using community-based monitoring data and Landsat time series. PLoS One **11**:e0147121.
Dodds, W. K., J. R. Jones, and E. B. Welch. 1998. Suggested classification of stream trophic state: distributions of temperate stream types by chlorophyll, total nitrogen, and phosphorus. Water Research **32**:1455-1462.
Doering, O., J. Galloway, T. Theis, V. Aneja, E. Boyer, K. Cassman, E. Cowling, R. Dickerson, W. Herz, and D. Hey. 2011. Reactive Nitrogen in the United States: an

analysis of inputs, flows, consequences, and management options. United States Environmental Protection Agency.
Dotterer, D. 2017. Nutrient Management Law and Regulations Overview.*in* M. D. o. Agriculture, editor., https://mda.maryland.gov/resource_conservation/Pages/nutrient_management_overview.aspx.
Doucet, A., M. M. Savard, C. Bégin, and A. Smirnoff. 2012. Tree-ring δ 15 N values to infer air quality changes at regional scale. Chemical Geology **320**:9-16.
Driscoll, C. T., K. M. Driscoll, H. Fakhraei, and K. Civerolo. 2016. Long-term temporal trends and spatial patterns in the acid-base chemistry of lakes in the Adirondack region of New York in response to decreases in acidic deposition. Atmospheric Environment **146**:5-14.
Driscoll, C. T., K. M. Driscoll, K. M. Roy, and M. J. Mitchell. 2003. Chemical response of lakes in the Adirondack region of New York to declines in acidic deposition. ACS Publications.
Driscoll, C. T., G. B. Lawrence, A. J. Bulger, T. J. Butler, C. S. Cronan, C. Eagar, K. F. Lambert, G. E. Likens, J. L. Stoddard, and K. C. Weathers. 2001. Acidic Deposition in the Northeastern United States: Sources and Inputs, Ecosystem Effects, and Management Strategies: The effects of acidic deposition in the northeastern United States include the acidification of soil and water, which stresses terrestrial and aquatic biota. AIBS Bulletin **51**:180-198.
Dupas, R., C. Minaudo, G. Gruau, L. Ruiz, and C. Gascuel□Odoux. 2017. Multi□decadal trajectory of riverine nitrogen and phosphorus dynamics in rural catchments. Water Resources Research.
Durán, J., J. L. Morse, P. M. Groffman, J. L. Campbell, L. M. Christenson, C. T. Driscoll, T. J. Fahey, M. C. Fisk, G. E. Likens, and J. M. Melillo. 2016. Climate change decreases nitrogen pools and mineralization rates in northern hardwood forests. Ecosphere **7**.
Elmore, A. J., D. M. Nelson, and J. M. Craine. 2016. Earlier springs are causing reduced nitrogen availability in North American eastern deciduous forests. Nature plants **2**:16133.
Eshleman, K. N. 2000. A linear model of the effects of disturbance on dissolved nitrogen leakage from forested watersheds. Water Resources Research **36**:3325-3335.
Eshleman, K. N., B. E. McNeil, and P. A. Townsend. 2009. Validation of a remote sensing based index of forest disturbance using streamwater nitrogen data. Ecological Indicators **9**:476-484.
Eshleman, K. N., R. P. Morgan, J. R. Webb, F. A. Deviney, and J. N. Galloway. 1998. Temporal patterns of nitrogen leakage from mid□Appalachian forested watersheds: Role of insect defoliation. Water Resources Research **34**:2005-2016.
Eshleman, K. N., and R. D. Sabo. 2016. Declining nitrate-N yields in the Upper Potomac River Basin: What is really driving progress under the Chesapeake Bay restoration? Atmospheric Environment **146**:280-289.
Eshleman, K. N., R. D. Sabo, and K. M. Kline. 2013. Surface water quality is improving due to declining atmospheric N deposition. Environmental science & technology **47**:12193-12200.

Fixen, P. E., R. Williams, and Q. B. Rund. 2012. NUGIS: A nutrient use geographic information system for the US. International Plant Nutrition Institute, Brookings, SD.

Fox, J. 2002. An R and S-Plus companion to applied regression. Sage.

Galloway, J. N., J. D. Aber, J. W. Erisman, S. P. Seitzinger, R. W. Howarth, E. B. Cowling, and B. J. Cosby. 2003. The nitrogen cascade. AIBS Bulletin **53**:341-356.

Galloway, J. N., A. R. Townsend, J. W. Erisman, M. Bekunda, Z. Cai, J. R. Freney, L. A. Martinelli, S. P. Seitzinger, and M. A. Sutton. 2008. Transformation of the nitrogen cycle: recent trends, questions, and potential solutions. Science **320**:889-892.

Gao, W., R. Howarth, B. Hong, D. Swaney, and H. Guo. 2014. Estimating net anthropogenic nitrogen inputs (NANI) in the Lake Dianchi basin of China. Biogeosciences **11**:4577.

GAP, U. 2011. GAP/LANDFIRE National Terrestrial Ecosystems 2011: U.S. Geological Survey. USGS, https://doi.org/10.5066/F7ZS2TM0.

García, A. M., R. B. Alexander, J. G. Arnold, L. Norfleet, M. J. White, D. M. Robertson, and G. Schwarz. 2016. Regional effects of agricultural conservation practices on nutrient transport in the Upper Mississippi River Basin. Environmental science & technology **50**:6991-7000.

Garmo, Ø. A., B. L. Skjelkvåle, H. A. de Wit, L. Colombo, C. Curtis, J. Fölster, A. Hoffmann, J. Hruška, T. Høgåsen, and D. S. Jeffries. 2014. Trends in surface water chemistry in acidified areas in Europe and North America from 1990 to 2008. Water, Air, & Soil Pollution **225**:1880.

Garten Jr, C. T. 1992. Nitrogen isotope composition of ammonium and nitrate in bulk precipitation and forest throughfall. International Journal of Environmental Analytical Chemistry **47**:33-45.

Gerhart, L. M., and K. K. McLauchlan. 2014. Reconstructing terrestrial nutrient cycling using stable nitrogen isotopes in wood. Biogeochemistry **120**:1-21.

Goyette, J. O., E. M. Bennett, R. W. Howarth, and R. Maranger. 2016. Changes in anthropogenic nitrogen and phosphorus inputs to the St. Lawrence sub□basin over 110 years and impacts on riverine export. Global Biogeochemical Cycles **30**:1000-1014.

Graham, M. H. 2003. Confronting multicollinearity in ecological multiple regression. Ecology **84**:2809-2815.

Griffis, T. J., Z. Chen, J. M. Baker, J. D. Wood, D. B. Millet, X. Lee, R. T. Venterea, and P. A. Turner. 2017. Nitrous oxide emissions are enhanced in a warmer and wetter world. Proceedings of the National Academy of Sciences **114**:12081-12085.

Grigal, D. 2012. Atmospheric deposition and inorganic nitrogen flux. Water, Air, & Soil Pollution **223**:3565-3575.

Groffman, P. M., M. L. Cadenasso, J. Cavender-Bares, D. L. Childers, N. B. Grimm, J. M. Grove, S. E. Hobbie, L. R. Hutyra, G. D. Jenerette, and T. McPhearson. 2017. Moving towards a new urban systems science. Ecosystems **20**:38-43.

Groffman, P. M., C. T. Driscoll, J. Durán, J. L. Campbell, L. M. Christenson, T. J. Fahey, M. C. Fisk, C. Fuss, G. E. Likens, and G. Lovett. 2018. Nitrogen oligotrophication in northern hardwood forests. Biogeochemistry:1-17.

Groffman, P. M., M. C. Fisk, C. T. Driscoll, G. E. Likens, T. J. Fahey, C. Eagar, and L. H. Pardo. 2006. Calcium additions and microbial nitrogen cycle processes in a northern hardwood forest. Ecosystems **9**:1289-1305.

Groffman, P. M., N. L. Law, K. T. Belt, L. E. Band, and G. T. Fisher. 2004. Nitrogen fluxes and retention in urban watershed ecosystems. Ecosystems **7**:393-403.

Gronberg, J. A. M., and N. E. Spahr. 2012. County-level estimates of nitrogen and phosphorus from commercial fertilizer for the conterminous United States, 1987–2006. 2328-0328, US Geological Survey.

Haagen-Smit, A. J. 1952. Chemistry and physiology of Los Angeles smog. Industrial & Engineering Chemistry **44**:1342-1346.

Hale, R. L., N. B. Grimm, C. J. Vörösmarty, and B. Fekete. 2015. Nitrogen and phosphorus fluxes from watersheds of the northeast US from 1930 to 2000: Role of anthropogenic nutrient inputs, infrastructure, and runoff. Global Biogeochemical Cycles **29**:341-356.

Halman, J. M., P. G. Schaberg, G. J. Hawley, C. F. Hansen, and T. J. Fahey. 2014. Differential impacts of calcium and aluminum treatments on sugar maple and American beech growth dynamics. Canadian Journal of Forest Research **45**:52-59.

Healey, S. P., W. B. Cohen, Y. Zhiqiang, and O. N. Krankina. 2005. Comparison of Tasseled Cap-based Landsat data structures for use in forest disturbance detection. Remote sensing of environment **97**:301-310.

Hedin, L. O., J. J. Armesto, and A. H. Johnson. 1995. Patterns of nutrient loss from unpolluted, old□growth temperate forests: Evaluation of biogeochemical theory. Ecology **76**:493-509.

Hirsch, R. M., S. A. Archfield, and L. A. De Cicco. 2015. A bootstrap method for estimating uncertainty of water quality trends. Environmental Modelling & Software **73**:148-166.

Hirsch, R. M., D. L. Moyer, and S. A. Archfield. 2010. Weighted regressions on time, discharge, and season (WRTDS), with an application to Chesapeake Bay river inputs. JAWRA Journal of the American Water Resources Association **46**:857-880.

Hobbie, E. A., S. A. Macko, and M. Williams. 2000. Correlations between foliar δ15N and nitrogen concentrations may indicate plant-mycorrhizal interactions. Oecologia **122**:273-283.

Hobbie, S. E., J. C. Finlay, B. D. Janke, D. A. Nidzgorski, D. B. Millet, and L. A. Baker. 2017. Contrasting nitrogen and phosphorus budgets in urban watersheds and implications for managing urban water pollution. Proceedings of the National Academy of Sciences:201618536.

Homer, C., J. Dewitz, L. Yang, S. Jin, P. Danielson, G. Xian, J. Coulston, N. Herold, J. Wickham, and K. Megown. 2015. Completion of the 2011 National Land Cover Database for the conterminous United States–representing a decade of land cover change information. Photogrammetric Engineering & Remote Sensing **81**:345-354.

Hong, B., D. P. Swaney, and R. W. Howarth. 2013. Estimating net anthropogenic nitrogen inputs to US watersheds: comparison of methodologies. Environmental science & technology **47**:5199-5207.

Hong, B., D. P. Swaney, M. McCrackin, A. Svanbäck, C. Humborg, B. Gustafsson, A. Yershova, and A. Pakhomau. 2017. Advances in NANI and NAPI accounting for the Baltic drainage basin: spatial and temporal trends and relationships to watershed TN and TP fluxes. Biogeochemistry **133**:245-261.

Horn, K. J., R. Q. Thomas, C. M. Clark, and L. Pardo. 2018. Growth and survival relationships of 71 tree species with nitrogen and sulfur deposition across the conterminous U.S. PLoS One.

Houlton, B. Z., E. Boyer, A. Finzi, J. Galloway, A. Leach, D. Liptzin, J. Melillo, T. S. Rosenstock, D. Sobota, and A. R. Townsend. 2013. Intentional versus unintentional nitrogen use in the United States: trends, efficiency and implications. Biogeochemistry **114**:11-23.

Houston, D. 1994. Major new tree disease epidemics: beech bark disease. Annual review of phytopathology **32**:75-87.

Howard, I., and K. K. McLauchlan. 2015. Spatiotemporal analysis of nitrogen cycling in a mixed coniferous forest of the northern United States. Biogeosciences **12**:3941-3952.

Howarth, R., D. Swaney, G. Billen, J. Garnier, B. Hong, C. Humborg, P. Johnes, C.-M. Mörth, and R. Marino. 2012. Nitrogen fluxes from the landscape are controlled by net anthropogenic nitrogen inputs and by climate. Frontiers in Ecology and the Environment **10**:37-43.

Hu, M., Y. Liu, J. Wang, R. A. Dahlgren, and D. Chen. 2018. A modification of the Regional Nutrient Management model (ReNuMa) to identify long-term changes in riverine nitrogen sources. Journal of Hydrology **561**:31-42.

Hu, W., J. Xie, H. W. Chau, and B. C. Si. 2015. Evaluation of parameter uncertainties in nonlinear regression using Microsoft Excel Spreadsheet. Environmental Systems Research **4**:4.

Huggett, B. A., P. G. Schaberg, G. J. Hawley, and C. Eagar. 2007. Long-term calcium addition increases growth release, wound closure, and health of sugar maple (Acer saccharum) trees at the Hubbard Brook Experimental Forest. Canadian Journal of Forest Research **37**:1692-1700.

Hwang, T., L. E. Band, C. F. Miniat, C. Song, P. V. Bolstad, J. M. Vose, and J. P. Love. 2014. Divergent phenological response to hydroclimate variability in forested mountain watersheds. Global Change Biology **20**:2580-2595.

Jaworski, N. A., P. M. Groffman, A. A. Keller, and J. C. Prager. 1992. A watershed nitrogen and phosphorus balance: the upper Potomac River basin. Estuaries **15**:83-95.

Jia, G., and F. Chen. 2010. Monthly variations in nitrogen isotopes of ammonium and nitrate in wet deposition at Guangzhou, south China. Atmospheric Environment **44**:2309-2315.

Johnson, C. E., C. T. Driscoll, J. D. Blum, T. J. Fahey, and J. J. Battles. 2014. Soil chemical dynamics after calcium silicate addition to a northern hardwood forest. Soil Science Society of America Journal **78**:1458-1468.

Jokela, W. E. 1992. Nitrogen fertilizer and dairy manure effects on corn yield and soil nitrate. Soil Science Society of America Journal **56**:148-154.

Jordan, T. E., and D. E. Weller. 1996. Human contributions to terrestrial nitrogen flux. BioScience **46**:655-664.

Jung, K., W.-J. Choi, S. X. Chang, and M. Arshad. 2013. Soil and tree ring chemistry of Pinus banksiana and Populus tremuloides stands as indicators of changes in atmospheric environments in the oil sands region of Alberta, Canada. Ecological Indicators **25**:256-265.

Kaushal, S. S., P. M. Groffman, L. E. Band, C. A. Shields, R. P. Morgan, M. A. Palmer, K. T. Belt, C. M. Swan, S. E. Findlay, and G. T. Fisher. 2008. Interaction between urbanization and climate variability amplifies watershed nitrate export in Maryland. Environmental science & technology **42**:5872-5878.

Keisman, J., J. Bloomquist, S. Phillips, G. Shenk, and E. Yagow. 2015. Estimating land management effects on water quality status and trends. Proceedings of the March 25-26, 2014 workshop. . STAC Publiclation **Number 15-002**.

Keisman, J. L., O. H. Devereux, A. E. LaMotte, A. J. Sekellick, and J. D. Blomquist. 2018. Manure and fertilizer inputs to land in the Chesapeake Bay watershed, 1950–2012. 2328-0328, US Geological Survey.

Kirchner, J. W., X. Feng, and C. Neal. 2000. Fractal stream chemistry and its implications for contaminant transport in catchments. Nature **403**:524-527.

Kirchner, J. W., and C. Neal. 2013. Universal fractal scaling in stream chemistry and its implications for solute transport and water quality trend detection. Proceedings of the National Academy of Sciences **110**:12213-12218.

Kline, K. M., K. N. Eshleman, J. E. Garlitz, and S. H. U'Ren. 2016. Long-term response of surface water acid neutralizing capacity in a central Appalachian (USA) river basin to declining acid deposition. Atmospheric Environment **146**:195-205.

Kopáček, J., J. Hejzlar, J. Kaňa, P. Porcal, and J. Turek. 2016. The sensitivity of water chemistry to climate in a forested, nitrogen-saturated catchment recovering from acidification. Ecological Indicators **63**:196-208.

Kothawala, D. N., S. A. Watmough, M. N. Futter, L. Zhang, and P. J. Dillon. 2011. Stream nitrate responds rapidly to decreasing nitrate deposition. Ecosystems **14**:274-286.

Larsson, L. A. 2009. CDENDRO: CooRecorder.*in* CDendro, editor., http://www.cybis.se/forfun/dendro/.

Latysh, N. E., and G. A. Wetherbee. 2012. Improved mapping of National Atmospheric Deposition Program wet-deposition in complex terrain using PRISM-gridded data sets. Environmental monitoring and assessment **184**:913-928.

Lawrence, G. 2002. Persistent episodic acidification of streams linked to acid rain effects on soil. Atmospheric Environment **36**:1589-1598.

Lawrence, G., H. Simonin, B. P. Baldigo, K. Roy, and S. Capone. 2011. Changes in the chemistry of acidified Adirondack streams from the early 1980s to 2008. Environmental Pollution **159**:2750-2758.

Lawrence, G., T. Sullivan, D. Burns, S. Bailey, B. Cosby, M. Dovciak, H. Ewing, T. McDonnel, R. Minocha, and K. Rice. 2015a. Acidic deposition along the Appalachian Trail corridor and its effects on acid-sensitive terrestrial and aquatic resources: results of the Appalachian Trail MEGA-transect atmospheric deposition effects study. Natural Resource Report NPS/NRSS/ARD/NRR—2015/996. National Park Service, Fort Collins, Colorado.

Lawrence, G. B., J. E. Dukett, N. Houck, P. Snyder, and S. Capone. 2013. Increases in dissolved organic carbon accelerate loss of toxic Al in Adirondack lakes

recovering from acidification. Environmental science & technology **47**:7095-7100.
Lawrence, G. B., P. W. Hazlett, I. J. Fernandez, R. Ouimet, S. W. Bailey, W. C. Shortle, K. T. Smith, and M. R. Antidormi. 2015b. Declining acidic deposition begins reversal of forest-soil acidification in the northeastern US and eastern Canada. Environmental science & technology **49**:13103-13111.
Lawrence, G. B., B. Momen, and K. M. Roy. 2004. Use of stream chemistry for monitoring acidic deposition effects in the Adirondack region of New York. Journal of environmental quality **33**:1002-1009.
Lawrence, G. B., K. M. Roy, B. P. Baldigo, H. A. Simonin, S. B. Capone, J. W. Sutherland, S. A. Nierzwicki-Bauer, and C. W. Boylen. 2008. Chronic and episodic acidification of Adirondack streams from acid rain in 2003–2005. Journal of environmental quality **37**:2264-2274.
Likens, G. E. 2013. Biogeochemistry of a forested ecosystem. Springer Science & Business Media.
Likens, G. E. 2017. Fifty years of continuous precipitation and stream chemistry data from the Hubbard Brook ecosystem study (1963–2013). Ecology **98**:2224-2224.
Linker, L. C., R. Dennis, G. W. Shenk, R. A. Batiuk, J. Grimm, and P. Wang. 2013. Computing atmospheric nutrient loads to the Chesapeake Bay watershed and tidal waters. JAWRA Journal of the American Water Resources Association **49**:1025-1041.
Lloret, J., and I. Valiela. 2016. Unprecedented decrease in deposition of nitrogen oxides over North America: the relative effects of emission controls and prevailing air-mass trajectories. Biogeochemistry **129**:165-180.
Lovett, G. M., and C. L. Goodale. 2011. A new conceptual model of nitrogen saturation based on experimental nitrogen addition to an oak forest. Ecosystems **14**:615-631.
Lovett, G. M., and M. J. Mitchell. 2004. Sugar maple and nitrogen cycling in the forests of eastern North America. Frontiers in Ecology and the Environment **2**:81-88.
Lumley, T., and A. Miller. 2009. Leaps: regression subset selection. R package version 2.9. See http://CRAN. R-project. org/package= leaps.
MacDonald, J., N. Dise, E. Matzner, M. Armbruster, P. Gundersen, and M. Forsius. 2002. Nitrogen input together with ecosystem nitrogen enrichment predict nitrate leaching from European forests. Global Change Biology **8**:1028-1033.
Mallin, M. A., M. R. McIver, H. A. Wells, D. C. Parsons, and V. L. Johnson. 2005. Reversal of eutrophication following sewage treatment upgrades in the New River Estuary, North Carolina. Estuaries and Coasts **28**:750-760.
Maryland. 2004. SENATE BILL 320: Water Pollution - State Waters - The Bay Restoration Fund.*in* M. Senate, editor. 320.
Mathias, J. M., and R. B. Thomas. 2018. Disentangling the effects of acidic air pollution, atmospheric CO 2, and climate change on recent growth of red spruce trees in the Central Appalachian Mountains. Global Change Biology.
McLauchlan, K., and J. Craine. 2012. Species-specific trajectories of nitrogen isotopes in Indiana hardwood forests, USA. Biogeosciences **9**:867.
McLauchlan, K. K., J. M. Craine, W. W. Oswald, P. R. Leavitt, and G. E. Likens. 2007. Changes in nitrogen cycling during the past century in a northern hardwood forest. Proceedings of the National Academy of Sciences **104**:7466-7470.

McLauchlan, K. K., C. J. Ferguson, I. E. Wilson, T. W. Ocheltree, and J. M. Craine. 2010. Thirteen decades of foliar isotopes indicate declining nitrogen availability in central North American grasslands. New Phytologist **187**:1135-1145.

McLauchlan, K. K., L. M. Gerhart, J. J. Battles, J. M. Craine, A. J. Elmore, P. E. Higuera, M. Mack, B. E. McNeil, D. M. Nelson, and N. Pederson. 2017. Centennial-scale reductions in nitrogen availability in temperate forests of the United States. Scientific Reports **7**.

McNeil, B. E., K. M. de Beurs, K. N. Eshleman, J. R. Foster, and P. A. Townsend. 2007. Maintenance of ecosystem nitrogen limitation by ephemeral forest disturbance: An assessment using MODIS, Hyperion, and Landsat ETM+. Geophysical Research Letters **34**.

Michelsen, A., C. Quarmby, D. Sleep, and S. Jonasson. 1998. Vascular plant 15 N natural abundance in heath and forest tundra ecosystems is closely correlated with presence and type of mycorrhizal fungi in roots. Oecologia **115**:406-418.

Miller, M. P., A. J. Tesoriero, P. D. Capel, B. A. Pellerin, K. E. Hyer, and D. A. Burns. 2016. Quantifying watershed□scale groundwater loading and in□stream fate of nitrate using high□frequency water quality data. Water Resources Research **52**:330-347.

Monteith, D. T., J. L. Stoddard, C. D. Evans, H. A. De Wit, M. Forsius, T. Høgåsen, A. Wilander, B. L. Skjelkvåle, D. S. Jeffries, and J. Vuorenmaa. 2007. Dissolved organic carbon trends resulting from changes in atmospheric deposition chemistry. Nature **450**:537-540.

Morse, J. L., J. Durán, F. Beall, E. M. Enanga, I. F. Creed, I. Fernandez, and P. M. Groffman. 2015. Soil denitrification fluxes from three northeastern North American forests across a range of nitrogen deposition. Oecologia **177**:17-27.

Moyer, D. L. 2016. Water Quality Loads and Trends at Nontidal Monitoring Stations in the Chespeake Bay Watershed. *.in* U. S. G. Survey, editor., Water Quality Loads and Trends at Nontidal Monitoring Stations in the Chespeake Bay Watershed. .

Mueller, N. D., J. S. Gerber, M. Johnston, D. K. Ray, N. Ramankutty, and J. A. Foley. 2012. Closing yield gaps through nutrient and water management. Nature **490**:254-257.

Nadelhoffer, K., G. Shaver, B. Fry, A. Giblin, L. Johnson, and R. McKane. 1996. 15 N natural abundances and N use by tundra plants. Oecologia **107**:386-394.

NADP. 2015. NTN Maps.*in* N. A. D. Program, editor., http://nadp.isws.illinois.edu/NTN/maps.aspx.

Norby, R. J., M. G. De Kauwe, T. F. Domingues, R. A. Duursma, D. S. Ellsworth, D. S. Goll, D. M. Lapola, K. A. Luus, A. R. MacKenzie, and B. E. Medlyn. 2016. Model–data synthesis for the next generation of forest free□air CO2 enrichment (FACE) experiments. New Phytologist **209**:17-28.

Norby, R. J., J. M. Warren, C. M. Iversen, B. E. Medlyn, and R. E. McMurtrie. 2010. CO2 enhancement of forest productivity constrained by limited nitrogen availability. Proceedings of the National Academy of Sciences **107**:19368-19373.

NRCS, U. 2009. Web soil survey. URL http://www. websoilsurvey. ncsc. usda. gov/app/[verified October 29, 2009].

NYSERDA. 2012. A Long-Term Monitoring Program For Evaluating Changes in Water Quality in Selected Adirondack Waters: Core Program Report 2011. New York State Energy Research and Development Authority

Oelsner, G. P., L. A. Sprague, J. C. Murphy, R. E. Zuellig, H. M. Johnson, K. R. Ryberg, J. A. Falcone, E. G. Stets, A. V. Vecchia, M. L. Riskin, L. A. De Cicco, T. J. Mills, and W. H. Farmer. 2017. Water-quality trends in the nation's rivers and streams, 1972–2012—Data preparation, statistical methods, and trend results. Report 2017-5006, Reston, VA.

Ollinger, S. V., J. D. Aber, P. B. Reich, and R. J. Freuder. 2002. Interactive effects of nitrogen deposition, tropospheric ozone, elevated CO2 and land use history on the carbon dynamics of northern hardwood forests. Global Change Biology **8**:545-562.

Oulehle, F., T. Chuman, J. Hruška, P. Krám, W. H. McDowell, O. Myška, T. Navrátil, and M. Tesař. 2017. Recovery from acidification alters concentrations and fluxes of solutes from Czech catchments. Biogeochemistry **132**:251-272.

Oulehle, F., C. D. Evans, J. Hofmeister, R. Krejci, K. Tahovska, T. Persson, P. Cudlin, and J. Hruska. 2011. Major changes in forest carbon and nitrogen cycling caused by declining sulphur deposition. Global Change Biology **17**:3115-3129.

Pardo, L., H. Hemond, J. Montoya, and J. Pett-Ridge. 2007. Natural abundance 15 N in soil and litter across a nitrate-output gradient in New Hampshire. Forest Ecology and management **251**:217-230.

Pardo, L., P. Templer, C. Goodale, S. Duke, P. Groffman, M. Adams, P. Boeckx, J. Boggs, J. Campbell, and B. Colman. 2006. Regional Assessment of N Saturation using Foliar and Root\varvec {\delta}^{\bf 15}{\bf N}. Biogeochemistry **80**:143-171.

Peñuelas, J., P. Ciais, J. G. Canadell, I. A. Janssens, M. Fernández-Martínez, J. Carnicer, M. Obersteiner, S. Piao, R. Vautard, and J. Sardans. 2017. Shifting from a fertilization-dominated to a warming-dominated period. Nature Ecology & Evolution **1**:1438.

Perakis, S. S., A. J. Tepley, and J. E. Compton. 2015. Disturbance and topography shape nitrogen availability and δ15N over long-term forest succession. Ecosystems **18**:573-588.

Peterson, B. J., W. M. Wollheim, P. J. Mulholland, J. R. Webster, J. L. Meyer, J. L. Tank, E. Martí, W. B. Bowden, H. M. Valett, and A. E. Hershey. 2001. Control of nitrogen export from watersheds by headwater streams. Science **292**:86-90.

Piatek, K. B., M. J. Mitchell, S. R. Silva, and C. Kendall. 2005. Sources of nitrate in snowmelt discharge: evidence from water chemistry and stable isotopes of nitrate. Water, Air, & Soil Pollution **165**:13-35.

PRISM. 2015. 30-Year Normals Maps.*in* O. State, editor., http://www.prism.oregonstate.edu/normals/.

Qi, H., T. B. Coplen, H. Geilmann, W. A. Brand, and J. K. Böhlke. 2003. Two new organic reference materials for δ13C and δ15N measurements and a new value for the δ13C of NBS 22 oil. Rapid Communications in Mass Spectrometry **17**:2483-2487.

R, R. T. 2014. R: A language and environment for statistical computing. Vienna, Austria: R Foundation for Statistical Computing; 2014.

Rizopoulos, D. 2006. ltm: An R package for latent variable modeling and item response theory analyses. Journal of statistical software **17**:1-25.

Rogora, M., S. Arisci, and A. Marchetto. 2012. The role of nitrogen deposition in the recent nitrate decline in lakes and rivers in Northern Italy. Science of The Total Environment **417**:214-223.

Rosi-Marshall, E. J., E. S. Bernhardt, D. C. Buso, C. T. Driscoll, and G. E. Likens. 2016. Acid rain mitigation experiment shifts a forested watershed from a net sink to a net source of nitrogen. Proceedings of the National Academy of Sciences **113**:7580-7583.

Ross, D. S., J. B. Shanley, J. L. Campbell, G. B. Lawrence, S. W. Bailey, G. E. Likens, B. C. Wemple, G. Fredriksen, and A. E. Jamison. 2012. Spatial patterns of soil nitrification and nitrate export from forested headwaters in the northeastern United States. Journal of Geophysical Research: Biogeosciences **117**.

Runkel, R. L., C. G. Crawford, and T. A. Cohn. 2004. Load Estimator (LOADEST): A FORTRAN program for estimating constituent loads in streams and rivers. 2328-7055.

Russell, M. J., D. E. Weller, T. E. Jordan, K. J. Sigwart, and K. J. Sullivan. 2008. Net anthropogenic phosphorus inputs: spatial and temporal variability in the Chesapeake Bay region. Biogeochemistry **88**:285-304.

Rustad, L., J. Campbell, G. Marion, R. Norby, M. Mitchell, A. Hartley, J. Cornelissen, and J. Gurevitch. 2001. A meta-analysis of the response of soil respiration, net nitrogen mineralization, and aboveground plant growth to experimental ecosystem warming. Oecologia **126**:543-562.

Sabo, R. D., D. M. Nelson, and K. N. Eshleman. 2016a. Episodic, seasonal, and annual export of atmospheric and microbial nitrate from a temperate forest. Geophysical Research Letters **43**:683-691.

Sabo, R. D., S. E. Scanga, G. B. Lawrence, D. M. Nelson, K. N. Eshleman, G. A. Zabala, A. A. Alinea, and C. D. Schirmer. 2016b. Watershed-scale changes in terrestrial nitrogen cycling during a period of decreased atmospheric nitrate and sulfur deposition. Atmospheric Environment **146**:271-279.

Sanford, W. E., and J. P. Pope. 2013. Quantifying groundwater's role in delaying improvements to Chesapeake Bay water quality. Environmental science & technology **47**:13330-13338.

Saurer, M., P. Cherubini, M. Ammann, B. De Cinti, and R. Siegwolf. 2004. First detection of nitrogen from NOx in tree rings: a 15 N/14 N study near a motorway. Atmospheric Environment **38**:2779-2787.

Savard, M. M., C. Bégin, A. Smirnoff, J. l. Marion, and E. Rioux-Paquette. 2009. Tree-ring nitrogen isotopes reflect anthropogenic NO x emissions and climatic effects. Environmental science & technology **43**:604-609.

Sawicka, K., D. Monteith, E. Vanguelova, A. J. Wade, and J. M. Clark. 2016. Fine-scale temporal characterization of trends in soil water dissolved organic carbon and potential drivers. Ecological Indicators **68**:36-51.

Scanlon, T. M., S. M. Ingram, and A. L. Riscassi. 2010. Terrestrial and in□stream influences on the spatial variability of nitrate in a forested headwater catchment. Journal of Geophysical Research: Biogeosciences **115**.

Sebestyen, S. D., E. W. Boyer, and J. B. Shanley. 2009. Responses of stream nitrate and DOC loadings to hydrological forcing and climate change in an upland forest of the northeastern United States. Journal of Geophysical Research: Biogeosciences **114**.

Sha, J., Z.-L. Wang, R. Lu, Y. Zhao, X. Li, and Y.-T. Shang. 2018. Estimation of the Source Apportionment of Phosphorus and Its Responses to Future Climate Changes Using Multi-Model Applications. Water **10**:468.

Shcherbak, I., N. Millar, and G. P. Robertson. 2014. Global metaanalysis of the nonlinear response of soil nitrous oxide (N2O) emissions to fertilizer nitrogen. Proceedings of the National Academy of Sciences **111**:9199-9204.

Shenk, G. W., and L. C. Linker. 2013. Development and application of the 2010 Chesapeake Bay watershed total maximum daily load model. JAWRA Journal of the American Water Resources Association **49**:1042-1056.

Shields, C. A., L. E. Band, N. Law, P. M. Groffman, S. S. Kaushal, K. Savvas, G. T. Fisher, and K. T. Belt. 2008. Streamflow distribution of non–point source nitrogen export from urban□rural catchments in the Chesapeake Bay watershed. Water Resources Research **44**.

Simkin, S. M., E. B. Allen, W. D. Bowman, C. M. Clark, J. Belnap, M. L. Brooks, B. S. Cade, S. L. Collins, L. H. Geiser, and F. S. Gilliam. 2016. Conditional vulnerability of plant diversity to atmospheric nitrogen deposition across the United States. Proceedings of the National Academy of Sciences **113**:4086-4091.

Simmons, J. A., J. B. Yavitt, and T. J. Fahey. 1996. Watershed liming effects on the forest floor N cycle. Pages 79-102 Experimental Watershed Liming Study. Springer.

Sinha, E., A. Michalak, and V. Balaji. 2017. Eutrophication will increase during the 21st century as a result of precipitation changes. Science **357**:405-408.

Sinha, E., and A. M. Michalak. 2016. Precipitation Dominates Interannual Variability of Riverine Nitrogen Loading across the Continental United States. Environmental science & technology **50**:12874-12884.

Sinsabaugh, R., D. Zak, M. Gallo, C. Lauber, and R. Amonette. 2004. Nitrogen deposition and dissolved organic carbon production in northern temperate forests. Soil Biology and Biochemistry **36**:1509-1515.

Sinsabaugh, R. L. 2010. Phenol oxidase, peroxidase and organic matter dynamics of soil. Soil Biology and Biochemistry **42**:391-404.

Smith, D., P. Owens, A. Leytem, and E. Warnemuende. 2007. Nutrient losses from manure and fertilizer applications as impacted by time to first runoff event. Environmental Pollution **147**:131-137.

Sobota, D. J., J. E. Compton, and J. A. Harrison. 2013. Reactive nitrogen inputs to US lands and waterways: how certain are we about sources and fluxes? Frontiers in Ecology and the Environment **11**:82-90.

Stets, E. G., V. J. Kelly, and C. G. Crawford. 2015. Regional and Temporal Differences in Nitrate Trends Discerned from Long□Term Water Quality Monitoring Data. JAWRA Journal of the American Water Resources Association **51**:1394-1407.

Stoddard, J. L., D. Jeffries, A. Lükewille, T. Clair, P. Dillon, C. Driscoll, M. Forsius, M. Johannessen, J. Kahl, and J. Kellogg. 1999. Regional trends in aquatic recovery from acidification in North America and Europe. Nature **401**:575-578.

Sullivan, T. J., G. B. Lawrence, S. W. Bailey, T. C. McDonnell, C. M. Beier, K. Weathers, G. McPherson, and D. A. Bishop. 2013. Effects of acidic deposition and soil acidification on sugar maple trees in the Adirondack Mountains, New York. Environmental science & technology **47**:12687-12694.

Sutton, M. A., C. M. Howard, J. W. Erisman, G. Billen, A. Bleeker, P. Grennfelt, H. Van Grinsven, and B. Grizzetti. 2011. The European nitrogen assessment: sources, effects and policy perspectives. Cambridge University Press.

Swaney, D. P., R. W. Howarth, and B. Hong. 2018. Nitrogen use efficiency and crop production: Patterns of regional variation in the United States, 1987–2012. Science of The Total Environment **635**:498-511.

Templer, P. H., M. A. Arthur, G. M. Lovett, and K. C. Weathers. 2007. Plant and soil natural abundance δ15N: indicators of relative rates of nitrogen cycling in temperate forest ecosystems. Oecologia **153**:399-406.

Thomas, R. Q., C. D. Canham, K. C. Weathers, and C. L. Goodale. 2010. Increased tree carbon storage in response to nitrogen deposition in the US. Nature Geoscience **3**:13.

Tian, J., D. M. Nelson, and F. S. Hu. 2011. How well do sediment indicators record past climate? An evaluation using annually laminated sediments. Journal of Paleolimnology **45**:73-84.

Tomlinson, G., N. Buchmann, R. Siegwolf, P. Weber, A. Thimonier, E. G. Pannatier, M. Schmitt, M. Schaub, and P. Waldner. 2016. Can tree-ring δ15N be used as a proxy for foliar δ15N in European beech and Norway spruce? Trees **30**:627-638.

Townsend, P. A., K. N. Eshleman, and C. Welcker. 2004. Remote sensing of gypsy moth defoliation to assess variations in stream nitrogen concentrations. Ecological Applications **14**:504-516.

Townsend, P. A., A. Singh, J. R. Foster, N. J. Rehberg, C. C. Kingdon, K. N. Eshleman, and S. W. Seagle. 2012. A general Landsat model to predict canopy defoliation in broadleaf deciduous forests. Remote sensing of environment **119**:255-265.

van Grinsven, H. J., L. Bouwman, K. G. Cassman, H. M. van Es, M. L. McCrackin, and A. H. Beusen. 2015. Losses of ammonia and nitrate from agriculture and their effect on nitrogen recovery in the European Union and the United States between 1900 and 2050. Journal of environmental quality **44**:356-367.

Van Meter, K., N. Basu, and P. Van Cappellen. 2017. Two centuries of nitrogen dynamics: Legacy sources and sinks in the Mississippi and Susquehanna River Basins. Global Biogeochemical Cycles **31**:2-23.

Velthof, G., J. Lesschen, J. Webb, S. Pietrzak, Z. Miatkowski, M. Pinto, J. Kros, and O. Oenema. 2014. The impact of the Nitrates Directive on nitrogen emissions from agriculture in the EU-27 during 2000–2008. Science of The Total Environment **468**:1225-1233.

Vet, R., R. S. Artz, S. Carou, M. Shaw, C.-U. Ro, W. Aas, A. Baker, V. C. Bowersox, F. Dentener, and C. Galy-Lacaux. 2014. A global assessment of precipitation chemistry and deposition of sulfur, nitrogen, sea salt, base cations, organic acids, acidity and pH, and phosphorus. Atmospheric Environment **93**:3-100.

Vitousek, P. M., J. D. Aber, R. W. Howarth, G. E. Likens, P. A. Matson, D. W. Schindler, W. H. Schlesinger, and D. G. Tilman. 1997. Human alteration of the

global nitrogen cycle: sources and consequences. Ecological Applications **7**:737-750.
Vitousek, P. M., and J. M. Melillo. 1979. Nitrate losses from disturbed forests: patterns and mechanisms. Forest Science **25**:605-619.
Waller, K., C. Driscoll, J. Lynch, D. Newcomb, and K. Roy. 2012. Long-term recovery of lakes in the Adirondack region of New York to decreases in acidic deposition. Atmospheric Environment **46**:56-64.
Wang, R., D. Goll, Y. Balkanski, D. Hauglustaine, O. Boucher, P. Ciais, I. Janssens, J. Penuelas, B. Guenet, and J. Sardans. 2017. Global forest carbon uptake due to nitrogen and phosphorus deposition from 1850 to 2100. Global Change Biology.
Webster, J., J. Knoepp, W. Swank, and C. Miniat. 2016. Evidence for a regime shift in nitrogen export from a forested watershed. Ecosystems **19**:881-895.
Weier, K., J. Doran, J. Power, and D. Walters. 1993. Denitrification and the dinitrogen/nitrous oxide ratio as affected by soil water, available carbon, and nitrate. Soil Science Society of America Journal **57**:66-72.
White, P. S., and S. T. Pickett. 1985. Natural disturbance and patch dynamics: An introduction. Academic Press, Incorporated:3-13.
Xiao, H.-W., H.-Y. Xiao, A.-m. Long, and Y.-L. Wang. 2012. Who controls the monthly variations of NH 4+ nitrogen isotope composition in precipitation? Atmospheric Environment **54**:201-206.
Zhang, Q. 2018. Synthesis of nutrient and sediment export patterns in the Chesapeake Bay watershed: Complex and non-stationary concentration-discharge relationships. Science of The Total Environment **618**:1268-1283.
Zhang, Q., D. C. Brady, W. R. Boynton, and W. P. Ball. 2015a. Long□Term Trends of Nutrients and Sediment from the Nontidal Chesapeake Watershed: An Assessment of Progress by River and Season. JAWRA Journal of the American Water Resources Association **51**:1534-1555.
Zhang, X., E. A. Davidson, D. L. Mauzerall, T. D. Searchinger, P. Dumas, and Y. Shen. 2015b. Managing nitrogen for sustainable development. Nature **528**:51-59.
Zheng, M., L. G. Salmon, J. J. Schauer, L. Zeng, C. Kiang, Y. Zhang, and G. R. Cass. 2005. Seasonal trends in PM2. 5 source contributions in Beijing, China. Atmospheric Environment **39**:3967-3976.
Zhu, Z., C. E. Woodcock, and P. Olofsson. 2012. Continuous monitoring of forest disturbance using all available Landsat imagery. Remote sensing of environment **122**:75-91.